

Plasma-activated polymer films
for mesenchymal stem cell differentiation

Inauguraldissertation

zur Erlangung der Würde eines Doktors der Philosophie

vorgelegt der

Medizinischen Fakultät

der Universität Basel

im Rahmen einer Cotutelle de thèse

von

Jasmin Waser-Althaus

aus Lauperswil, Kanton Bern, Schweiz

Basel, 2014

Prof. Dr. med. Christoph Beglinger

Dekan

Aus dem Arbeitsbereich Zellbiologie

Direktor: Prof. Dr. Wolfgang Schareck

und zur

Erlangung des akademischen Grades

Doktor der Medizinwissenschaften

Doctor rerum humanarum

der Universitätsmedizin Rostock

im Rahmen einer Cotutelle de thèse

von

Jasmin Waser-Althaus, geb. am 02.07.1981 in Rheinfelden

aus Rheinfelden

Rostock, 2014

Genehmigt von der medizinischen Fakultät

auf Antrag von

Prof. Dr. Bert Müller (Fakultätsverantwortlicher, Dissertationsleiter)
Biomaterials Science Center, Universität Basel

Prof. Dr. Uwe Pieleles (Korreferent)
Abteilung Chemie und Bioanalytik, Fachhochschule Nordwestschweiz

PD Dr. rer. nat. et med. habil. Kirsten Peters (Externe Expertin)
Arbeitsbereich Zellbiologie, Universität Rostock

Prof. Dr. med. Jürg A. Schifferli (Prüfungsvorsitzender)
Abteilung Biomedizin, Universität Basel

Basel, den 19.06.2012

ABSTRACT

Polyetheretherketone (PEEK) is a biomaterial utilized for spine, orthopedic and trauma implants. Its inertness prevents osseointegration, so that coatings with titanium or hydroxyapatite are required for load-bearing PEEK implants. Compared to metals, PEEK is iso-elastic, magnetic resonance imaging compatible and radiolucent. To activate the PEEK surface directly, oxygen and ammonia plasma treatments of plasma powers between 10 to 200 W were applied on films with thicknesses between 12 to 50 μm . Oxygen plasma treatment introduced carboxylic and ester groups at the PEEK surface, whereas ammonia plasma treatment generated amine groups. In both cases, scanning electron microscopy revealed pillar-like nanostructures in the range of 10 to 100 nm, differing in density and size dependent on plasma power, exposure time and composition of plasma. Analysis of the nanostructures by atomic force microscopy showed that the roughness increased and island density decreased linearly with plasma power for oxygen and ammonia plasma-treated PEEK substrates. Anisotropic structures, found in human tissue, can be copied to PEEK implants, for example by means of injection molding or glass casting. Such anisotropy was analyzed on the nanometer scale using wide-angle and small-angle X-ray scattering and using optical transmission measurements. The rather simple optical experiments also permit the determination of the intermolecular binding energies, originating from the $\pi - \pi$ stacks of the phenyl moieties from annealed PEEK films.

On PEEK films treated with plasma powers of 10 and 50 W, which exhibited water contact angles of 40 to 50° and an enhanced protein adsorption, increased adhesion and proliferation of adipose tissue-derived stem cells was found. Osteogenic differentiation, monitored by alkaline phosphatase activity and mineralization, was doubled on these oxygen and ammonia plasma-treated PEEK films in comparison to the original PEEK films and the polystyrene control. These *in vitro* data indicated an osteopromotive effect of plasma-treated PEEK on tissue-resident mesenchymal stem cells. Before application to medical implants, however, the results have to be confirmed by *in vivo* studies.

ZUSAMMENFASSUNG

Polyetheretherketon (PEEK) wird als Biomaterial für Wirbelsäulen-, orthopädische sowie Trauma-Implantate verwendet. Für lasttragende Implantate benötigt das inerte PEEK Beschichtungen aus Titan oder Hydroxyapatit um die Einheilung am Knochen zu gewährleisten. Im Vergleich zu Metallimplantaten ist PEEK isoelastisch, magnetresonanzkompatibel und strahlendurchlässig. Um die PEEK Oberfläche direkt zu aktivieren wurden 12-50 µm dicke PEEK-Folien zwischen 10 und 200 W Sauerstoff- und Ammoniakplasma behandelt. Durch Sauerstoffplasma wurden Carboxyl- und Estergruppen auf der PEEK Oberfläche generiert, Ammoniakplasma resultierte in Aminogruppen. Beide Prozessgase induzierten säulenartige Strukturen im Bereich von 10 bis 100 nm. Die Strukturen variierten in Dichte und Grösse abhängig von der Plasmaintensität, Behandlungsdauer und Zusammensetzung des Prozessgases. Die Analyse mittels Atomkraftmikroskopie zeigte eine lineare Erhöhung der Rauigkeit und Verringerung der Inseldichte mit steigender Plasmaintensität für beide Prozessgase. Anisotrope Strukturen welche in menschlichem Gewebe vorkommen, können durch Spritz- oder Glasguss auf PEEK übertragen werden. Diese Anisotropie wurde im Nanometerbereich mittels Röntgenkleinwinkel- und Röntgengrosswinkelstreuung sowie optischen Transmissionsmessungen untersucht. Die einfachen optischen Experimente erlauben die Bestimmung der intermolekularen Bindungsenergien von getemperten PEEK Folien, welche von den $\pi - \pi$ Wechselwirkungen der Phenylringe stammen.

PEEK Folien welche mit Plasmaintensitäten von 10 und 50 W behandelt wurden zeigten Wasserkontaktwinkel zwischen 40 und 50°. Zudem wurde eine erhöhte Proteinadsorption, sowie erhöhte Adhäsion und Proliferation von isolierten Stammzellen aus Fettgewebe beobachtet. Auf diesen Sauerstoff- und Ammoniakplasma behandelten PEEK Oberflächen war die osteogene Differenzierung im Bezug auf die alkalische Phosphatase Aktivität und Mineralisierung doppelt so hoch wie auf unbehandelten PEEK Folien und Polystyrenkontrollen. Diese *in vitro* Ergebnisse deuten auf einen knochenwachstumsfördernden Effekt von plasmabehandeltem PEEK auf mesenchymale Stammzellen hin, welche direkt aus Gewebe isoliert wurden. Vor der Anwendung auf Implantaten müssen diese Resultate mit *in vivo* Studien verifiziert werden.

TABLE OF CONTENTS

Acknowledgements	1
Chapter 1 Introduction and thesis tasks	4
Chapter 2 Materials and methods	8
Chapter 3 Thesis contributions (results and discussion)	12
Chapter 4 Anisotropy in polyetheretherketone films	20
Chapter 5 Nanostructuring polyetheretherketone for medical implants	32
Chapter 6 Micro- and nano-structured polymer substrates for biomedical applications	41
Chapter 7 Differentiation of human mesenchymal stem cells on plasma-treated polyetheretherketone	57
Chapter 8 Conclusions and outlook	68
Curriculum Vitae	70
References	74

ACKNOWLEDGEMENTS

It would not have been possible to write this doctoral thesis without the help and support of the kind people around me, to only some of whom it is possible to give particular mention here.

First of all, I would like to express my gratitude to my supervisor Prof. Bert Müller, who gave me a challenging interdisciplinary topic and the freedom to find my own way through the thesis. His patience, persistence and support enabled me to realize this thesis.

I am deeply grateful for gaining a second supervisor, P.D. Dr. Kirsten Peters, during my thesis. She adopted me straight away into her lovely group in Rostock and taught me to be patient with my stem cell experiments. Kirsten, thank you for the interesting discussions, encouragement, sound advice and good company.

Very special thanks to my co-referee, Prof. Uwe Pieleles, who motivated me to accept the challenge of a doctoral thesis. He fostered and accompanied me since my diploma thesis at FH and I admire his never-ending support and encouragement in so many ways during all these years.

I am especially indebted to Prof. Jens Gobrecht and Dr. Helmut Schiff, who gave me the opportunity to be a part of the marvelous LMN group at PSI.

I am very thankful to Dr. Prabitha Urwyler, my DICANS colleague, for interesting discussions, good collaboration and very kind support, especially during the last phase of my thesis. Thank you for sharing your Indian mentality.

I am most grateful to Dr. Celestino Padeste for all his contributions, great support and advice. I truly thank you for always having time and an ear for me and being my anchor at PSI. I hope that you accompany many more PhD students.

Special thanks go to Dr. Jochen Köser for sharing his knowledge and for interesting and fruitful discussions throughout my thesis.

My deepest gratitude goes to Achim Salamon and Stefanie Adam, who have contributed immensely to my personal and professional time in Rostock. The “Nachwuchsgruppe” has been a source of friendship as well as good advice and collaboration. Steffi, thank you for handling the massive amount of experiments with me, I will always remember our microscope-sessions.

I extend my gratitude to Hans Deyhle, Prof. Magnus Kristiansen and Dr. Oliver Bunk, who supported me discovering the world of small and wide-angle x-ray scattering. Thank you for the interesting discussions and insights. Hans, I truly appreciate your immense patience.

It is my great pleasure to thank all the members of the Nanotechnology group at FHNW for great support and for providing a stimulating and jovial environment. Special thanks go to Theodor Bühler for his great technical support and ideas. Furthermore, I would like to thank Prof. Patrick Shahgaldian for stimulating discussions and advice. Many thanks to our girls jogging group, Sabrina Küpfer, Lucy Kind and Annemarie Schönfeld, for keeping me fit and cheering me up! I look forward to our first half-marathon.

Furthermore, I would like to thank the members of the cell biology department at the University of Rostock for hosting me in a friendly and supportive environment. I especially thank Prof. Joachim Richly for supporting the Cotutelle de thèse.

I would also like to show my deep gratitude to the LMN members at PSI. Amongst others, Konrad Vogelsang, Mirco Altana, Stefan Stutz and Dr. Vitaly Guzenko greatly supported me with technical and scientific knowledge during my thesis.

In addition, I want to thank the members of BMC at University of Basel for their kind support. Hans Deyhle, Georg Schulz, Dr. Simone Hieber, Therese Bormann, Maggie Holme and Florian Weiss, it was nice to have you around especially while writing up.

The funding sources of the Swiss Nanoscience Institute (project 6.2), the Rectors' Conference of the Swiss Universities (CRUS) and the Federal State of Mecklenburg-Vorpommern are gratefully acknowledged.

Moreover, I would like to express my gratitude to Prof. Dieter Scharnweber and Anja Caspari who enabled me to perform Zeta-Potential measurements in Dresden. Special thanks go to Dr. Roman Heuberger for introducing me into the complexity of XPS measurements.

I deeply acknowledge my friends who helped me to keep my balance during the last years. Claude and Fabian, spending time with you on holiday or having cooking sessions sharing a glass of wine is the best battery reload I can think of. My-Hanh, Silke, Ronja, Maria, Arina, Selina and Marianne, thank you for so many years of true friendship. Thank you for bearing me with bad moods, listening to me, for endless discussions and also for honest criticism. I share tears of pain and joy with you and I hope we always support each other through life.

I wish to thank my family for all their support, for providing a loving environment to me, and for being a safe harbor in difficult times. Oma and Opa, thank you for being there, keeping the family together. Dropping in for a coffee in your kitchen means home to me. Onkel Harald, thank you for your humor, I know, I got all my skills from you ;-) Rita, thank you for being a friend, I am glad to have you in my life. Mami, I deeply thank you for all your never ending support and giving me the freedom I need. I love you all.

Marcus, dir gilt min letschte und allergröschte Dank. Ohni dini Unterstützig während dere mängmol harte Zit wär die Arbet eso nid möglich gsii. Du hesch mi nid nur mental begleitet, ushalte und ufbaut, au im Labor hämmer einigi Stunde zäme krampft. Du hesch mich immer ermunteret, aatribe und a mich glaubt. Dini Fürsorg isch unglaublich. Das bechunnsch zrug, versproche! Du hesch Rueh und Glück i mis Läbe brocht und für das bin ich dir us tiefschtem Härze dankbar. Ich lieb dich.

INTRODUCTION

Polyetheretherketone (PEEK) is a high-performance, thermoplastic polymer mainly used in aerospace engineering and for biomedical applications. It consists of an aromatic backbone chain interconnected by ketone and ether functional groups (Fig 1 A). Owing to its chemical structure, PEEK is inert versus a wide variety of solvents and chemicals, which explains its biocompatibility. Compared to other polymer materials, PEEK possesses excellent mechanical properties. The glass transition temperature T_g is around 143 °C and the melting temperature T_m ranges from 330 °C to 350 °C. Amorphous PEEK is readily obtained by rapid quenching from the melt below T_g , whereas semi-crystalline PEEK forms by controlled crystallization from the melt or by annealing from the amorphous state. The crystalline content in PEEK varies from 0 to 40% depending on the thermal history of the manufacturing process and has an influence on the mechanical properties of the material [1]. Based on X-ray diffraction studies, the c long-axis of the orthorhombic unit cell of PEEK spans three aryl groups, with a center-to-center distance between aryl groups of 5 Å, corresponding to a long-axis length of 15 Å (Fig 1 B) [2].

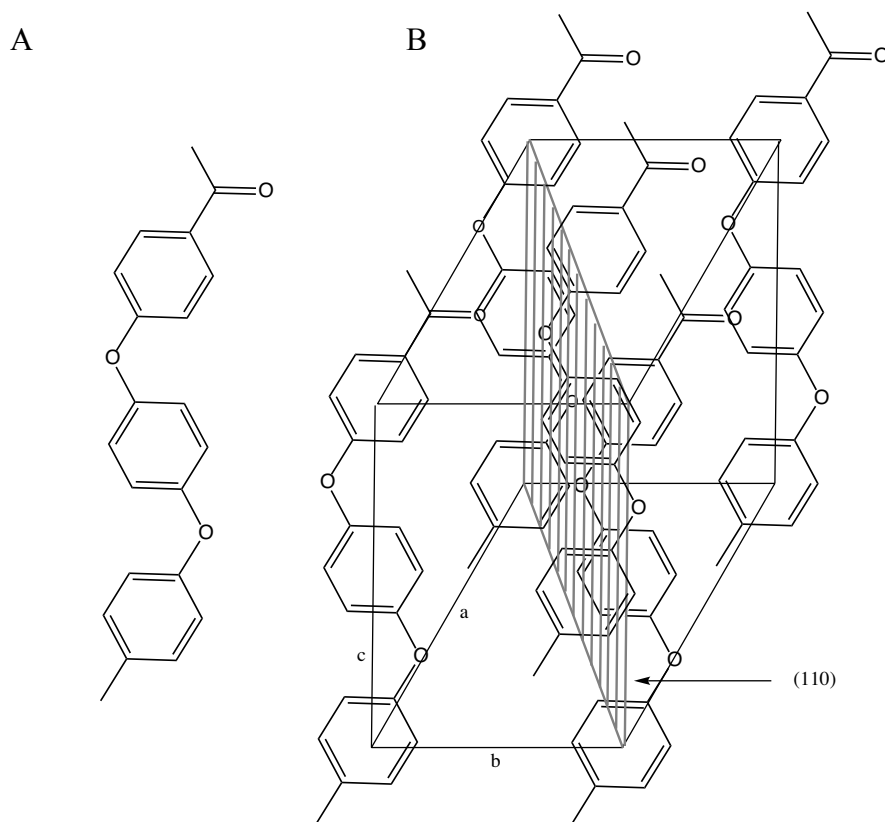


Fig. 1 Chain conformation of PEEK and orthorhombic crystal unit cell for PEEK. Adapted from [1].

PEEK as a biomaterial

PEEK is used since the 1980s as a biomaterial for spine, orthopedic and trauma applications. Also pacemaker housings are made of PEEK [5]. It has had the greatest clinical impact in the field of spine implant design and PEEK is now broadly accepted as a radiolucent alternative to metallic biomaterials in the spine community. For mature fields such as total joint replacement and fracture fixation implants, radiolucency is an attractive but not necessarily critical material feature [1]. Nonetheless, the interest in producing isoelastic load-bearing orthopedic PEEK implants with osseointegrative properties is ubiquitous [6]. The Young's modulus E of pure PEEK is between 3 and 4 GPa [7]. To improve the mechanical properties of PEEK implants, carbon fiber reinforcement is used to increase E to that of cortical bone (18 GPa) [8]. Due to its relative inertness, several attempts were made to activate PEEK implant surfaces. Coatings with Ti and hydroxyapatite [9, 10] as well as plasma deposition were shown to be compatible with PEEK [9, 11]. Processing without coating, i.e. wet chemical activation [12-14] and plasma treatments [4, 14, 15] were shown to be alternatives.

Versys Epoch Fullcoat is an isoelastic composite femoral implant produced by Zimmer since 2006. The core is made of CoCr, which is surrounded by PEEK. To achieve bone in-growth, the PEEK material is coated with Ti. The parent femoral implant, which consisted of PEKEKK (Polyetherketoneetherketoneketone) instead of PEEK, achieved convincing results in an extensive clinical study regarding bone-ingrowth and reduced bone loss [16]. Also bioactive PEEK composites using beta-tricalcium phosphate [17] or hydroxyapatite (HA) [18] showed promising *in vitro* data, however, the load-bearing capacity was reduced in such composite materials, especially with HA contents of 40% [19-21]. Therefore, rendering the PEEK surface itself bioavailable is a promising method, since the bulk properties of the PEEK material remain unaffected.

Anisotropy of biomaterials

Anisotropy plays a major role in the body since almost all tissues exhibit preferential orientations of macroscopic, microscopic and nanoscopic features. For instance, trabecular bone is organized in trabeculae oriented according to the direction of the physiological load. Therefore, anisotropic materials might improve implant performance, mimicking the structures naturally appearing in the body.

Auto-fluorescence of PEEK

To study the cell-biomaterial interactions including cell morphology, fluorescence microscopy and confocal laser scanning microscopy (CLSM) are widely used. In case of PEEK substrates, the application of fluorescence microscopy is critical because of the strong auto-fluorescence of the polymeric material which is only scarcely described in literature. Hunter and colleagues [3], who investigated the attachment and proliferation of osteoblasts and fibroblasts on biomaterials for orthopedic use, explicitly excluded PEEK from the immuno-fluorescence study due to the prominent auto-fluorescence of the material. To overcome the problem, Briem et al. [4] replaced the immuno-fluorescence stains by Giemsa stains to investigate the response of primary fibroblasts and osteoblasts to plasma-treated PEEK. In order to address the problem of the auto-fluorescence, we have carefully analyzed the auto-fluorescence of commercially available PEEK films (APTIV™ Series from Victrex) to explore the possible origin of the strong background fluorescence, which could arise from fluorescent additives.

Activation of PEEK with plasma treatment

Plasma treatment is a common method to activate low energy polymeric surfaces. We applied oxygen and ammonia plasma on PEEK substrates and investigated the effect of this treatment on the PEEK material itself and on human mesenchymal stem cell differentiation *in vitro*. Plasma treatments generate functional groups at the surface of polymers, which increase the surface energy (hydrophilicity) and modify the surface topography [22]. It was shown that plasma treatment generates nanostructures on polymer surfaces such as PDMS (polydimethylsiloxane) [23], PMMA (polymethyl methacrylate) and PEEK [24].

Biomaterial – cell interface

The interaction of cells and tissues with implant materials is affected by the surface chemistry [26, 31], stiffness [27] and topography on the micrometer [36] and nanometer [34, 35] scale. As the properties of the biomaterial surface conduct the protein adsorption, which mediates cell adhesion, it is necessary to characterize the implant surface thoroughly. The types and the amounts of proteins adsorbed determine the types and surface density of the bioactive sites that may be available for cell interactions [33]. It is well known that the surface properties of materials may affect healing processes by modulating cell proliferation and differentiation [32]. Therefore, investigators aim at correlating surface chemistry and structure to protein adsorption and cell adhesion. Recently, Dalby and colleagues [34] showed that patterns of nanostructures on polymeric substrates cause osteogenic differentiation of mesenchymal stem

cells. They have found that, in contrast to highly ordered nanostructures, randomly arranged nanostructures induce osteogenic differentiation.

Mesenchymal stem cells from adipose tissue

In order to study the response of cells to a biomaterial *in vitro*, primary cells taken from living tissue are preferred over continuous tumor or immortalized cell lines since they have undergone only very few population doublings and are more representative for the main functional component of the tissue they are derived from. Human mesenchymal stem cells (hMSCs) are multipotent adult stem cells and can differentiate into a variety of cell types including osteoblasts, chondrocytes, adipocytes and myocytes. Therefore, they are attractive to study bone regeneration *in vitro*. In 2001, Zuk et al. [37] found a cell population in lipoaspirates from human adipose tissue that were able to differentiate *in vitro* into osteogenic, chondrogenic, adipogenic and myogenic cells in the presence of lineage-specific induction factors. These cells were termed adipose tissue derived stem cells (ASC). Nowadays even a broader differentiation spectrum of ASC is demonstrated, in that also neurogenic [38], and hepatic-like [39] differentiation capacity is described. Due to their primarily mesenchymal differentiation potential, their frequent occurrence and the ease to harvest, they are a potential alternative to mesenchymal stem cells from bone marrow (MSC) for utilization in regenerative therapies such as bone regeneration [40, 41].

Thesis task

The aim of this thesis was to activate the surface of thin PEEK films improve cell adhesion and differentiation. Plasma treatments using different reactive gases should be applied to create high-energy surfaces. The chemical as well as the topographical changes resulting from the treatment has to be investigated with appropriate methods. Furthermore, the effect of the plasma treatment was studied on ASC adhesion, proliferation and differentiation.

MATERIALS AND METHODS

PEEK sheet pretreatment

Commercially available amorphous and semi-crystalline PEEK films (APTIV™ 2000 and 1000 series, respectively, Victrex Europa GmbH, Hofheim, Germany) of 12, 25 and 50 μm were subjected to annealing under pressure. Also microstructuring of the PEEK films by hot embossing was performed. For details please refer to the materials and methods in chapter 4 (annealing) and chapter 6 (embossing).

Optical measurements and x-ray scattering

In order to investigate the anisotropy occurring in the thin PEEK films, optical measurements and x-ray scattering were performed. Transmission and absorbance spectra of the PEEK films were recorded with a UV/VIS/NIR spectrometer (Lambda 19, Perkin Elmer, Überlingen, Germany). For optical anisotropy measurements, PEEK films were mounted on a rotation table. The small- and wide-angle X-ray scattering (SAXS/WAXS) data were recorded at the cSAXS beamline of the Swiss Light Source (Paul Scherrer Institut, Villigen, Switzerland) using a 2D scanning setup [42]. For details please refer to the materials and methods in chapter 4.

Transmission and fluorescence scans of PEEK

The auto-fluorescence was studied using transmission and fluorescence scans. PEEK was synthesized according to Risse et al. [44]. The transmission measurements were recorded for wavelengths ranging from 240 nm to 1000 nm. The fluorescence experiments were performed with a TECAN micro-plate reader infinite 200, equipped with a UV Xenon flash lamp (TECAN trading AG, Switzerland). The excitation wavelengths were varied between 350 nm to 800 nm in steps of 10 nm. The corresponding emission was acquired 30 nm above excitation wavelengths to 850 nm in 5 nm steps. For details please refer to the materials and methods in chapter 5.

Plasma treatment

To activate the surface, oxygen/argon or ammonia plasma treatments (Piccolo system, Plasma Electronic, Neuenburg, Germany) were applied on the annealed or embossed PEEK films. The plasma treatments using a power of 10 W to 200 W always lasted 5 min at a gas flow of 20/10 sscm oxygen/argon or 30 sscm ammonia. For details please refer to the materials and

methods in chapter 5. In addition, other polymer materials were oxygen plasma treated (materials and methods chapter 6).

Atomic force microscopy (AFM) and scanning electron microscopy (SEM)

The nanostructuring caused by the plasma treatment was visualized and quantified by AFM and SEM. AFM measurements were performed in TappingMode[®] in air under dry conditions. From these images, the RMS roughness and the island density were derived. For rapid investigation of the nanostructures, the PEEK substrates were Pd/Au coated and investigated with the field emission scanning electron microscope Supra 40 VP (Carl Zeiss, Jena, Germany) with an electron energy of 10 keV using the InLens detector. For details please refer to the materials and methods in chapter 5 (AFM) and chapter 6 (SEM).

Zeta-potential, x-ray photon spectroscopy (XPS) and contact angle measurements

Investigation of the chemical effects of the plasma treated PEEK surfaces was done by means of zeta-potential measurements to determine the electrochemical charging state, XPS to gain information about the chemical composition of the surfaces and contact angle measurements to measure the wettability of the plasma treated PEEK surfaces.

All streaming potential measurements to determine the zeta potential values were performed with the Electrokinetic Analyzer (Anton Paar KG, Graz, Austria) and the measuring cell for flat plates as described previously [5]. XPS studies were carried out by means of an Axis Nova photoelectron spectrometer (Kratos Analytical, Manchester, England). The spectrometer was equipped with a monochromatic Al K α ($h\nu = 1486.6$ eV) X-ray source. Quantitative elemental compositions were determined from peak areas. The wettability of the plasma-treated PEEK films and controls was determined with double distilled water (ddH₂O) by the sessile drop contact angle method using a contact angle goniometer (Drop Shape Analysis System PSA 10Mk2, Krüss, Hamburg, Germany). For details please refer to the materials and methods in chapter 6 (zeta-potential and XPS) and chapter 7 (contact angle).

Protein adsorption

The adsorbed bovine serum albumin (BSA) or fetal calf serum (FCS) protein amount on the plasma treated PEEK substrates was quantified via the colorimetric microBCA assay. The protein concentration of the supernatant was determined via the optical density at 562 nm. For details please refer to the materials and methods in chapter 7.

Cell culture

Cell culture experiments were performed with Rat-2-fibroblasts and human ASC. Rat-2 fibroblasts were cultured in DMEM medium under standard conditions (5% CO₂, 37 °C). ASC isolation was performed as described previously [40]. ASC isolations were conducted with the approval of the ethics committee (Medical Faculty, University of Rostock) and the full consent of the patients.

In the fourth passage seeding of ASC into experimentation was done at 20,000 cells per cm². After seeding, ASC were cultured until confluence was reached (2-3 days) and then stimulated to differentiate using osteogenic differentiation stimulating medium (OS: basal medium plus 0.25 g/l asorbic acid, 1 μM dexamethasone and 10 mM beta-glycerophosphate) or adipogenic differentiation stimulating medium (AS: basal medium plus 1 μM dexamethasone, 500 μM IBMX, 500 μM indomethacin, 10 μM insulin). US indicates the basal medium not containing any specific differentiation factors and used for the non-stimulated ASC control cultures. For details please refer to the materials and methods in chapter 3 (Rat-2) and chapter 5 (ASC). The plasma treated PEEK films were punched out to fit into a 96 well format, sterilized with 70% ethanol (LiChrosolv, MERCK, Darmstadt, Germany) washed two times with Dulbecco's PBS (without Ca²⁺ and Mg²⁺, sterile; PAA Laboratories GmbH, Cölbe, Germany), and incubated with medium for 2 h before ASC seeding. For details please refer to the materials and methods in chapter 7.

Fluorescence cell staining

Rat-2 cells were stained for focal adhesions and the actin cytoskeleton. The cells were washed, fixed, permeabilized and stained with mouse anti-human vinculin/ goat anti-mouse Alexa 488 antibodies (Sigma-Aldrich) and TRITC-conjugated phalloidin (Sigma-Aldrich). The cells were visualized on a BX-51 fluorescence microscope equipped with a fluorescence unit, and a Fluo-View 1000 confocal laser scanning microscope, both Olympus (Hamburg, Germany). For details please refer to the materials and methods in chapter 5.

ASC live cell staining

Visualization of living cells was done by fluorescence staining with calcein AM. Cells were incubated in basal medium containing calcein AM (Biomol GmbH, Hamburg, Germany) at 1 μM and incubated for 15 min. Then, this staining solution was exchanged by basal medium and cells were then examined under the microscope in standard filter-based fluorescence microscopy (Axio Scope.A1 with AxioCam MRc, both Carl Zeiss MicroImaging GmbH, Göttingen, Germany). For details please refer to the materials and methods in chapter 7.

ASC cell number quantification

Quantification of ASC number at the distinct experimental conditions was done indirectly using the basic dye crystal violet. Due to its positive charge, crystal violet binds negatively charged cellular macromolecules, most of which being DNA, via ionic attraction [51]. Due to a linear correlation, cell numbers can indirectly be determined quantifying the optical density of the re-solubilized dye at 600 nm [52]. For details please refer to the materials and methods in chapter 7.

Analysis of osteogenic differentiation of ASC in vitro

Osteogenic differentiation of ASC on plasma treated PEEK substrates was monitored by alkaline phosphatase activity (day 14, 21 and 28) and *in vitro* mineralization (day 28).

Alkaline phosphatase (ALPL) activity was quantified by the conversion of the synthetic substrate para-nitrophenyl phosphate (pNPP) into the colored product paranitrophenol [53]. Extracellular matrix calcium content was quantified optically using cresolphthalein. In a complexation mechanism, ortho-cresolphthalein complexon in solution binds divalent cations (i.e. mainly calcium and magnesium) and thereby develops a violet color whose intensity is proportional to the concentration of the ions present. The procedure used was adapted from Proudfoot et al. [54]. For details please refer to the materials and methods in chapter 7.

Analysis of adipogenic differentiation of ASC in vitro

Adipogenic differentiation of ASC on plasma treated PEEK substrates was monitored by the cellular lipid content using an unmodified lipophilic boron dipyrromethene (Bodipy) dye which dissolves well in cellular neutral lipids. For details please refer to the materials and methods in chapter 7.

ASC data normalization and illustration

To facilitate statistical analysis of the metrical data obtained, data were normalized. The position of a distinct value x obtained for this parameter and individual with respect to the extremes x_{\min} and x_{\max} was then represented as $x_{\text{norm}} = (x - x_{\min}) / (x_{\max} - x_{\min})$. This operation scales the values for each individual and parameter to a range from zero to one. Data are habitually presented as box plots. The solid box represents 50% of the measured values that assemble around the median indicated by a horizontal line. The box ranges from the 25th to the 75th percentile. Error bars starting below and above the box indicate the 5th and 95th percentile. For details please refer to the materials and methods in chapter 7.

THESIS CONTRIBUTIONS (RESULTS AND DISCUSSION)

First of all, I like to emphasize the “Cotutelle de thèse” between the medical faculties of the universities in Basel and Rostock. Highly interested in primary cell culture, I had the opportunity to visit the group of K. Peters at the University of Rostock (Department of Cell Biology), who works with adipose tissue derived mesenchymal stem cells (ASC). Promising initial cell experiments on plasma-treated PEEK substrates resulted in an application for a “Cotutelle de thèse” at the Rectors’ Conference of the Swiss Universities, which was accepted and included a travel grant to finance my working stays in Rostock. In total, I spent five months working in the lab of K. Peters during the last one and half years of my thesis. I met with a very kind reception and had great support from the team leader and the group members, especially from A. Salamon and S. Adam, who helped me to manage the massive amount of experiments.

The summarized chapters in this section correspond to the following publications:

Chapter 4 J. Althaus, H. Deyhle, O. Bunk, P.M. Kristiansen, B. Müller. Anisotropy in polyetheretherketone films. *Journal of Nanophotonics* 6 (2012) 063510.

Chapter 5 J. Althaus, C. Padeste, J. Köser, U. Pieves, K. Peters, B. Müller. Nanostructuring polyetheretherketone for medical implants. *European Journal of Nanomedicine* 4 (1) (2012) 7-15.

Chapter 6 J. Althaus, P. Urwyler, C. Padeste, R. Heuberger, H. Deyhle, H. Schiff, J. Gobrecht, U. Pieves, D. Scharnweber, K. Peters, B. Müller Micro- and nanostructured polymer substrates for biomedical applications. *Proc. SPIE* 8339 (2012) 83390Q.

Chapter 7 J. Waser-Althaus, A. Salamon, M. Waser, C. Padeste, M. Kreutzer, U. Pieves, B. Müller, K. Peters. Differentiation of human mesenchymal stem cells on plasma-treated polyetheretherketone. *Journal of Materials Science: Materials in Medicine* 25 (2014) 515-525.

Chapter 4 of my thesis describes the anisotropy of glass casted thin PEEK films by optical and X-ray methods. I selected commercially available APTIV™ PEEK films with micrometer thickness for my work due to several reasons: the commercial product underlies a specified production process, and is available in amorphous (2000 series) and semi-crystalline (1000 series) films of different thicknesses. Furthermore, it is translucent which facilitates cell culture work regarding microscopy. Using optical measurements, I investigated amorphous and semi-crystalline PEEK films for their anisotropic behavior, which is characteristic for thin polymeric films. Linear anisotropy was discovered oriented in machine direction (MD) of the

processed films upon annealing. The anisotropy coefficient AC was in the range of 1.19 to 1.27, indicating a fairly weak anisotropy. Selected films were investigated by small-angle and wide-angle X-ray scattering (SAXS and WAXS) to understand the origin of the anisotropy. In SAXS measurements, we found an anisotropic long-range order oriented in MD with a periodicity of 14.6 nm, which corresponds to the amorphous/crystalline long period (δ) of the lamellar stacks and is bulk thickness dependent. According to WAXS measurements, the long period is oriented in the *c*-axis direction, parallel to the machine direction. Discussing and understanding the obtained data with H. Deyhle, B. Müller and M. Kristiansen, I learned a lot about the complexity of polymer crystallography. I was able to derive the intermolecular binding energies in PEEK from optical transmission of annealed PEEK films. This Arrhenius behavior might be found for other materials as well.

In Chapter 5, the nano-structuring effect of plasma treatment on PEEK films is described. Furthermore, the auto-fluorescence of PEEK was investigated in detail. To activate the hydrophobic PEEK surfaces for cell adhesion studies, I chose the plasma technology available at University of Applied Sciences and Arts (FH NW) because it is a fast, dry and reproducible method for polymer surface activation. The used plasma oven from Plasma Electronics, made for industrial applications, enabled large surface treatment and the choice of a variety of process gases. Oxygen and ammonia as process gasses were selected because they were successfully used to activate polymer surfaces according to literature. Oxygen plasma induces negatively charged functional groups whereas ammonia plasma induces positively charged functional groups on the surface. Therefore, I decided to work with both reaction gases to investigate the opposing chemical effects on the PEEK substrates and also on stem cell behavior. Applying different oxygen plasma powers under the same conditions, homogenous nano-structuring on the PEEK surface was discovered, which increased in roughness with increasing plasma power. Ammonia plasma had the same effect, but was weaker than oxygen plasma using identical power and exposure time (Fig 2).

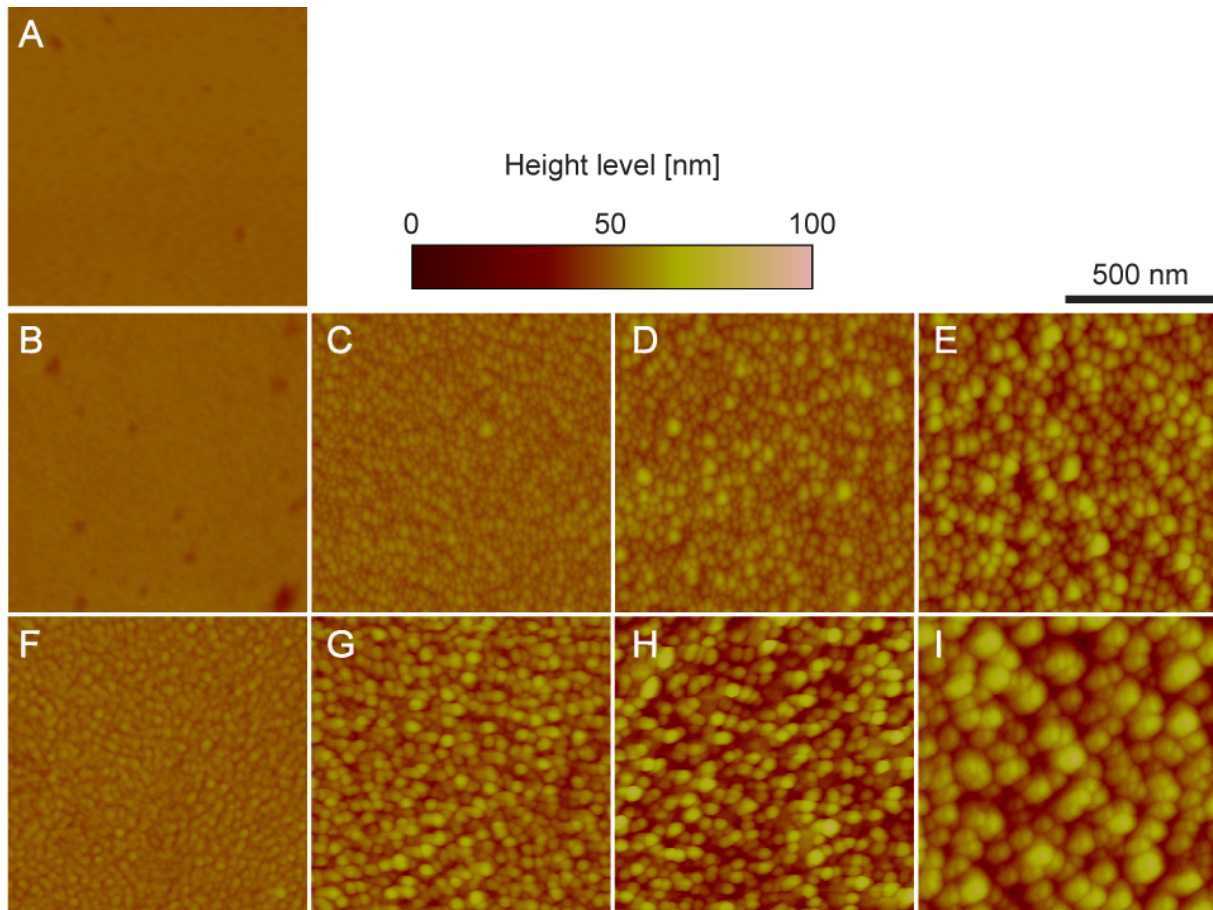


Fig. 2. AFM images of plasma-treated PEEK films. The 25 μm -thick films were plasma-treated for 5 min. A: untreated, B-E: ammonia-plasma-treated, plasma power from left to right: 10 W, 50 W 100 W and 200 W. F-I: oxygen-plasma-treated, plasma power from left to right: 10 W, 50 W 100 W and 200 W.

Correlating the induced nano-structuring with plasma powers, a linear relationship between plasma power and roughness as well as island density was found. This simple method allows us to tailor the size of homogenous pillar-like nanostructures on large PEEK surfaces varying reaction gas, plasma power and reaction time. With time and intensity dependent experiments, I showed that the nano-structuring is induced by a pure etching effect. Initial cell seeding experiments revealed that mild oxygen plasma treatment is necessary to achieve homogenous and reproducible ASC adhesion. Harsh oxygen plasma treatment resulted in reduced cell attachment.

Performing fluorescence based actin and vinculin stainings, I discovered a strong fluorescence background from the PEEK films that made the use of conventional, filter-based microscopy impossible. The use of confocal microscopy enabled the visualization of the cytoskeleton and the focal adhesions of Rat-2 fibroblasts (Fig 3).

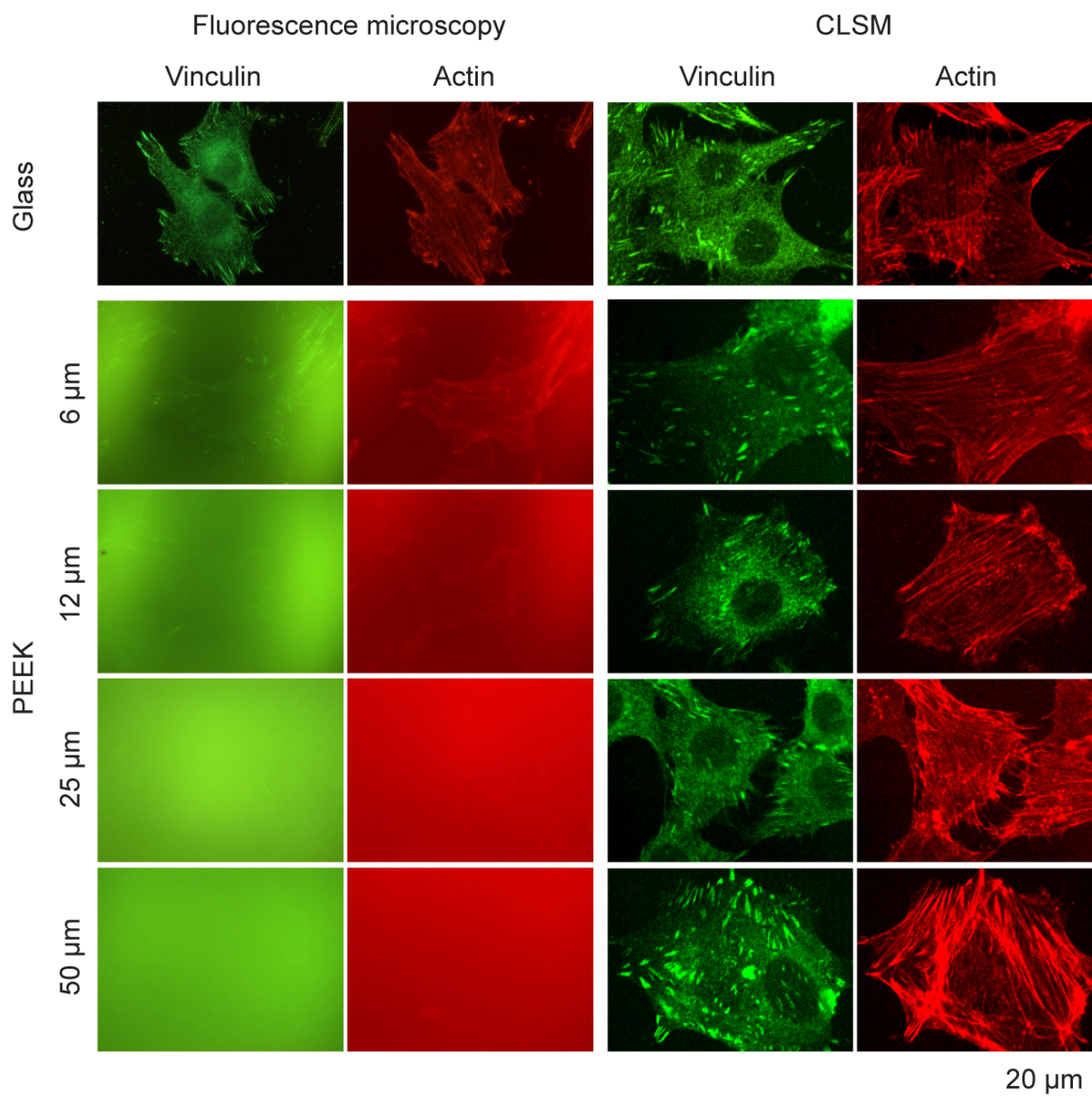


Fig. 3. Rat-2 fibroblasts seeded on glass and differently thick APTIVTM PEEK films. Actin stain: phalloidin-TRITC, vinculin stain: monoclonal anti-vinculin and goat-anti-mouse A-488.

Nevertheless, the non-confocal localization of the cells remained challenging. As the autofluorescence of PEEK was only vaguely described in literature, I investigated this phenomenon in more detail. Fluorescence scans revealed a broadband fluorescent behavior for excitation wavelengths from 350 to 550 nm. The synthesis of pure PEEK (by M. Waser, according to ref. [44]) enabled me to prove that the fluorescent behavior originates from the molecular structure of PEEK and not from any additives used in the manufacturing process.

Chapter 6 deals with the manufacturing of micro- and nanostructured polymer surfaces for cantilever-based cell force measurements. Next to PEEK, also other polymer materials such as injection molded cantilevers (P. Urwyler) or other films were plasma treated and investigated for the resulting nano-structuring. Oxygen plasma treatment revealed material

specific nano-structuring. Interestingly, injection molded polymer samples showed clear anisotropic nano-structuring. After investigating the cantilevers and fleshes of the cantilevers, we hypothesize that the plasma etching reveals the polymer chain orientation, but this suggestion has to be confirmed with dedicated experiments. Further characterization of the plasma treated PEEK substrates by zeta-potential and XPS measurements was performed. As only few groups are capable of measuring surface charges of films I carried out these experiments at the Leibnitz Institute for Polymer Research in Dresden through the help of D. Scharnweber. The pH-dependent streaming measurements required a lot of handling knowledge. During my one-week stay in Dresden, A. Caspari kindly introduced me to the experimental setup, enabling me to perform self-contained measurements. XPS measurements and data analysis were performed at the RMS foundation. I was able to attend the measurements and gain basic knowledge about the experimental setup and data analysis. Zeta-potential and XPS revealed that ammonia plasma treatment induced positively charged amine groups at the surface, whereas oxygen plasma induced negatively charged carboxylic or ester groups. Initial short-term experiments included human dermal microvascular endothelial cells (HDMEC) and adipose tissue derived stem cells (ASC). Both primary cell types did not homogeneously adhere on original PEEK films. Upon ammonia plasma treatment at different intensities, HDMEC and ASC adhered, spread and proliferated similar to the polystyrene control. Micro-grooved PEEK films for cell adhesion studies were realized by hot embossing. Micro-patterns from a 4-inch silicon master were transferred into the thin PEEK films using a hot press in a clean room at PSI. ASC clearly aligned along the 1 μm deep and 20 μm wide grooves, and pretreatment of the PEEK films by plasma treatment and/or a thin 5 nm titanium coating allowed homogeneous cell attachment and proliferation. It is known that the cell shape has an influence on the differentiation of human mesenchymal stem cells involving the rearrangement of the actin cytoskeleton of the cell. Therefore, cantilever based cell force measurements of such phenotypically changed ASC might be of great value.

Human mesenchymal stem cell differentiation on the plasma-activated PEEK substrates was studied in chapter 7. The substrates were additionally characterized by means of static water contact angle and protein adsorption. The original PEEK film revealed a contact angle of more than 80°. Increasing oxygen plasma power resulted in reduction of contact angles, i.e. between 40° for 10 W and below 5° for 200 W. In contrast, ammonia plasma treatment also resulted in a decrease, but a plasma power dependent increase of contact angles, i.e. between 45° for 10 W and 90° for 200 W. For the protein adsorption, I adapted the commercially available microBCA assay so that the protein density could be determined directly adsorbed

to the PEEK substrates. In all cases, the amount of adsorbed protein gained with increasing plasma power. Whereas the BSA density on oxygen and ammonia plasma-treated films as well as FCS on ammonia plasma-treated PEEK was doubled with respect to the original films for powers of 200 W, FCS density on oxygen plasma-treated films raised by a factor of six.

Extensive differentiation experiments on plasma treated PEEK substrates were performed with ASC quantifying cell number, metabolic activity, alkaline phosphatase activity, *in vitro* mineralization and cellular lipid staining under unstimulated, osteogenic stimulation conditions and adipogenic stimulation conditions at different time points from 14 to 28 days. Fluorescent vital stains at all time points were recorded as a control. Osteogenic differentiation was investigated analyzing the ALPL activity (day 14, 21 and 28) and the mineralization degree (day 28) (Fig 4). We observed a plasma power dependent regulation of ALPL activity and mineralization, being increased on 10 W and 50 W plasma-treated PEEK substrates compared to polystyrene control, the original PEEK substrate and the US controls, but decreased for higher plasma powers. This phenomenon was observed for both reaction gases, while oxygen plasma showed a stronger impact. Furthermore, the adipogenic differentiation potential of ASC on plasma-treated PEEK substrates was investigated. Cellular lipid accumulation was analyzed at day 14 and day 21 under AS and US conditions. Quantification of cellular lipid content revealed a slight and homogenous increase on ammonia plasma-treated PEEK between 10 and 100 W, whereas the lipid content was reduced on 200 W ammonia plasma-treated PEEK. The lipid accumulation on oxygen plasma-treated PEEK substrates was generally low compared to original and ammonia plasma-treated PEEK.

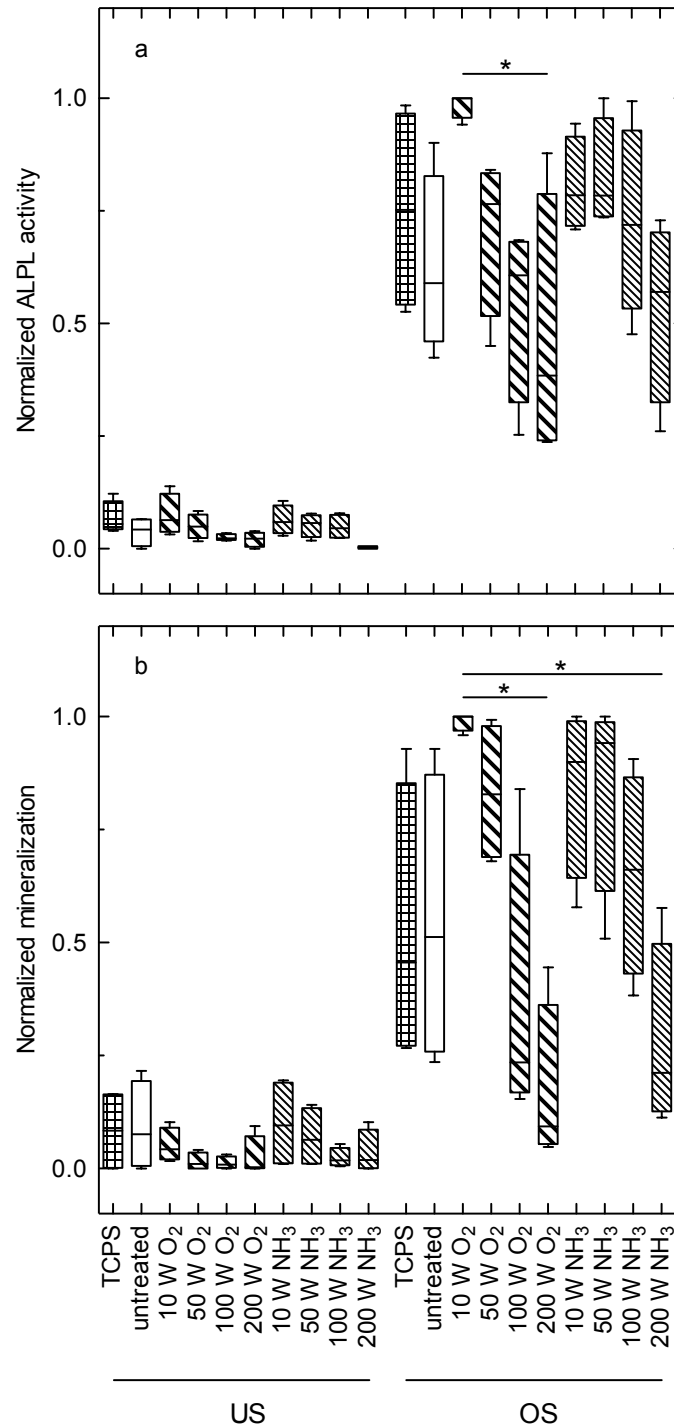


Fig. 4. Osteogenic differentiation of ASC on tissue culture polystyrene TCPS, original, oxygen and ammonia plasma-treated PEEK substrates. a) ALPL activity at day 14 of culture under US and OS conditions. b) In vitro mineralization at day 28 under US and OS conditions. Data were normalized to values between 0 and 1, $n = 4$.

Although the ammonia and oxygen plasma-treated PEEK films significantly differ with respect to surface chemistry and roughness, ASC adhesion, proliferation and differentiation were largely similar. This raises the question whether surface nanostructure or surface chemistry dominates the observed ASC differentiation. The nanostructure may be of

secondary importance, as the nanostructures on oxygen and ammonia plasma-treated substrates significantly differ in height and density and there is no direct correlation with the protein adsorption. The chemical modification of the PEEK surfaces through the oxygen and ammonia plasma treatments, reproduced by the XPS and contact angle measurements, is complex. The electrochemical properties showed reaction gas, but not plasma power dependent effects. Therefore, we have to conclude that both surface chemistry and nanostructuring lead to the positive effect on ASC differentiation. 10 W and 50 W oxygen and ammonia plasma-treated PEEK proved to be suitable substrates to promote osteogenic differentiation *in vitro*.

Parallel to the ASC differentiation experiments on the nanostructured plasma treated PEEK substrates, the same experiments were performed on micro-grooved PEEK substrates in the frame of a bachelor thesis under my supervision. This project will continue with further bachelor students from FHNW. I was allowed to design a silicon master dedicated for these cell culture experiments with 4 large micro-grooved areas that was produced at PSI.

Journal of Nanophotonics

SPIDigitalLibrary.org/jnp

Anisotropy in polyetheretherketone films

Jasmin Althaus
Hans Deyhle
Oliver Bunk
Per Magnus Kristiansen
Bert Müller

Anisotropy in polyetheretherketone films

Jasmin Althaus,^a Hans Deyhle,^{a,b} Oliver Bunk,^b Per Magnus Kristiansen,^c
and Bert Müller^a

^aUniversity of Basel, Biomaterials Science Center, c/o University Hospital Basel,
4031 Basel, Switzerland
bert.mueller@unibas.ch

^bPaul Scherrer Institute, Swiss Light Source, 5232 Villigen, Switzerland

^cUniversity of Applied Sciences and Arts Northwestern Switzerland, Institutes of Polymer
Engineering & Polymer Nanotechnology, 5210 Windisch, Switzerland

Abstract. Optical measurements reveal the preferential orientation of nanostructures within polymer films, which results from the fabrication process including mechanical and thermal treatments. As the wavelength of the incident light is generally much larger than the characteristic dimensions of the molecular arrangement in semi-crystalline or amorphous polymers, the optical signal originates not directly from the nanostructure of the polymers. Linear dichroism measurements were correlated with synchrotron radiation-based x-ray scattering data on commercially available polyetheretherketone (PEEK) thin films (12 to 50 μm). Annealing changed the structure of amorphous films to semi-crystalline ones associated with the measured linear dichroism. The intensity of the measured anisotropic signal depended on the film thickness. While for wavelengths between 450 and 1100 nm the transmission was higher when the polarizer was parallel to the machine direction, for larger wavelengths maximum transmission was observed with the polarizer perpendicular to the machine direction indicating excitations parallel and perpendicular to the PEEK molecule axis, respectively. Annealing PEEK films at temperatures between 160 and 240°C decreased the transmission at 540 nm by a factor of two, whereas the anisotropy remained constant. x-ray scattering revealed strongest anisotropy for a periodicity of 15 nm in the machine direction of the cast film extrusion process. The long-range order of amorphous and semi-crystalline entities can explain the x-ray scattering data and the related optical anisotropy of casted PEEK films. © 2012 Society of Photo-Optical Instrumentation Engineers (SPIE). [DOI: [10.1117/1.JNP.6.063510](https://doi.org/10.1117/1.JNP.6.063510)]

Keywords: anisotropy; polyetheretherketone; x-ray scattering; synchrotron radiation; long-range order.

Paper 12014 received Feb. 16, 2012; revised manuscript received Mar. 29, 2012; accepted for publication Apr. 2, 2012; published online Jul. 2, 2012.

1 Introduction

As a result of the fabrication process, polymer films often exhibit an optical anisotropy.¹⁻⁵ This anisotropy can simply be quantified from transmission measurements of the film between crossed polarizers at wavelengths from ultraviolet to infrared.^{1,6} Usually, these wavelengths from 200 to 2,500 nm are much larger than the structures within the nano-crystalline or even amorphous polymers and the origin of the detected optical anisotropy cannot be resolved.

Polyetheretherketone (PEEK) is a high-performance, thermoplastic polymer used in a number of applications including medical implants.⁷ Due to its structure and related inertness, PEEK is biocompatible and used, e.g., for pacemaker housings⁸ and load-bearing spine implants.⁷ Very recently, it has been demonstrated that dedicated plasma treatments of PEEK films result in nanostructures on the surface with feature sizes depending on the choice of process gas, applied power and treatment duration.⁹ By tailoring the nanostructure of implant surfaces, tissue integration might be accomplished, which broadens the fields of application for PEEK. As human tissues usually exhibit an anisotropic nanostructure,¹⁰ PEEK implants should preferably also

display anisotropy at these length scales. Appropriate methods to characterize the oriented structure and anisotropy properties of PEEK are necessary.

In this article we demonstrate that micrometer-thin, commercially available PEEK films show an optical anisotropy, represented by the linear dichroism, which relates to nanostructures revealed by means of x-ray scattering. The combination of small- and wide-angle x-ray scattering should permit the development of a structural model for PEEK that also explains the mechanically and thermally induced transitions from amorphous to (partially) crystalline states in PEEK films. In order to differentiate between surface and bulk phenomena, specimens of different thickness were incorporated in the study.

2 Materials and Methods

2.1 Materials and Preparation

Commercially available amorphous and semi-crystalline PEEK films (APTIV™ 2000 and 1000 series, respectively, Victrex Europa GmbH, Hofheim, Germany) of 12, 25, and 50 μm thickness were marked to identify machine and transverse directions with respect to the extrusion process. They were subjected to annealing under pressure. For this purpose, the films were placed between two polished, 500 μm thick, 4-inch Si(100) wafers (Si-Mat, Kaufenring, Germany) in a precision hot press (HEX03, JENOPTIK Mikrotechnik GmbH, Jena, Germany) at temperatures between 160 and 240°C with a pressure of 12.3 MPa for a period of 10 min and subsequently cooled down with an average rate of 0.26 K/min.

2.2 Optical Measurements

Transmission spectra of the PEEK films were recorded with a spectrometer (Lambda 19, Perkin Elmer, Überlingen, Germany) covering the wavelength range between 200 and 2,500 nm. The system was equipped with a rotatable polarizer (analyzer). For optical anisotropy measurements, PEEK films were mounted on a rotation table, and rotated in steps of 10 degrees. The angle of zero degree corresponded to the machine direction. The 0.7 mm-thick polarizer film HN 32 (SreenLab, Elmshorn, Germany) was made of polyvinyl alcohol.

2.3 x-Ray Scattering

The small- and wide-angle x-ray scattering (SAXS/WAXS) data were recorded at the cSAXS beamline of the Swiss Light Source (Paul Scherrer Institut, Villigen, Switzerland) using a two-dimensional (2-D) scanning setup.¹¹ The measurements were performed at a photon energy of 8.7 keV, corresponding to a wavelength of $\lambda = 1.43 \text{ \AA}$. The films were mounted over apertures of an aluminum frame. This frame was moved by a translation stage in two orthogonal directions. Scattering patterns were recorded by a PILATUS 2M detector¹² with a pixel size of 172 μm . The exposure time was set to 0.5 s per frame. The data were averaged over 100 frames recorded in a line scan with a step size of 5 μm . The specimen-detector distance, which corresponded to 2.17 m, was calculated from the first scattering order of a silver behenate powder. WAXS measurements with 2 s exposure time per frame were performed at a photon energy of 11.2 keV ($\lambda = 1.11 \text{ \AA}$) and a detector distance of 0.578 m. Data evaluation was performed with dedicated self-written MATLAB® (2010b, TheMathWorks, Natick, USA) code.

3 Results

3.1 Optical Measurements

To characterize the potentially anisotropic structure of annealed micrometer-thin PEEK films, a transmission scan varying the wavelength from ultraviolet to infrared was performed. As shown in Fig. 1(b), the 50 μm -thin APTIV™ 2000 PEEK film annealed at 160°C, revealed differences in absorbance parallel and perpendicular to the machine direction. At wavelengths between 400

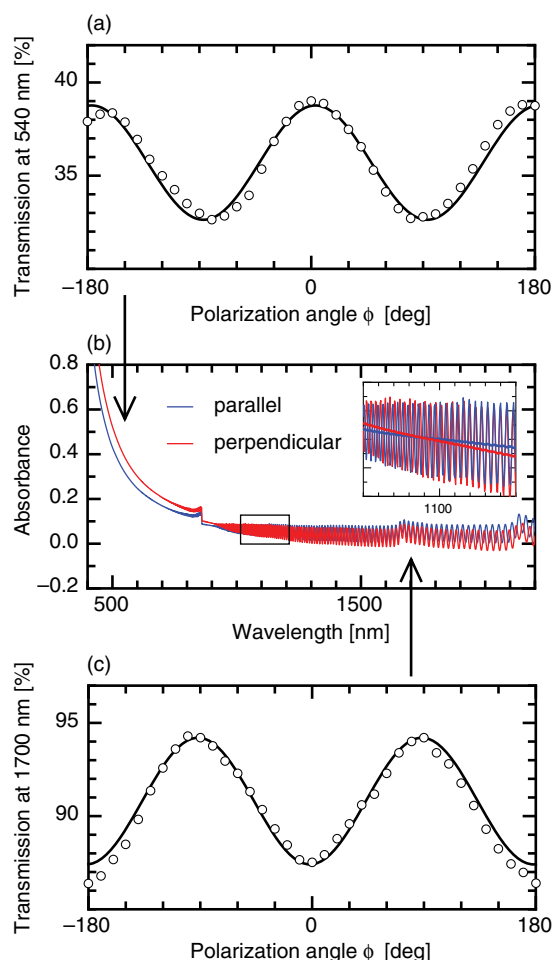


Fig. 1 Anisotropic characteristics of a 50- μm APTIV™ 2000 PEEK film, annealed at 160°C, in a polarizer setup. (b) The middle graph shows the absorbance with the polarizer position parallel and perpendicular to machine direction. Maximum anisotropy is reached at approximately 540 nm and a phase shift occurs around 1100 nm (see inset). The inset shows in addition to the absorbance the values averaged along ± 100 nm. (a) At 540 nm, below the phase shift around the maximum of the anisotropy, a 360 deg transmission measurement followed a sinusoidal curve with the transmission maximum in machine direction. (c) At 1700 nm, above the phase shift, the 360 deg rotation resulted in a sinusoidal curve with the transmission maximum in transverse direction.

and 1100 nm, the absorbance was lower when the analyzer was oriented in machine direction. For wavelengths above 1100 nm, the absorbance in machine direction was higher than in transverse direction. This phase shift clearly indicates anisotropic behavior. Note the Fabry-Pérot fringes, that occur in the near infrared range, originate from interferences due to the thin film nature of the PEEK sheets. Optical anisotropy is often identified with linear dichroism.¹³ It is defined as the difference in the absorbance parallel and perpendicular to the molecular axis. The linear dichroism is related to the molecular structure and the interactions of the molecules with the incident electromagnetic waves. Therefore, the PEEK film was further investigated below and above the phase shift at 1100 nm. Below this neutral point [see inset of Fig. 1(b)], the anisotropy reached a maximum at a wavelength of about 540 nm. A characteristic transmission curve, recorded at 540 nm as a function of the rotation angle, is shown in Fig. 1(a). The transmission follows a sinusoidal function with maxima along the machine direction, indicating a preferential alignment of the molecules within the plane of incidence. For the wavelength of 1700 nm [Fig. 1(c)], well above the phase shift wavelength, the sinusoidal function was shifted by 90 deg with respect to the one recorded at 540 nm. The transmission showed maxima in transverse direction. In a control experiment, the amorphous APTIV™ 2000 PEEK films

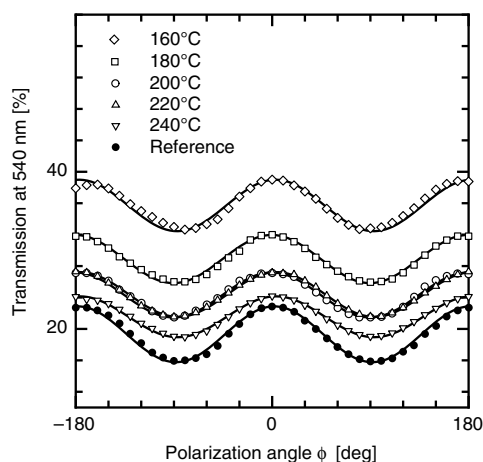


Fig. 2 Transmission at 540 nm of 50 μm APTIV™ 2000 PEEK films subjected to annealing at the temperatures indicated. Reference is a 50 μm -thin APTIV™ 1000 PEEK film. Sinusoidal behavior of the transmission with a maximum in machine direction is observed for all samples including the reference.

(not annealed) did not show any linear anisotropy. These optical measurements confirm the apparent isotropy of the source material prior to the annealing process. In order to investigate this orientation effect in more detail, the anisotropy in absorbance of APTIV™ 2000 PEEK films was studied as a function of the annealing temperature above the glass transition temperature at 143°C. Annealing of 50 μm -thin APTIV™ 2000 PEEK films at temperatures between 160 and 240°C induced similar anisotropy as found in a semi-crystalline APTIV™ 1000 PEEK film of same thickness (Fig. 2). The amplitude of the sinusoidal curves slightly decreased with increasing annealing temperature. Annealing at a temperature of 240°C led to a similar transmission as found for the APTIV™ 1000 PEEK films. The higher annealing temperatures are associated with enhanced crystallinity. This effect decreases the transmission due to light scattering. The annealing supports the molecule alignment into crystallite assemblies detectable as optical anisotropy in the originally amorphous PEEK films. Table 1 quantitatively summarizes the anisotropy by the amplitude and the ratio of transmissions in machine and transverse directions

Table 1 Anisotropy quantification of APTIV™ 1000 and 2000 PEEK films and a polarizer foil HN32 by transmission measurements. The mean transmission τ_M and the amplitude τ_A were derived from fitting the sinusoidal transmission behavior between crossed polarizers at the wavelength of 540 nm. The ratio of transmission measurements in machine and transverse directions τ_{MD}/τ_{TD} characterizes the PEEK film anisotropy.

Film	$T_{\text{annealing}}$ [°C]	Film thickness [μm]	τ_M [%]	τ_A [%]	τ_{MD}/τ_{TD}
APTIV™ 1000		25	35.8 ± 0.1	4.0 ± 0.1	1.3 ± 0.0
APTIV™ 1000		50	19.3 ± 0.1	3.6 ± 0.1	1.5 ± 0.0
APTIV™ 2000		50	18.3 ± 0.1	0	0
APTIV™ 2000	160	50	35.7 ± 0.1	3.2 ± 0.2	1.2 ± 0.1
APTIV™ 2000	180	50	28.9 ± 0.1	3.0 ± 0.2	1.2 ± 0.1
APTIV™ 2000	200	50	24.3 ± 0.1	2.9 ± 0.2	1.3 ± 0.1
APTIV™ 2000	220	50	24.4 ± 0.1	2.9 ± 0.2	1.3 ± 0.1
APTIV™ 2000	240	50	21.5 ± 0.1	2.6 ± 0.1	1.3 ± 0.1
HN32 polarizer		700	19.4 ± 0.1	19.3 ± 0.1	552 ± 6

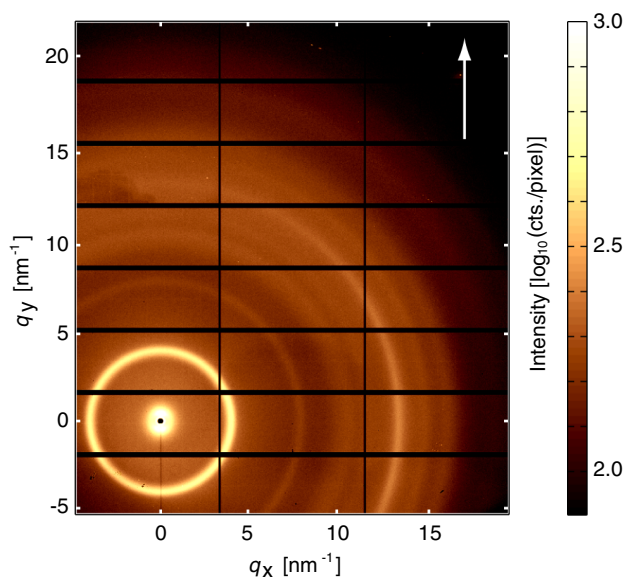


Fig. 3 WAXS pattern of a 50 μm -thin 2000 APTIV™ PEEK film annealed at 160°C for 10 min, featuring the characteristic peaks of PEEK. The most prominent anisotropic ring relates to the (110) plane. The white-colored arrow indicates the machine direction.

calculated from sinusoidal fits for the 25 and 50 μm -thin 2000, annealed and 1000 APTIV™ PEEK films investigated at a wavelength of 540 nm. The transmission ratios rose from 1.19 to 1.27, while the mean transmission decreased from 35.72% to 21.54% when increasing annealing temperatures from 160 to 240°C. A 50 μm -thin APTIV™ 1000 PEEK film showed a transmission of 19.32% and a transmission ratio of 1.45. The 50 μm -thin APTIV™ 2000 PEEK film exhibited low transmission since it had a rough surface on one side, which caused significant light scattering. As a reference, we examined a commercially available linear polarizer film (HN32). In comparison to the PEEK films, we found a transmission ratio of more than 500 for the HN32 polarizer film, stating that the polarization and therefore anisotropy of the PEEK films is fairly weak. The absolute amplitude of the polarizer film, however, was only 4 to 5 times larger.

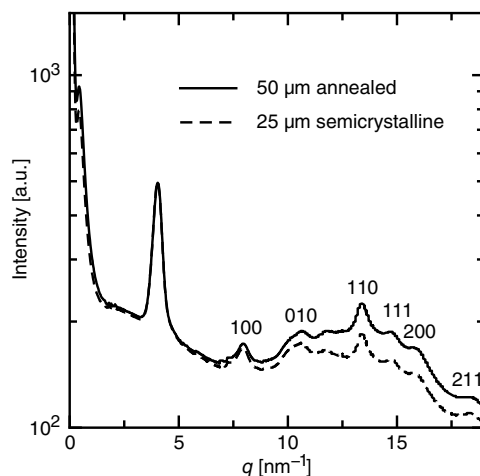


Fig. 4 Radially integrated WAXS intensities (q -plot) of a 25 μm -thin APTIV™ 1000 PEEK film (dashed line) and a 50 μm -thin APTIV™ 2000 PEEK film (solid line) after annealing at 160°C for 10 min. Miller indices are given for peaks of the PEEK unit cell.

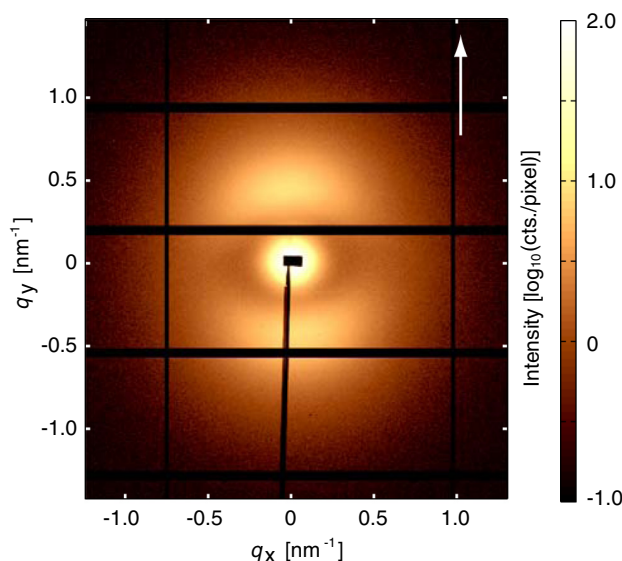


Fig. 5 SAXS pattern of a 50 μm -thin APTIV™ 2000 PEEK film annealed at 160°C for 10 min. The anisotropic scattered intensity distribution with a maximum q -value of 0.43 nm^{-1} indicates preferential long-range order in the machine direction, see white arrow. Data were recorded in a q -range between 0.09 to 3.4 nm^{-1} .

3.2 x-Ray Scattering Measurements Using Synchrotron Radiation

In order to gain more detailed information about the investigated anisotropy of the PEEK films on the molecular scale, WAXS data of the PEEK films were recorded. As shown in Fig. 3, the APTIV™ PEEK films give rise to intensity distributions at well-defined scattering angles of 0.4 nm^{-1} , 4.0 nm^{-1} , 8.0 nm^{-1} , 10.7 nm^{-1} , and 13.4 nm^{-1} , corresponding to feature sizes of 14.66 nm, 1.56 nm, 0.79 nm, 0.59 nm, and 0.47 nm, respectively. Anisotropic sinusoidal intensity modulations along the ring were clearly identified for the features with sizes of 14.66 nm and 0.47 nm, oriented in machine and transverse directions, respectively. The crystallographic unit

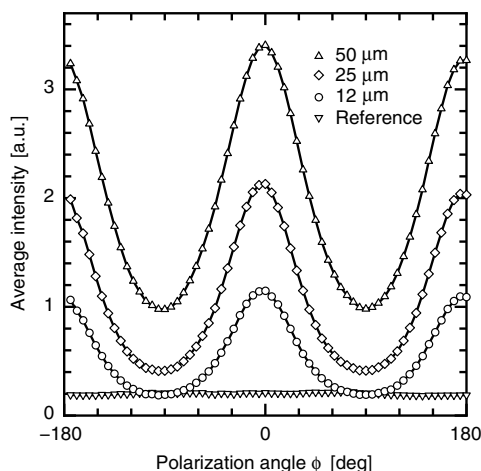


Fig. 6 Azimuthal intensity plot (from 2-D SAXS data integrated over the q -range related to real space periodicities between 5.2 and 22.5 nm) for PEEK films of different film thickness (after annealing to 160°C). A 50 μm -thin amorphous PEEK film is also included as reference, revealing the distinct anisotropy of the scattered intensity in the annealed films. Maxima were found in the machine direction. Their intensity was almost directly proportional to the material thickness while no modulation was found in the amorphous PEEK.

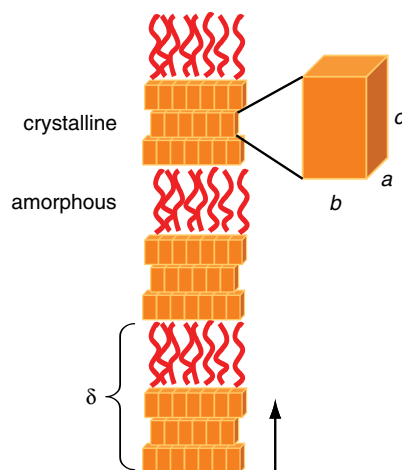


Fig. 7 Molecular semi-crystalline PEEK film model. The parameter δ describes the alternating crystalline/amorphous long-range order stacks with a periodicity of 14.66 nm. One crystalline subunit consists of a unit cell with the axes a , b , and c . The semi-crystalline/amorphous repeats are oriented along the machine direction.

cell of PEEK is orthorhombic ($a = 0.775$ nm, $b = 0.589$ nm, and $c = 0.988$ nm)^{14,15} comprising two chains aligned in direction of the c -axis, one chain positioned at the center of the ab -projection and four chains at the corners. The observed WAXS signals at q -values of 8.0 nm⁻¹ and 10.7 nm⁻¹ corresponding to 0.79 and 0.59 nm, respectively, are in reasonable agreement (less than 2% difference) with the a - and b -lattice constants reported. The pronounced ring at 4.0 nm⁻¹, which corresponds to a periodicity of 1.56 nm, however, does not agree with a single lattice constant but may originate from two times a . Figure 4 shows an I - q -plot of the integrated WAXS data of a 25 μ m-thin APTIV™ 1000 PEEK film and a 50 μ m-thin APTIV™ 2000 PEEK film that was annealed at a temperature of 160°C for a period of 10 min.

The diffraction ring corresponding to anisotropic long-range ordering of 14.66 nm was measured with higher angular resolution in SAXS geometry. A SAXS pattern of an originally amorphous 50 μ m-thin PEEK film annealed at 160°C for a period of 10 min is shown in Fig. 5. The main orientation of the scattering signal, and thus of the long-range order, is parallel to the machine direction, fitting the orientation found in the optical measurements. Therefore, one may assume the same source of anisotropy is detected with the two methods. The intensity of the anisotropic scattering signal increased with film thickness from 12 via 25 to 50 μ m (see Fig. 6).

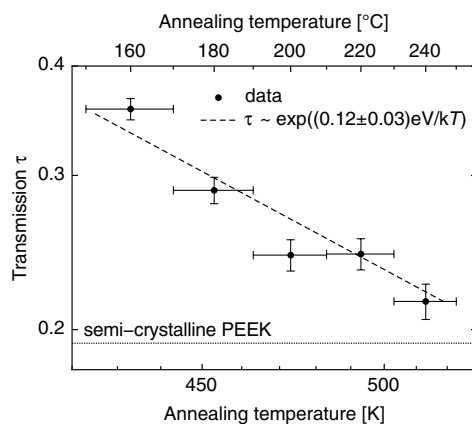


Fig. 8 The Arrhenius-plot of the optical transmission of 50 μ m APTIV™ 2000 PEEK films at 540 nm shows the growth of crystallites with a long-range order and a related activation barrier of (0.12 ± 0.03) eV associated with intermolecular interactions.

While the APTIV™ 1000 PEEK films and annealed films exhibited an anisotropic signal, the untreated APTIV™ 2000 PEEK films (reference) were isotropic. This indicates that the anisotropy of the film arises from the bulk of the PEEK films.

3.3 Nanostructure of Semi-Crystalline PEEK Films

The following model, which is known from polymers¹⁶⁻¹⁸ and is in agreement with the optical and x-ray measurements, is represented in Fig. 7. The long-range order with a periodicity of 14.66 nm describes the amorphous/semi-crystalline long period δ . The unit cell parameter c of PEEK is parallel to machine direction. The long period is oriented in the c -axis direction, and the related q -peak intensities are therefore film thickness dependent.

4 Discussion and Conclusions

The description of semi-crystalline PEEK by means of stacked long-range ordered amorphous and crystalline units agrees with previously published results. Lovinger et al.¹⁹ studied PEEK crystallization from solution and melt, and concluded that both routes produce spherulites with narrow, elongated lamellae, that radially grow in the crystallographic b -axis direction. In this structure, the c -axis lies parallel to the spherulite plane and the a -axis lies vertical to the plane. The interpretation of SAXS data, concerning the lamellar structure is, however, a more difficult task and subject of debates (see Ref. 16 and references therein). Two main models were discussed. In a three-phase model, thick lamellar crystals (7 to 12 nm) separated by thinner amorphous interlayers (3 to 4 nm) pack into stacks of finite size. Extended purely amorphous PEEK regions lie between these stacks. A two-phase model suggests stacks of thin lamellae alternating with thicker amorphous interlayers.¹⁶ The size range of one repeating unit consisting of a crystalline and an amorphous layer is in reasonable agreement with the obtained periodicity of 14.66 nm. Also, the orientation of the lamellae perpendicular to the ab -projection plane fits well to the assumption that the orientation measured in optical transmission and WAXS/SAXS originates from the lamellar stacks.

DSC thermograms of PEEK 2000 films (data not shown) exhibited a pronounced re-crystallization peak around 170°C. This is a common phenomenon observed for polymers that have been cooled down rapidly during processing, thus kinetically preventing crystallization (prominent examples are polyethylene terephthalate and polylactic acid) despite molecular chains being oriented. The present pre-orientation of molecular strands in the amorphous film, upon heating above T_g , facilitates re-crystallization as the molecular motions are deliberated. We suggest that the pre-orientation of the molecules in the 2000 APTIV™ PEEK film, induced by the production process, becomes detectable upon crystallization. This annealing process can be monitored using optical transition measurements as evidenced in Fig. 8. The transmission at a wavelength of 540 nm exhibits the Arrhenius behavior with an activation energy of (0.12 ± 0.03) eV. Similar to organic systems on surfaces²⁰ this value is associated with the intermolecular bond strength within PEEK. For benzene dimers, the π - π binding energy is reported to be in the range of 2 to 3 kcal mol⁻¹,²¹ which corresponds to 0.09 to 0.13 eV per molecule, and therefore reasonably agrees with the activation energy obtained from the Arrhenius plot. Note that for the three-dimensional epitaxial growth of para-hexaphenyl the activation energy corresponds to (0.90 ± 0.04) eV,²² a value which has to be divided by six to deduce the π - π binding energy, and thus it is in agreement with the activation energy derived from the rather simple transmission measurements of annealed PEEK films. One may, therefore, deduce the scenario for the optical measurements on PEEK films. First, amorphous PEEK films are transparent and do not show any anisotropy, because the nanostructures are well below the wavelength of the probe. Second, annealing results in the formation of crystallites within the amorphous matrix, which show a long-range order according to the film processing direction and hence reduce the optical transmission of the PEEK films until the semi-crystalline state has been reached. Both methods, x-ray scattering and optical characterization, sensitive to different length scales, revealed a process-induced anisotropy in PEEK films.

Anisotropic polymer films with a preferential orientation on different lengths are promising materials for medical implants, as most human tissues also show anisotropic structure and properties.¹⁰ In order to realize nature-analogue and biomimetic polymer implants, rather simple optical transmission or reflection measurements could become a vital tool to optimize the structural anisotropy on the nanometer scale.

Acknowledgments

The SAXS experiments were performed on the cSAXS beamline at the Swiss Light Source, Paul Scherrer Institut, Villigen, Switzerland. The support of Teemu Ikonen and Xavier Donath is gratefully acknowledged. We also thank Stefan Stutz for the technical setup and support regarding the optical measurements. This work was funded by the Swiss Nanoscience Institute (project 6.2).

J.A., O.B., H.D., and B.M. have designed the study. J.A. recorded the optical data and prepared the related figures. J.A. and H.D. acquired the x-ray scattering data. All authors significantly contributed to data analysis and interpretation as well as approved the final version of the submitted manuscript. B.M. is the guarantor of integrity of the entire study.

References

1. M. Escuti, D. Cairns, and G. Crawford, "Optical-strain characteristics of anisotropic polymer films fabricated from a liquid crystal diacrylate," *J. Appl. Phys.* **95**(5), 2386–2390 (2004), <http://dx.doi.org/10.1063/1.1643192>.
2. K. Kirov and H. Assender, "Quantitative ATR-IR analysis of anisotropic polymer films: extraction of optical constants," *Macromolecules* **37**(3), 894–904 (2004), <http://dx.doi.org/10.1021/ma030369j>.
3. T. Shimo and M. Nagasawa, "Stress and birefringence relaxations of noncrystalline linear polymer," *Macromolecules* **25**(19), 5026–5029 (1992), <http://dx.doi.org/10.1021/ma00045a032>.
4. I. Ward, *Structure and Properties of Oriented Polymers*, Applied Science, London (1975).
5. X. Zhang et al., "Oriented structure and anisotropy properties of polymer blown films: HDPE, LLDE and LDPE," *Polymer* **45**(1), 217–229 (2004), <http://dx.doi.org/10.1016/j.polymer.2003.10.057>.
6. S. Shoji et al., "Optical polarizer made of uniaxially aligned short single-wall carbon nanotubes embedded in a polymer film," *Phys. Rev. B* **77**(15), 153407 (2008), <http://dx.doi.org/10.1103/PhysRevB.77.153407>.
7. S. M. Kurtz and J. N. Devine, "PEEK biomaterials in trauma, orthopedic, and spinal implants," *Biomaterials* **28**, 4845–4869 (2007), <http://dx.doi.org/10.1016/j.biomaterials.2007.07.013>.
8. "Protecting batteries in heart pacemakers," *Kunststoffe* **2**, 98 (2011).
9. J. Althaus et al., "Nanostructuring polyetheretherketone for medical implants," *Eur. J. Nanomed.* **4**(1), 7–15 (2012), <http://dx.doi.org/10.1515/ejnm-2011-0001>.
10. B. Müller et al., "Scanning x-ray scattering: evaluating the nanostructure of human tissues," *Eur. J. Nanomed.* **3**(1), 30–33 (2010), <http://dx.doi.org/10.1515/EJNM.2010.3.1.30>.
11. O. Bunk et al., "Multimodal x-ray scatter imaging," *New J. Phys.* **11**(12), 123016 (2009), <http://dx.doi.org/10.1088/1367-2630/11/12/123016>.
12. B. Heinrich et al., "PILATUS: a single photon counting pixel detector for x-ray applications," *Nucl. Instrum. Methods* **607**(1), 247–249 (2009), <http://dx.doi.org/10.1016/j.nima.2009.03.200>.
13. A. Rodger and B. Nordén, *Circular Dichroism and Linear Dichroism*, Oxford University Press, Oxford and New York (1997).
14. P. C. Dawson and D. J. Blundell, "X-ray data for poly(aryl ether ketones)," *Polymer* **21**(5), 577–578 (1980), [http://dx.doi.org/10.1016/0032-3861\(80\)90228-1](http://dx.doi.org/10.1016/0032-3861(80)90228-1).
15. J. N. Hay et al., "The structure of crystalline PEEK," *Polym. Commun.* **25**(6), 175–178 (1984).

16. G. Reiter and J.-U. Sommer, "Polymer crystallization: observations, concepts and interpretations," *Lect. Notes Phys.* **606**, 1–382 (2003), <http://dx.doi.org/10.1007/3-540-45851-4>.
17. J. I. Lauritzen and J. D. Hoffman, "Theory of formation of polymer crystals with folded chains in dilute solution," *J. Res. Nat. Bur. Stand.* **64A**(1), 73–102 (1960).
18. A. Ryan et al., "A synchrotron x-ray study of melting and recrystallization in isotactic polypropylene," *Polymer* **38**(4), 759–768 (1997), [http://dx.doi.org/10.1016/S0032-3861\(96\)00583-6](http://dx.doi.org/10.1016/S0032-3861(96)00583-6).
19. A. J. Lovinger and D. D. Davis, "Solution crystallization of poly(ether ether ketone)," *Macromolecules* **19**(7), 1861–1867 (1986), <http://dx.doi.org/10.1021/ma00161a014>.
20. B. Müller, "Natural formation of nanostructures: from fundamentals in metal heteroepitaxy to applications in optics and biomaterials science," *Surf. Rev. Lett.* **8**(1–2), 169–228 (2001), [http://dx.doi.org/10.1016/S0218-625X\(01\)00085-9](http://dx.doi.org/10.1016/S0218-625X(01)00085-9).
21. M. Sinnokrot, E. Valeev, and C. Sherrill, "Estimates of the ab initio limit for π - π interactions: the benzene dimer," *J. Am. Chem. Soc.* **124**(36), 10887–10893 (2002), <http://dx.doi.org/10.1021/ja025896h>.
22. B. Müller et al., "MBE growth of para-hexaphenyl on GaAs(001)-2 \times 4," *Surf. Sci.* **418**(1), 256–266 (1998), [http://dx.doi.org/10.1016/S0039-6028\(98\)00720-1](http://dx.doi.org/10.1016/S0039-6028(98)00720-1).



Jasmin Althaus received a diploma in chemistry from the University of Applied Sciences, Northwestern, Switzerland, in 2004. After working at the Friedrich Miescher Institute in Basel as a research assistant with Jan Hofsteenge, she moved on to the Biocenter in Basel, where she earned a molecular biology MSc in 2008. She is currently working towards her PhD degree in biomedical engineering on the effect of plasma-treated PEEK films on human mesenchymal stem cell differentiation at University of Basel, University of Rostock, Paul Scherrer Institute and University of Applied Sciences, and Arts Northwestern Switzerland with the aim to obtain the degree from the medical faculties of the universities in Basel and Rostock.



Hans Deyhle received a MSc diploma in experimental physics from ETH, Zurich, in 2008. He has worked as scientist and later as PhD student in the team of Bert Müller at the Biomaterials Science Center of the University of Basel. He is mainly dealing with micro- and nano-imaging of human teeth using x-rays from synchrotron radiation sources in Villigen/Switzerland, Hamburg/Germany, and Grenoble/France.



Oliver Bunk received a PhD in physics from the University of Hamburg. He is currently heading the laboratory for macromolecules and bioimaging of the Swiss Light Source at the Paul Scherrer Institute. Recurrent themes of his research include cross-disciplinary work using x-ray techniques, which he has developed towards perfection step-wise. The current focus relates to bioimaging of hierarchically structured materials using scanning small-angle x-ray scattering and coherent diffractive imaging.



Per Magnus Kristiansen received a MSc diploma in materials sciences from the ETH, Zurich, in 2000. He then joined the polymer technology group of Paul Smith at ETH, Zürich for a PhD project on nucleation and clarification of semi-crystalline polymers. In 2004 he started to conduct applied research on functional supramolecular additives at Ciba. From 2007 to 2009 he was responsible for customer support for light stabilizers, functional additives, and nanoparticles. In 2009 he became a professor at the Institutes of Polymer Engineering and Polymer Nanotechnology. He deals with micro- and nano-structuring by injection molding, nanoimprint lithography, roll embossing, and microthermoforming.



Bert Müller received a MSc degree in physics from the Dresden University of Technology and a PhD in physics from the University of Hannover, Germany, in 1989 and 1994, respectively. From 1994 to 2001, he worked as a researcher at the Paderborn University, Germany, and subsequently in Switzerland at EPF Lausanne, and ETH Zurich. He became a faculty member of the Physics Department at ETH, Zurich, in 2001. After his election as Thomas Straumann-Chair for Materials Science in Medicine at the University of Basel, Switzerland and his appointment at the Surgery Department of the University Hospital Basel in 2006, he founded the Biomaterials Science Center. He teaches physics and materials science at the Universities of Basel and Bern as well as at ETH, Zurich. He is a member of SPIE and Associate Editor of the *Journal of Nanophotonics*.

Nanostructuring polyetheretherketone for medical implants

Jasmin Althaus¹⁻⁴, Celestino Padeste², Joachim Köser³, Uwe Pieleš³, Kirsten Peters⁴ and Bert Müller^{1,*}

¹Biomaterials Science Center (BMC), University of Basel, c/o University Hospital Basel, 4031 Basel, Switzerland

²Laboratory for Micro- and Nanotechnology, Paul Scherrer Institute, 5232 Villigen, Switzerland

³Institute of Chemistry and Bioanalytics, University of Northwestern Switzerland, School of Life Sciences, 4132 Muttenz, Switzerland

⁴Department of Cell Biology, University of Rostock, 18057 Rostock, Germany

Abstract

Surface roughness is a vital factor for medical implants since the cells of the surrounding tissue interact with the underlying substrate on the micro- and nanometer scales. In order to improve the surface morphology of implants, appropriate large-area micro- and nanostructuring techniques have to be identified being applicable to irregularly shaped structures. We demonstrate that plasma treatments of polyetheretherketone (PEEK) thin films produce nanostructured surfaces in a reproducible manner. They are easily tailored by varying plasma intensity using oxygen and ammonia as process gases. It was observed that roughness and nanostructure density linearly depend on plasma intensity. Oxygen plasma turned out to exhibit a stronger effect compared to ammonia plasma at the same processing conditions. For cell interaction studies, the mean size of the nanostructures was intentionally varied between 10 nm and 100 nm. In vitro experiments revealed that human mesenchymal stem cells (hMSC) adhere inhomogeneously on untreated PEEK films, but the plasma treatment with oxygen or ammonia allows the hMSC to adhere and proliferate. Fluorescence microscopy of the cells on the PEEK films turned out to be difficult because of the strong auto-fluorescence of the PEEK substrate. Stains including the whole cell vital stain Calcein-AM allowed cell morphology studies on plasma-treated PEEK films. In the case of the analysis of cell compartments such as the actin cytoskeleton, confocal laser scanning microscopy (CLSM) was successfully applied.

*Corresponding author: Dr. Bert Müller, Thomas Straumann
Professor für Materialwissenschaft in der Medizin, Biomaterials
Science Center (BMC), Universität Basel, c/o Universitätsspital,
4031 Basel, Schweiz
Phone: +41 61 265 9660
E-mail: bert.mueller@unibas.ch, www.bmc.unibas.ch

Keywords: atomic force microscopy; auto-fluorescence; confocal laser scanning microscopy; human mesenchymal stem cells; nanostructures; oxygen and ammonia plasma treatments; polyetheretherketone (PEEK); Rat-2 fibroblasts.

Introduction

The surface chemistry, the surface roughness, and the stiffness of an implant play a crucial role in the biocompatibility of medical implants (1–3) because adherent cells interact with the accessible micro- and nanometer-size features (4–6). Titanium bone implants are usually sandblasted and etched to reach the necessary micro- and nanometer-scale roughness for appropriate osseointegration. For an increasing number of musculo-skeletal applications polymer materials have been used, which exhibit the advantage of being radiolucent which is beneficial following the soft tissue formation around the implant. Their limited mechanical properties, however, restrict the materials selection. Therefore, the high-performance polymer polyetheretherketone (PEEK), which exhibits the desired mechanical properties, received the FDA-approval for trauma, orthopedic and spinal implants in 1982, and experiences an increasing use for medical implants and beyond. Besides reasonable mechanical properties it also exhibits outstanding chemical resistance, which makes it suitable as a biocompatible material and is already used in applications such as spinal disc cages and housings of pacemakers (7). For bone implants, PEEK surfaces have to be activated to allow for proper cell attachment. Plasma treatment belongs to the promising methods because of the ease of the process and the reproducible control of the final surface chemistry. We hypothesize that the plasma treatment can be exploited to generate and tailor nanostructures for improved osseointegration. Our hypothesis is also based on the recent observation of Dalby et al. (8), that patterns of nanostructures on polymeric substrates cause osteogenic differentiation of mesenchymal stem cells. They have found that, in contrast to highly ordered nanostructures, the randomly arranged nanostructures induce osteogenic differentiation. Therefore, we assume that the plasma etching, which leads to a random distribution of nanostructures on the PEEK surfaces, could be well suited for bone implants.

To study the cell-biomaterial interactions including cell morphology, fluorescence microscopy and confocal laser scanning microscopy (CLSM) are widely used. In the case of PEEK substrates, the application of fluorescence microscopy is critical because of the strong auto-fluorescence of the polymeric material. Hunter et al. (9), investigated the attachment and proliferation of osteoblasts and fibroblasts on biomaterials for orthopedic use, and explicitly excluded PEEK from the

immuno-fluorescence study due to the prominent auto-fluorescence of the material. To overcome the problem, Briem et al. (10) replaced the immuno-fluorescence stains with Giemsa stains when investigating the response of primary fibroblasts and osteoblasts to plasma-treated PEEK. In order to address the problem of the auto-fluorescence, we have carefully analyzed the auto-fluorescence of commercially available PEEK films (APTIV™ Series from VICTREX, Hofheim, Germany) to explore the possible origin of the strong background fluorescence. One cause could arise from fluorescent additives. Therefore, PEEK has been chemically synthesized without any additive according to Risse et al. (11). Finally, we demonstrate that utilizing CLSM allows for the investigation of fluorescence-stained cells on micrometer-thin PEEK sheets with minimized background signal.

Materials and methods

PEEK sheet pretreatment

Hot embossing with a HEX03 press (JENOPTIK Mikrotechnik GmbH, Germany) at a temperature of 160°C and a pressure of 100 kN served to flatten commercially available amorphous APTIV™ PEEK films (Series 2000, Victrex Europa GmbH, Hofheim, Germany) with nominal thicknesses of 6 µm, 12 µm, 25 µm and 50 µm between two polished 4-inch silicon wafers.

Plasma treatment

Oxygen/argon or ammonia plasma treatments (Piccolo system, Plasma Electronic, Neuenburg, Germany) activated the embossed PEEK sheets. The embossing-marked films were placed at the bottom of the plasma chamber. Subsequently, the chamber was evacuated, flushed for a period of 5 min with a 2:1 mixture of oxygen/argon (200/100 sccm, 99.5/99.2%, Messer, Lenzburg, Switzerland) or ammonia (200 sccm, 99.98%, Messer, Lenzburg, Switzerland) and then equilibrated for further 5 min with oxygen/argon (20/10 sccm) or ammonia (30 sccm). The plasma treatments using a power of 10 W, 25 W, 50 W, 75 W, 100 W, 125 W, 150 W, 175 W, or 200 W always lasted 5 min.

Atomic force microscopy measurements (AFM)

AFM measurements enabled us to determine the surface roughness and island density of plasma-activated PEEK sheets. Measurements were performed in TappingMode® in air under dry conditions on a Dimension IIIa instrument (Veeco, Mannheim, Germany) using silicon cantilevers with a Si₃N₄ coating and a tip radius of 20 nm, a spring constant of 40 N/m and a resonance frequency of 325 kHz (NSC15/A1BS, Mikromasch, CA, USA; manufacturers specifications). The scan area was set to 2×2 µm². Data processing and roughness evaluation was done using the Nanoscope software. For each specimen the island density was determined from three individual characteristic square areas, each with approximately 100 islands.

Transmission and fluorescence scans

PEEK was synthesized according to Risse et al. (11). A tert-butyl substituted PEEK was prepared by nucleophilic substitution of tert-

butylhydroquinone and 4,4'-difluorobenzophenone (Sigma-Aldrich). The tert-butyl substituent was cleaved via reversed Friedel-Crafts alkylation using trifluoromethanesulfonic acid. The specially synthesized PEEK and corresponding starting materials in powder form were filled into 96-well plates until the bottom was covered.

The PEEK films were stamped out to fit into the 96-well plate format. The transmission measurements carried out in a 96-well quartz glass plate (Hellma, Müllheim, Germany) were recorded for wavelengths ranging from 240 nm to 1000 nm. The fluorescence experiments in black 96-well plates were performed with a TECAN micro-plate reader infinite 200, equipped with a UV Xenon flash lamp (TECAN trading AG, Switzerland) using bottom reading with a detector gain of 60. The excitation wavelengths were varied between 350 nm and 800 nm in steps of 10 nm. The corresponding emission was acquired 30 nm above excitation wavelengths to 850 nm in 5 nm steps.

Cell culture

Rat-2 fibroblasts were cultured in DMEM medium under standard conditions (5% CO₂, 37°C). The fibroblasts were seeded over night on 70% ethanol sterilized class cover slips and PEEK sheets.

Human mesenchymal stem cells (hMSC) were isolated from liposuction-derived adipose tissue as described previously by Peters et al. (12) and seeded (96-well plate, 10⁴ cells/cm², triplicates) on the differently plasma-treated PEEK substrates for a period of 14 days. Cell cultivation was done under standard conditions.

Fluorescence staining

Cells were washed with phosphate buffered saline (PBS) and fixed with 4% paraformaldehyde in PBS for 10 min at room temperature. The cells were then permeabilized with 0.2% Triton X-100, washed, and incubated with a 1:40 dilution of mouse anti-human vinculin (Sigma-Aldrich, Buchs, Switzerland) and a 1:2000 dilution of TRITC-conjugated phalloidin (Sigma-Aldrich, Buchs, Switzerland) in PBS for 1 h at room temperature. Subsequently, the cells were labeled using a 1:1000 dilution of goat anti-mouse Alexa 488 secondary antibody (Invitrogen) in PBS during 30 min. The cells were visualized on a BX-51 fluorescence microscope equipped with a fluorescence unit, and a Fluo-View 1000 confocal laser scanning microscope, both from Olympus (Hamburg, Germany).

hMSC were vital-stained with Hoechst 33324 (1:2000, Sigma-Aldrich, Taufkirchen, Germany) and Calcein-AM (Biomol GmbH, Hamburg, Germany; 1:200, ATT Bioquest) in DMEM medium during 15 min at a temperature of 37°C. The staining medium was exchanged with fresh solution before imaging.

Scanning electron microscopy (SEM)

The plasma-treated PEEK films were coated with Au/Pd during 30 s using a current of 20 mA and applied a vacuum of 6 Pa (sputter coater Polaron, Thermo VG Scientific, Germany). Substrates were investigated with the field emission scanning electron microscope Supra 40 VP (Carl Zeiss, Jena, Germany) with an applied acceleration voltage of 10 kV using the InLens detector.

Results

Plasma treatment is a common process to chemically activate polymer surfaces (10, 13–16), which is a prerequisite to

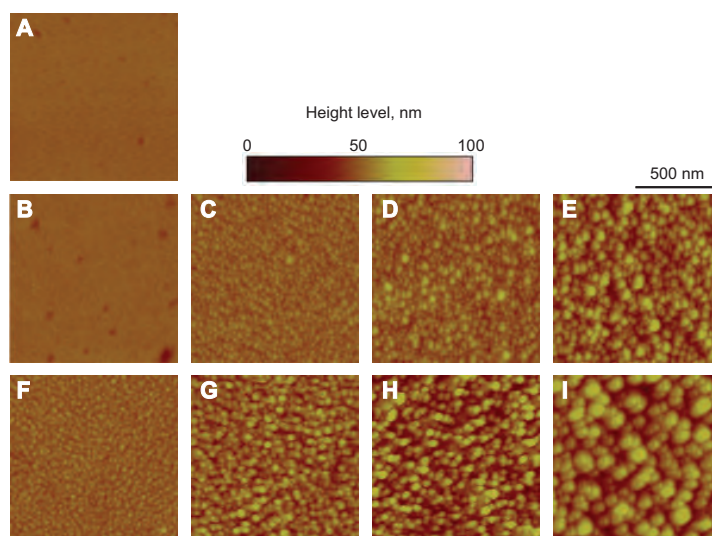


Figure 1 AFM images of plasma-treated PEEK films.

The 25 μm -thick films were plasma-treated for 5 min. (A) untreated, (B-E) ammonia-plasma-treated, plasma power from left to right: 10 W, 50 W, 100 W and 200 W. (F-I) oxygen-plasma-treated, plasma power from left to right: 10 W, 50 W, 100 W and 200 W.

achieve proper cell attachment. The process gases, oxygen and ammonia, modify the PEEK surface and lead to nanostructures as represented by the AFM images in Figure 1.

The plasma treatment with a duration of 5 min and the variation of the power between 10 and 200 W results in nanostructures of increasing size and PEEK surfaces with increasing roughness. This finding clearly indicates that plasma activation does not only change the chemical nature of the PEEK sheet but also induces significant changes in the surface morphology. These changes are also reflected in water contact angle measurements (data not shown). From the AFM measurements shown as an example in Figure 1, quantitative data were derived. The root-mean-square (RMS) roughness exhibits an almost perfectly linear behavior as a function of plasma power (see Figure 2A). The RMS roughness measurements of the oxygen plasma-treated surfaces show twice as large values to those of the ammonia treatments. Nevertheless, the island densities for the ammonia plasma treatments determined via area measurements of about 100 islands (island counting on certain areas), turned out to show values twice as high as the ones for the oxygen treatments (cp. Figure 2B).

The adipose tissue-derived hMSC, cultured on the differently treated PEEK substrates and the tissue culture polystyrene (TCPS) control for a period of 14 days, show a morphology characteristic for the plasma activation. While the hMSC on the PEEK sheet treated with a power of 10 W are similar to the ones on the control substrate, i.e., in a healthy state, the hMSC on the untreated PEEK have not properly adhered and spread out (see Figure 3). Also on harshly oxygen plasma-treated PEEK, the cells did not adhere and spread.

In order to study the cells on the PEEK films, fluorescence stains were applied with the aim to visualize the integrin-

mediated focal adhesions. Integrins are heterodimeric cell membrane spanning receptors and connect the extracellular matrix (ECM) with the actin cytoskeleton of the cell.

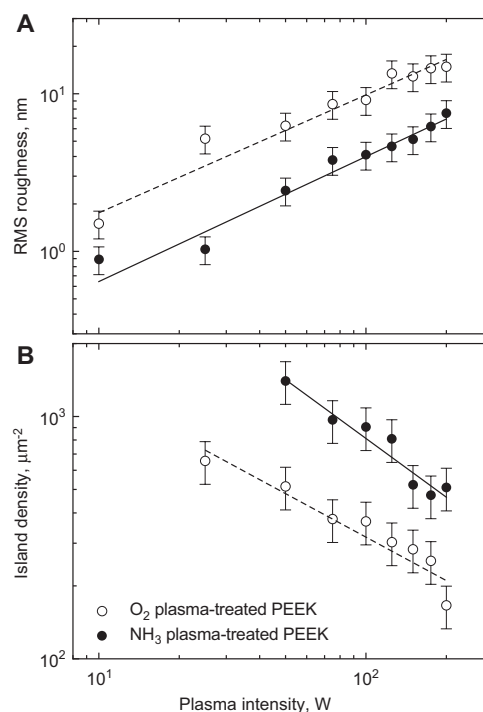


Figure 2 RMS roughness and island density of plasma-treated PEEK films.

The 25 μm -thick films were plasma-treated for 5 min.

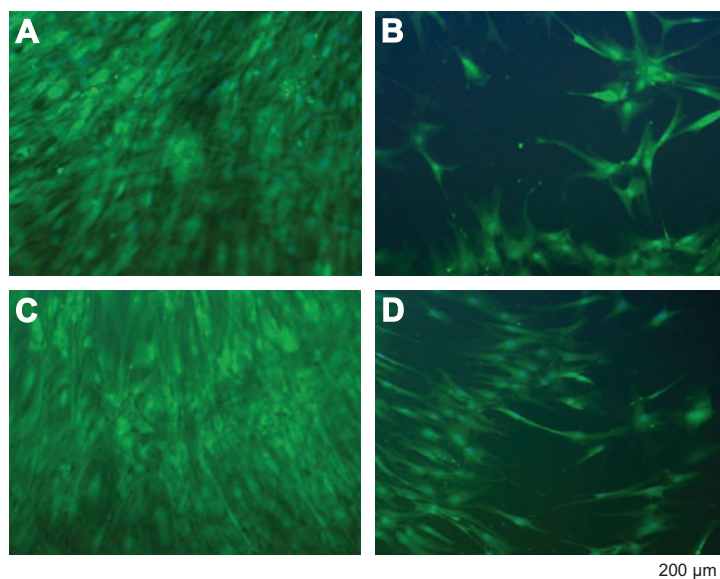


Figure 3 hMSC on oxygen-plasma-treated PEEK films.

hMSC from adipose tissue were cultured for 14 days under standard conditions. The 25 μm -thick films were plasma-treated for 5 min. (A) TCPS control, (B) untreated, (C) oxygen plasma power 10 W, (D) oxygen plasma power 200 W.

Here, the intracellular part of the integrin receptor binds to a protein complex including vinculin, which itself directly binds to actin. Therefore, co-localization of actin and vinculin is regarded as proper verification for the presence of focal adhesions (17). Rat-2 fibroblasts were seeded on APTIV™ PEEK sheets of different thicknesses and stained for vinculin and actin, giving rise to green- and red-colored features, respectively. Figure 4 shows the related images obtained with conventional epifluorescence microscopy and CLSM.

The images displayed in the first row of Figure 4 show the controls (rat-2 fibroblasts on glass slides). Here, the background is low and the green vinculin stain (FITC-labeled) clearly points to the focal adhesions of the cells. The red-colored actin cytoskeleton (TRITC-labeled) spans over the entire individual cells. The APTIV™ PEEK sheets exhibit a strong background fluorescence that seriously complicates the feature extraction using conventional fluorescence microscopy. This background fluorescence linearly increased with the film thickness. Hence, three-dimensional structures made out of PEEK, e.g., medical implants, can hardly be included into such fluorescence studies that strongly depend on the focal plane. In the model system studied, replacing the conventional fluorescence microscopy by CLSM, the background could significantly be reduced (see Figure 4). The characteristic pattern of the fluorescence stained cytoskeletal elements was obvious and similar to the control. The flexible 6 μm -thin PEEK films, however, exhibit an inhomogeneous background associated with their non-wavy surface. Therefore, one can reasonably assume that the investigation of cells on non-planar PEEK implant surfaces becomes complicated.

In order to characterize the optical properties of the PEEK films, the transmission spectra have been recorded (see Figure 5) for the four selected thicknesses.

With the exception of the Fabry-Pérot fringes that are very obvious for the 6 μm -thin sheets, the maximum transmission corresponds to about 80%. Below 370 nm, the PEEK sheets are opaque.

The background of the fluorescence images implies characteristic auto-fluorescence of PEEK. To obtain a detailed view about the auto-fluorescence of the PEEK sheets, spectroscopic fluorescence measurements for wavelengths ranging from 350 to 850 nm have been recorded and are presented in the diagrams of Figure 6.

To exclude that the fluorescence originates from any polymer additive, the PEEK polymer was synthesized according to the description of Risse et al. (11) and compared with the commercially available APTIV™ PEEK films from VICTREX. As shown in Figure 6, the PEEK films and the pure PEEK exhibit very similar emission spectra. Consequently, the auto-fluorescence is an inherent property of the PEEK polymer.

Strong emission resulted upon excitation at wavelengths between 370 and 550 nm with a broader maximum for excitation wavelengths between 370 and 450 nm. Oxygen and ammonia plasma treatments did not change the emission profiles. The materials for the PEEK synthesis, 4,4'-difluorobenzophenone and tert-butylhydroquinone, were analyzed concerning fluorescence emission as well. While 4,4'-difluorobenzophenone showed fluorescence behavior similar to PEEK, tert-butylhydroquinone did not emit light in the excitation wavelength range between 400 and 800 nm.

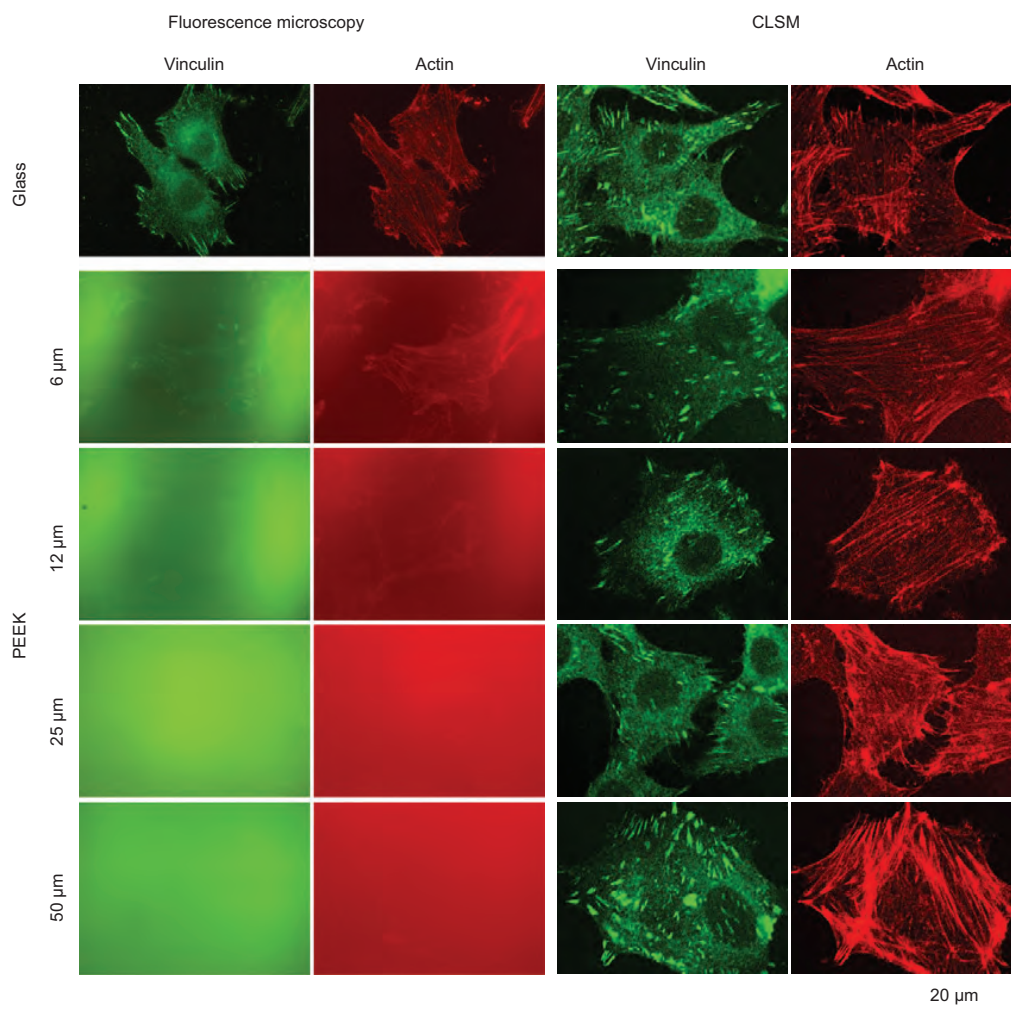


Figure 4 Rat-2 fibroblasts seeded on glass and differently thick APTIV™ PEEK films. Actin stain: phalloidin-TRITC, vinculin stain: monoclonal anti-vinculin and goat-anti-mouse A-488.

Discussion and conclusions

The observed nanostructuring of PEEK by oxygen and ammonia plasma treatments is likely due to etching. To exclude a thermal effect, as the temperature within the plasma chamber increases during the processing by several Kelvin, we have performed an additional experiment comparing the nanostructures of a 20-min treatment with a four times 5 min processing. After each 5-min treatment, we have opened the chamber to harvest a part of the PEEK sheet for scanning electron microscopy imaging. Figure 7 displays these images, which do not show any significant difference between step-wise and the one-step processes.

Therefore, one can conclude that thermal effects are negligible. We speculate that the local etching rate depends on the molecule orientation within the semi-crystalline polymer. When etching is described as a negative growth, similar to the facet-depending growth rates in single-crystalline solids, the orientations with fast etching rates gradually disappear, which

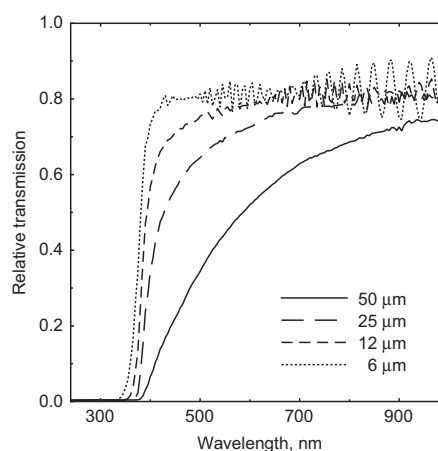


Figure 5 Transmission spectra of PEEK films. (Film thickness indicated.)

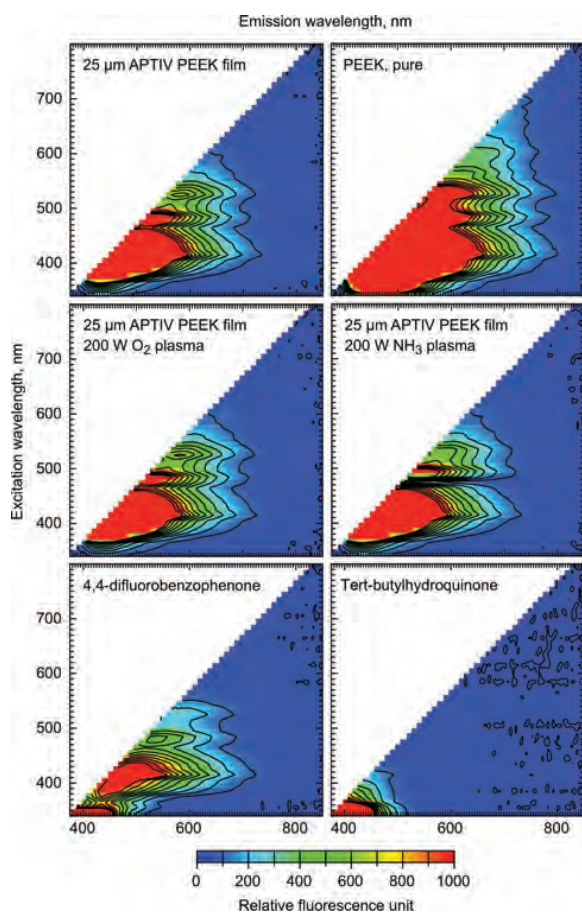


Figure 6 Fluorescence spectra from APTIV™ PEEK films, synthesized PEEK and starting materials.

Specimens were excited with wavelengths ranging from 350 nm to 800 nm in 10 nm-steps. Emission spectra up to a wavelength of 850 nm were recorded 30 nm above excitation wavelength (5 nm steps). The 25 μm -thick films were plasma-treated for 5 min.

is linked to the formation of larger and larger nanostructures. Oxygen plasma exhibits a higher etching rate than ammonia plasma. This phenomenon can be explained, because the two plasma-activated reaction gases exhibit a different level of chemical reactivity causing the difference in the etching rate. Consequently, the nanostructures on the PEEK sheets can be tailored using the plasma power, the duration of processing, and the choice of the process gas.

AFM measurements directly provide data on the substrate roughness. In many experiments one observes, however, that the roughness of nanostructured surfaces depends on the scanning speed and the choice of the scanning range (18). Counting the nanometer-size features is rather independent on the spatial resolution of the imaging method and therefore a reliable parameter to compare specimens from different batches (19). Hence, we recommend selecting the process parameters via the nanostructure density rather than using RMS values derived from AFM data.

Surface nanostructures have a vital influence on protein adsorption and cellular response, making them a key parameter in characterizing the interactions between biological systems and man-made biomaterials (4, 19–21). In contrast to metallic and ceramic biomaterials, however, nanostructuring polymer materials is still poorly understood, although this group of biomaterials has numerous advantages and the plasma-induced roughness increase of polymers has been known for more than a decade (22). First, the plasma treatment can be realized on large areas, as required for the treatment of medical implants. Second, it can be combined with other structuring technologies such as soft lithography, replica molding or polymer de-mixing (23). Third, the plasma treatment generates random nanostructures, which seem to be favored by hMSC for osteogenic differentiation over highly ordered structures as recently described by Dalby et al. (8). Fourth, plasma treatment is a fast, dry, and reproducible process and easy to apply on large scales and therefore suitable for mass production. As a consequence, this method enables the production of large substrate areas necessary for in vitro cell culture studies with primary cells like hMSC to reach statistically significant statements. However, one drawback of the plasma-induced activation (chemical modification) is the creation of instable surfaces, which change their properties including the water contact angle over time, due to decay of the reactive molecular species remaining.

A further drawback of optimizing PEEK for medical implants is the optical imaging of cells on PEEK surfaces due to auto-fluorescence (9, 10). The detailed investigation of the fluorescence of commercially available PEEK films (VICTREX) and pure PEEK revealed that the broadband auto-fluorescence is an inherent material property and not caused by any additive. As the aromatic ring structures of the PEEK monomers consist of highly delocalized electrons, they are expected to be excitable to a greater extent than tightly bound electrons. According to the results of the fluorescence analysis, fluorescent dyes that emit in the UV and infrared spectral regions should be less prone to background fluorescence interference. Therefore, Alexa Fluor 350 and Alexa Fluor 633 are promising candidates for fluorescence microscopy on PEEK substrates, since the corresponding filters are less common but available for most fluorescent microscopes. Due to the relatively long wavelength of 633 nm, a loss in resolution has to be taken into account. Notably, the cell live stain Calcein-AM, which has its emission maximum at 488 nm, can be applied to visualize cells on PEEK films. The cell stain is strong compared to a cell compartment stain and a cell has a height of several micrometers, shifting the focal plane away from the auto-fluorescent PEEK surface.

PEEK belongs to the promising biomaterials for a variety of medical implants. To reach cell attachment and the desired cell response, the surface has to be activated. Plasma treatment is a suitable method to activate the PEEK surface, associated with the generation of nanostructures. Their density and size can be tailored by the choice of the process gas, the plasma power, and the duration of the plasma treatment. In summary our results guide a path towards improving the biocompatibility of PEEK implants.

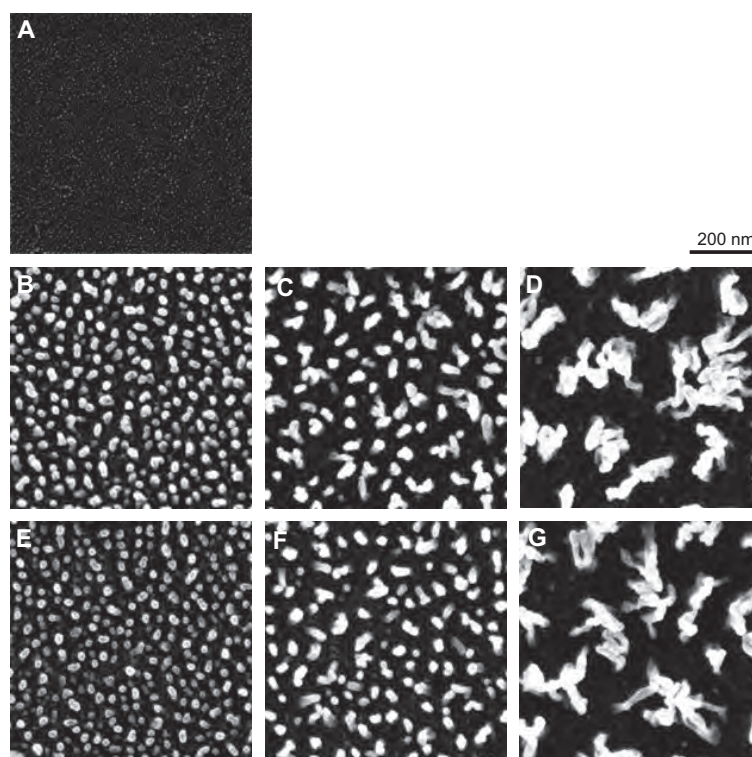


Figure 7 SEM images of 25 μm -thin PEEK films after 50 W oxygen plasma treatment with varying exposure time. (A) untreated, (B) 5 min, (C) 10 min, (D) 20 min, (E) 5 min, (F) 2 \times 5 min (G) 4 \times 5 min.

Acknowledgments

We gratefully acknowledge Nadja Chiapparelli for the AFM measurements and Marcus Waser for the synthesis of PEEK. We thank Helmut Schiff, Konrad Vogelsang and Mirco Altana for supporting us with knowledge about hot embossing and VICTREX for supplying us with APTIV™ PEEK films. Stefanie Adam kindly supported the cell culture work. Financial support was provided by grants from the Swiss Nanoscience Institute (project 6.2), the Rectors Conference of the Swiss Universities (CRUS), the European Union and the Federal State of Mecklenburg-Vorpommern, Germany (ESF/IV-WM-B34-0006/08).

References

1. Ponche A, Bigerelle M, Anselme K. Relative influence of surface topography and surface chemistry on cell response to bone implant materials. Part 1: physico-chemical effects. *Proc Inst Mech Eng H* 2010;224:1471–86.
2. Anselme K, Ponche A, Bigerelle M. Relative influence of surface topography and surface chemistry on cell response to bone implant materials. Part 2: biological aspects. *Proc Inst Mech Eng H* 2010;224:1487–507.
3. Engler AJ, Sen S, Sweeney HL, Discher DE. Matrix Elasticity Directs Stem Cell Lineage Specification. *Cell* 2006;126:677–89.
4. Riedel M, Müller B, Wintermantel E. Protein adsorption and monocyte activation on germanium nanopyramids. *Biomaterials* 2001;22:2307–16.
5. Variola F, Brunski JB, Orsini G, Tambasco de Oliveira P, Wazen R, Nanci A. Nanoscale surface modifications of medically relevant metals: state-of-the art and perspectives. *Nanoscale* 2011;3: 335–53.
6. Dohan Ehrenfest D, Coelho P, Kang B, Sul Y, Albrektsson T. Classification of osseointegrated implant surfaces: materials, chemistry and topography. *Trends Biotechnol* 2010;28:198–206.
7. Kurtz SM, Devine JN. PEEK biomaterials in trauma, orthopedic, and spinal implants. *Biomaterials* 2007;28:4845–69.
8. Dalby MJ, Gadegaard N, Tare R, Andar A, Riehle MO, Herzyk P, et al. The control of human mesenchymal cell differentiation using nanoscale symmetry and disorder. *Nat Mater* 2007;6:997–1003.
9. Hunter A, Archer CW, Walker PS, Blunn GW. Attachment and proliferation of osteoblasts and fibroblasts on biomaterials for orthopaedic use. *Biomaterials* 1995;16:287–95.
10. Briem D, Strametz S, Schröder K, Meenen NM, Lehmann W, Linhart W, et al. Response of primary fibroblasts and osteoblasts to plasma treated polyetheretherketone (PEEK) surfaces. *J Mater Sci-Mater M* 2005;16:671–7.
11. Risse W, Sogha DY. Synthesis of soluble high molecular weight poly(aryl ether ketones) containing bulky substituents. *Macromolecules* 1990;23:4029–33.
12. Peters K, Salamon A, Van Vlierberghe S, Richly J, Kreutzner M, Neumann H-G, et al. A new approach for adipose tissue regeneration based on human mesenchymal stem cells in contact to hydrogels-an in vitro study. *Adv Eng Mater* 2007;11:B155–61.
13. Ha SW, Hauert R, Ernst KH, Wintermantel E. Surface analysis of chemically-etched and plasma-treated polyetherether-

- ketone (PEEK) for biomedical applications. *Surf Coat Tech* 1997;96:293–9.
14. Ha SW, Kirch M, Birchler F, Eckert KL, Mayer J, Wintermantel E, et al. Surface activation of polyetheretherketone (PEEK) and formation of calcium phosphate coatings by precipitation. *J Mater Sci-Mater M* 1997;8:683–90.
 15. Cortese B, Morgan H. Controlling the wettability of hierarchically structured thermoplastics. *Langmuir* 2011; dx.doi.org/10.1021/la203741b.
 16. Tsougeni K, Vourdas N, Tseripi A, Gogolides E, Cardinaud C. Mechanisms of oxygen plasma nanotexturing of organic polymer surfaces: from stable super hydrophilic to super hydrophobic surfaces. *Langmuir*. 2009;6:11748–59.
 17. Geiger B. A 130K protein from chicken gizzard: its localization at the termini of microfilament bundles in cultured chicken cells. *Cell* 1979;18:193–205.
 18. Müller B, Riedel M, Michel R, Paul SMD, Hofer R, Heger D, et al. Impact of nanometer-scale roughness on contact-angle hysteresis and globulin adsorption. *J Vac Sci Technol B* 2001;19:1715–20.
 19. Müller B. Natural Formation of nanostructures: from fundamentals in metal heteroepitaxy to applications in optics and biomaterials science. *Surf Rev Lett* 2001;8:169–228.
 20. Lord MS, Foss M, Besenbacher F. Influence of nanoscale surface topography on protein adsorption and cellular response. *Nano Today* 2010;5:66–78.
 21. Latour R. Biomaterials: Protein-surface Interactions. *Encyclopedia of Biomaterials and Bioengineering*. 2008; pp. 27–284.
 22. Chan CM, Ko TM, Hiraoka H. Polymer surface modification by plasmas and photons. *Surf Sci Rep* 1996;24:1–54.
 23. Engel E, Michiardi A. Nanotechnology in regenerative medicine: the materials side. *Trends Biotechnol* 2008;26:39–47.



Jasmin Althaus received her diploma in chemistry from the University of Applied Sciences Northwestern Switzerland in 2004. After working at the Friedrich Miescher Institute in Basel as a research assistant in the group of Jan Hofsteenge, she moved on to the Biocenter in Basel where she earned her MSc in molecular biology in

2008. She is currently working towards her PhD degree in biomedical engineering on the effect of plasma-treated PEEK films on human mesenchymal stem cell differentiation at the University of Basel in close collaboration with Paul Scherrer Institute and University of Applied Sciences Northwestern Switzerland as well as the medical faculty of the University of Rostock.



Celestino Padeste studied chemistry at the University of Zürich from where he received a PhD degree on inorganic solid state-gas phase reactions in 1989. After a Post-doc at the University of New South Wales in Sydney/Australia in the field of surface analysis of catalyst systems he was employed at the Micro- and Nanotechnology Laboratory at the Paul Scherrer Institute in Villigen/Switzerland. His

work is focused on the design of functional surfaces by combination of nanostructuring methods including synchrotron radiation-based lithography with chemical surface modification, polymer grafting and protein immobilization.



Joachim Köser received a diploma in biology from the University of Heidelberg. Following his PhD thesis at the German Cancer Research Center he moved to the Biocenter in Basel to work in the group of Ueli Aebi on the nuclear pore complex. Subsequently, he joined the spin-off company Concentris GmbH where he was responsible for the application

development for cantilever sensors and now is working in the group of Uwe Pieles at the University for Applied Sciences Northwestern Switzerland in the field of medical nano-biotechnology.



Uwe Pieles studied chemistry at the universities in Bielefeld and Göttingen (1981–1985) and obtained his diploma (1985) and the PhD degree (1988) at the Max-Planck Institute for experimental medicine under the supervision of Friedrich Cramer. Between 1989 and 1991 he worked as a postdoctoral researcher at the European

Molecular Biology Laboratory. From 1991 to 1996 he worked as a laboratory head in the Central Research Laboratories of Ciba/Novartis in Switzerland (Basel). He became a group leader in the pharmaceutical research of Altana AG Germany (Konstanz, 1997–2000). Since 2000 he is a full professor and head of nanotechnology at the University of Applied Sciences Northwestern Switzerland in Muttens. In 2007 he was rewarded with the Collano Prize. His main research activities include surface science, surface chemistry in materials science, chemical and biochemical sensors, and nanoparticles in catalysis and biochemical applications.



Kirsten Peters studied biology and did her diploma thesis (1993–1994) at the Westfälische Wilhelms-University in Münster, Germany, where she also received her PhD under the supervision of Jürgen Rauterberg (1994–1998). Between 1999 and 2006 she worked as a senior post-doctoral researcher at the Institute of Pathology at the Johannes Gutenberg-University Mainz (C. James Kirkpatrick). Since 2006 she is the head of the Junior Research Group (Department of Cell Biology, University of Rostock, Germany). In 2008 she received her habilitation in molecular medicine from the Johannes Gutenberg-University in Mainz.



Bert Müller received a diploma in mechanical engineering (1982), followed by an MSc from the Dresden University of Technology and the PhD from the University of Hannover, Germany in 1989 and 1994, respectively. From 1994 to 2001, he worked as a researcher at the Paderborn University, Germany, EPF Lausanne, ETH Zurich. He became a faculty member of the Physics Department at ETH Zurich in April 2001. After his election as Thomas Straumann-Chair for Materials Science in Medicine at the University of Basel, Switzerland and his appointment at the Surgery Department of the University Hospital Basel in September 2006, he founded the Biomaterials Science Center. He also teaches physics and materials science at the ETH Zurich and the Universities of Basel and Bern.

Micro- and nanostructured polymer substrates for biomedical applications

Jasmin Althaus^{a,b,c,d}, Prabitha Urwyler^{a,b}, Celestino Padeste^b, Roman Heuberger^e, Hans Deyhle^a, Helmut Schiff^b, Jens Gobrecht^{b,f}, Uwe Pieves^c, Dieter Scharnweber^g, Kirsten Peters^d, and Bert Müller*^a

^aBiomaterials Science Center, University of Basel, c/o University Hospital, 4031 Basel, Switzerland;

^bLaboratory for Micro- and Nanotechnology, Paul Scherrer Institut, 5232 Villigen PSI, Switzerland;

^cInstitute of Chemistry and Bioanalytics, University of Applied Sciences and Arts Northwestern Switzerland, 4132 Muttenz, Switzerland;

^dDepartment of Cell Biology, University of Rostock, 18057 Rostock., Germany;

^eRMS Foundation, 2544 Bettlach, Switzerland;

^fInstitutes of Polymer Engineering and of Polymer Nanotechnology, University of Applied Sciences and Arts Northwestern Switzerland, 5210 Windisch, Switzerland;

^gMax Bergmann Center for Biomaterials, Technical University Dresden, 01069 Dresden, Germany

ABSTRACT

Polymer implants are interesting alternatives to the contemporary load-bearing implants made from metals. Polyetheretherketone (PEEK), a well-established biomaterial for example, is not only iso-elastic to bone but also permits investigating the surrounding soft tissues using magnetic resonance imaging or computed tomography, which is particularly important for cancer patients. The commercially available PEEK bone implants, however, require costly coatings, which restricts their usage. As an alternative to coatings, plasma activation can be applied. The present paper shows the plasma-induced preparation of nanostructures on polymer films and on injection-molded micro-cantilever arrays and the associated chemical modifications of the surface. In vitro cell experiments indicate the suitability of the activation process. In addition, we show that microstructures such as micro-grooves 1 μm deep and 20 μm wide cause cell alignment. The combination of micro-injection molding, simultaneous microstructuring using inserts/bioreplica and plasma treatments permits the preparation of polymer implants with nature-analogue, anisotropic micro- and nanostructures.

Keywords: Injection molding, embossing, PEEK film, plasma treatment, anisotropy, zeta-potential, XPS, mesenchymal stem cells

1. INTRODUCTION

Manufacturing of polymer micrometer-size components with nanostructures on top by mass fabrication is an emerging technology. For example, it is obvious to replace the currently dominating Si- or SiO₂-based MEMS/NEMS components by replicated polymer parts because of substantial cost reductions. These cost reductions, a prerequisite to open further applications, are even more significant, as single usage already required in medicine will become standard in other fields. Several attempts have been made to replace Si micro-cantilevers in sensor systems for biochemical applications by polymer-based microstructures. Either these micro-cantilevers were machined from bulk material [1, 2] or the microstructures were realized in photopolymers using optical lithography [3, 4]. Although it could be shown that polymer cantilevers can be used for sensing, even with substantially higher sensitivity compared to Si, both approaches do have severe drawbacks. The most severe ones are the limited choice of materials and the limited cost advantages expected, since machining of micro-parts and lithography processes are rather expensive. Attempts to apply injection molding in the fabrication of micro-cantilever arrays have been reported [5-7]. The reasons behind might be the precise machining of the molding tool and the control of the molding process for minimizing mechanical stresses in the micro-cantilever arrays.

*bert.mueller@unibas.ch; phone +41 61 265 9660; fax +41 61 265 9699; www.bmc.unibas.ch

The cantilever bending is well known for chemical sensors to identify small amounts of species including DNA. Sensors with cantilevers based on silicon micro-technology have found widespread applications, see e.g. F.M. Battiston [8]. Extreme sensitivity has been reported for detecting mass differences in molecules immobilized on the micro-cantilever's surface. Very recently, polypropylene micro-cantilevers have been introduced to detect bio-molecular interactions [6].

Micro-cantilevers can also be applied to determine the interactions of adherent cells with the underlying substrate. Recently, it has been shown that silicon cantilevers allow measuring the contractile forces of an ensemble of about one hundred fibroblasts [9]. Consequently, the forces of adherent biological cells on any underlying substrate should become accessible. The micro- and nanostructures of the substrate can be intentionally modified to mimic the bony tissue, which exhibits anisotropic features on the micro- and nanometer scale according to the loading direction. In a similar manner cells interact with man-made substrates. A decade ago, it was demonstrated for example that germanium nanopillars epitaxially grown on Si(100) can drastically reduce the inflammatory reactions [10] and it was postulated that the nanopillars behave in vitro similar to the apatite crystallites in vivo [11]. This is also the reason why the manufacturers of medical bone implants produce surfaces with a roughness on the micro- and nanometer scale using sandblasting and/or etching procedures. Such procedures, however, do not work equally for polymer implants. Although polymers have many advantages including iso-elasticity and compatibility with magnetic resonance imaging and computed tomography, their usage is still restricted. An appropriate structuring of polymers, which may include plasma treatments [12, 13], will allow the osseointegration of polymer implants and the realization of load-bearing implants with unique properties.

This proceedings communication deals with options to generate micro- and nanostructures on polymer biomaterials, which are supposed to be beneficial for bone implants. Polymer cantilevers, for example, can be straightforwardly micro-structured with a variety of pattern during the injection molding process or using nano-imprint technologies. Such microstructures can reveal directionally defined periodicities to guide and orient adherent cells or even be replicates of natural structures including cortical bone. Further processing, specifically plasma treatment, is necessary to chemically activate the polymer surface and to create nanostructures for improved protein adsorption and related cell behavior. Hence surface morphologies as found in nature (and beyond) are engineered with reasonable effort. Polyetheretherketone (PEEK), a high-performance, FDA-approved polymeric biomaterial is of special interest, since it has similar mechanical properties as human bone and is already used for implants such as housings for pacemakers because of its bio-inertness [14].

2. MATERIAL AND METHODS

2.1 Cantilever manufacture

Arrays of eight polymeric micro-cantilevers were produced using a modular injection molding tool [5, 7]. The molding tool represented in Figure 1 was installed in an Arburg 320 Allrounder (Arburg, Lossburg, Germany) with a maximum clamping force of 600 kN. The mirror unit of the molding tool, a polished steel surface ensured an optically flat and smooth surface. The micro-cantilever array was designed with an outline of $3.5 \times 2.5 \text{ mm}^2$ large holder. The eight nominally 45 μm -deep, 500 μm -long and 100 μm -wide micro-cantilever mold cavities were laser ablated. The injection molding process parameters were identical to those published recently [5, 7].

For adding a micro-relief onto the cantilever beam, a thin polycarbonate (PC: Makrofol ID 6-2, Bayer MaterialScience AG, Leverkusen, Germany) film patterned by hot embossing was placed at the mirror side of the molding tool [7]. The mold temperature was low enough to use the polymeric structures for several hundreds replications without degradation of the surface relief. Thus, a simple means to integrate gratings of different sizes and orientations into the micro-cantilever without changing their outlines (see Figure 2) became available.

2.2 Polymers used for injection molding

The polymer materials cyclic olefin copolymer (COC: Topas 8007x10, Topas Advanced Polymers GmbH, Frankfurt-Höchst, Germany), poly-oxymethylene (POM-C: 511P Delrin NC010, DuPont, Le Grand Saconnex, Switzerland), polyvinylidenefluoride (PVDF: Kynar 720, Arkema, Puteaux, France) and polypropylene (PP: Metocene HM648T, LyondellBasell, Bayreuth, Germany) were used for the injection molding experiments presented.

2.3 Polymer films used

For the experiments polyetheretherketone films (PEEK: Series 2000, Victrex Europa GmbH, Hofheim, Germany), polypropylene films (PP: Greiner, Huber, Reinach, Switzerland), polyethylene films (PE: Eppendorf, Huber, Reinach, Switzerland) and polyvinyl alcohol films (PVA: SreenLab, Elmshorn, Germany) were used.

2.4 PEEK sheet embossing

Hot embossing with a HEX03 press (JENOPTIK Mikrotechnik GmbH, Oberkochen, Germany) at a temperature of 160 °C and a pressure of 100 kN served to flatten commercially available amorphous APTIV™ PEEK films with thicknesses of 6, 12, 25 and 50 μm between two polished 4-inch silicon wafers. 20 μm-wide line structures were embossed from a silicon master. Due to processing conditions the PEEK films change from amorphous to partially crystalline phase [15].

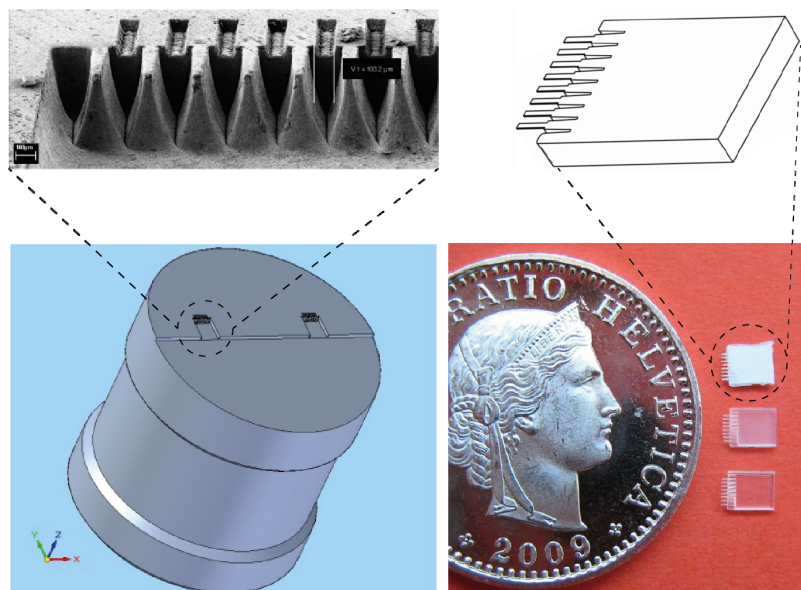


Figure 1. Scheme of the mold insert with two micro-cantilever array cavities each with eight 100 μm-wide micro-cantilevers cavities (left). Three selected injection molded micro-cantilever arrays compared in size to a Swiss coin (21.05 mm in diameter).

2.5 Plasma etching to generate nanostructures on polymer substrates

Oxygen/argon and ammonia plasma treatments (Piccolo system, Plasma Electronic, Neuenburg, Germany) were used to activate the polymer surfaces. First, the specimens were placed at the bottom of the plasma chamber (RF-system, 13.56 MHz). Second, the chamber was evacuated, flushed for a period of 5 min with oxygen/argon (200/100 sccm, 99.5/99.2%, Messer, Lenzburg, Switzerland) or ammonia (200 sccm, 99.98%, Messer, Lenzburg, Switzerland). Third, the system was equilibrated for 5 min with oxygen/argon (20/10 sccm) or ammonia (30 sccm). The plasma treatments with a duration of 5 min using a power of 10 to 200 W resulted in pressures within the chamber of 0.5 to 1.8 Pa and bias voltages from 55 to 400 V.

Since the plasma-activated polymer surfaces are known to exhibit significant changes with time, termed ageing [16], the XPS, zeta potential and presented cell culture experiments were started exactly seven days after the plasma treatments.

2.6 Scanning electron microscopy

The polymer films were coated with a 9 nm-thin Au/Pd film to obtain a conductive surface for scanning electron microscopy (SEM) imaging. During a sputtering time of 30 s (sputter coater Polaron, Thermo VG Scientific, East Grinstead, United Kingdom) with a current of 20 mA under vacuum conditions (6 Pa) the metal film is formed. The

nanostructured substrates were investigated with the field emission scanning electron microscope Supra 40 VP (Carl Zeiss, Jena, Germany) using an acceleration voltage of 10 kV and an InLens detector.

2.7 Zeta-potential measurements

All streaming potential measurements to determine the zeta potential quantitatively were carried out with the Electrokinetic Analyzer (Anton Paar KG, Graz, Austria) using silver/silver chloride electrodes and the measuring cell for flat plates as described previously [17]. The temperature, 24 to 28 °C during the experiments, was incorporated into the temperature-dependent viscosity and dielectric constant.

2.8 XPS measurements

X-ray photoelectron spectroscopy (XPS) studies were carried out by means of an Axis Nova photoelectron spectrometer (Kratos Analytical, Manchester, UK). The spectrometer was equipped with a monochromatic Al K α ($h\nu = 1486.6$ eV) X-ray source operated at a power of 225 W. The kinetic energy of the photoelectrons was detected using a hemispheric analyzer set to a pass energy of 160 eV for the wide-scan survey spectra and 40 eV for the detailed spectra (full-width-at-half-maximum of Ag3d_{5/2} 1.8 and 0.6 eV, respectively). During the measurements, electrostatic charging of the specimen was overcompensated by means of a low-energy electron source. The CasaXPS software (Version 2.3.15, Casa Software Ltd.) served for peak fittings. The energy scale of the spectra was calibrated against the C1s line peak of aliphatic aromatic carbon at $E_b = 284.0$ eV. An iterated Shirley background was subtracted from the spectra. Quantitative element compositions were determined from integrated peak areas below the measured curves and corrected by the sensitivity factors provided by Kratos. The residual pressure during the analysis was below $5 \cdot 10^{-6}$ Pa.

2.9 Cell culture experiments

Adipose tissue derived stem cells (ASC) were isolated from liposuction-derived adipose tissue as described previously [18]. Human dermal microvascular endothelial cells (HDMEC) were isolated from juvenile foreskin and cultivated as described in ref. [19]. These in vitro experiments were conducted after approval of the ethics committee (Medical Faculty, University of Rostock) and the full consent of the patients.

In the fourth passage, seeding of ASC was done at 20,000 cells per cm². Absence of contaminating monocytes/macrophages and endothelial cells was confirmed by flow cytometry (FACSCalibur; BD Biosciences AG, Heidelberg, Germany) proving the absence of CD14⁺/CD68⁺ (eBioscience, Frankfurt a. M., Germany) and CD31⁺ (Millipore, Schwalbach, Germany) cells, respectively.

The plasma-treated PEEK films were cut down to fit into a 96-well plates, sterilized with 70% ethanol (LiChrosolv, MERCK, Darmstadt, Germany), washed two times with Dulbecco's phosphate buffer saline (without Ca²⁺ and Mg²⁺, sterile; PAA Laboratories GmbH, Cölbe, Germany), and incubated with medium for a period of 2 h before cell seeding.

Cell cultivation was carried out under standard conditions, i.e. a temperature of 37 °C and 5% CO₂. Cells were cultured for a period of 48 h on the PEEK substrates and subsequently depicted by the fluorescence stain Calcein-AM (vital stain).

2.10 Live cell staining

Fluorescence staining with calcein AM permitted the visualization of live cells. Here, the cells were incubated in basal medium containing calcein AM (Biomol GmbH, Hamburg, Germany) at 1 μ M and incubated for a time period of 15 min at standard conditions, i.e. 37 °C and 5% CO₂ in a humidified atmosphere. Subsequently, the staining solution was exchanged by basal medium and cells were examined under the optical microscope in standard filter-based fluorescence microscopy (Axio Scope.A1 with AxioCam MRc, both Carl Zeiss MicroImaging GmbH, Göttingen, Germany). Calcein excitation and emission maxima are at wavelengths 496 and 516 nm, respectively.

3. RESULTS

3.1 Micro-cantilevers

Additional to micro-cantilever arrays with flat surface given by the polished steel molds, injection molding also permitted the manufacturing of patterned micro-cantilevers [7], i.e. the incorporation of micrometer-size surface topographies on one side of each cantilever. This was achieved by the placement of thermally and mechanically stable, pre-patterned polymer films in the mold. The SEM-images in Figure 2 show a variety of structures obtained for PP micro-cantilevers. The patterns display the high reproduction quality with a precision in the low micrometer range or even below. The rounded microstructures shown in the left image are supposed to be well comparable with cells, whereas the microindentations in the right image will only indirectly interact with cells via the adsorbed proteins.

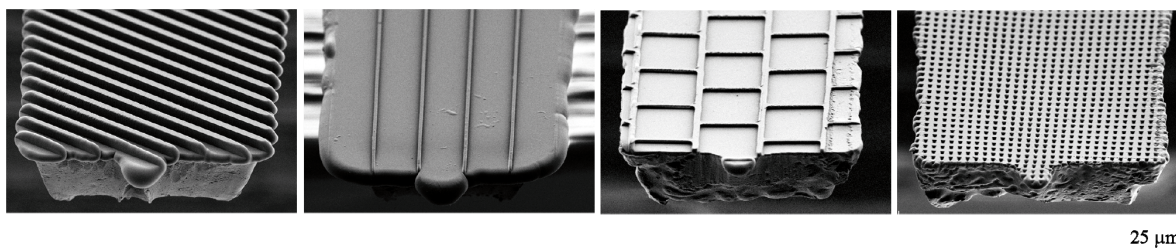


Figure 2. The SEM micrographs of polypropylene micro-cantilevers show the microstructures transferred to the micro-cantilevers during the injection molding process.

3.2 Plasma-treated polymer films

Figure 3 shows four different polymer films that were oxygen plasma treated for a duration of five minutes and a power of 50 W. Oxygen plasma treatments of the originally flat polymer films resulted in nanostructures (three dimensional islands). Although polymer films usually show preferential orientations of the molecules as the result of the casting [15], the plasma treatment yielded only isotropic nanostructures with isotropic distribution, see Figure 3. The larger nanostructures on PMMA, however, showed a ramified morphology.

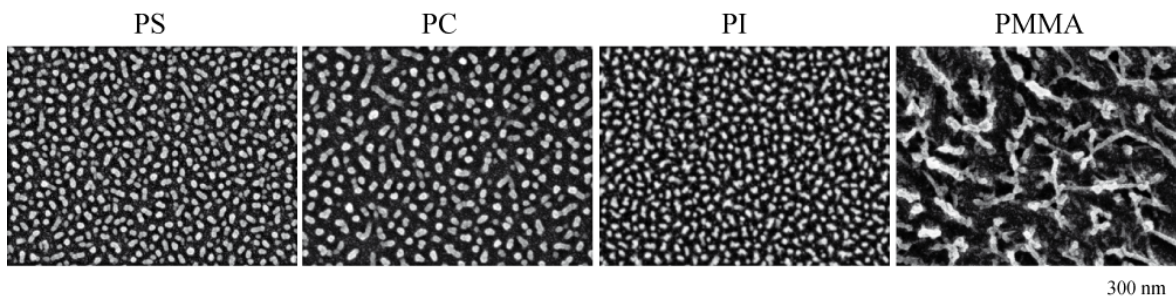


Figure 3. The SEM images of polymer films after oxygen plasma treatment with a power of 50 W show the occurrence of homogeneously distributed nanostructures with material specific size and shape. Whereas polystyrene (PS), polypropylene (PP) and polyimide (PI) give rise to circularly shaped nanostructures polymethyl metacrylate (PMMA) substrates show large ramified nanostructures with an arm width comparable to the diameter of the compact morphologies of the other polymer films investigated.

3.3 Plasma treatment of the micro-cantilevers to generate nanostructures on their surface

Figure 4 shows characteristic surface areas of injection-molded micro-cantilevers prepared from the polymer materials indicated that had been oxygen plasma treated with comparable conditions, i.e. with a power of 50 W and a duration of five minutes each. These SEM images reveal homogeneously distributed nanostructures, which are the result of oxygen plasma induced etching. The nanostructure's sizes and density are material dependent and can be further tailored by the choice of the plasma gas composition, the plasma power and the exposure time [12]. The nanostructures on the polypropylene (PP) and polyvinylidene (PVDF) substrates reveal a strong anisotropy. They are elongated and

preferentially oriented. None of the nanostructures observed were compact, although compact shapes are beneficial from an energetic point of view. Therefore, these surface structures represent a metastable configuration.

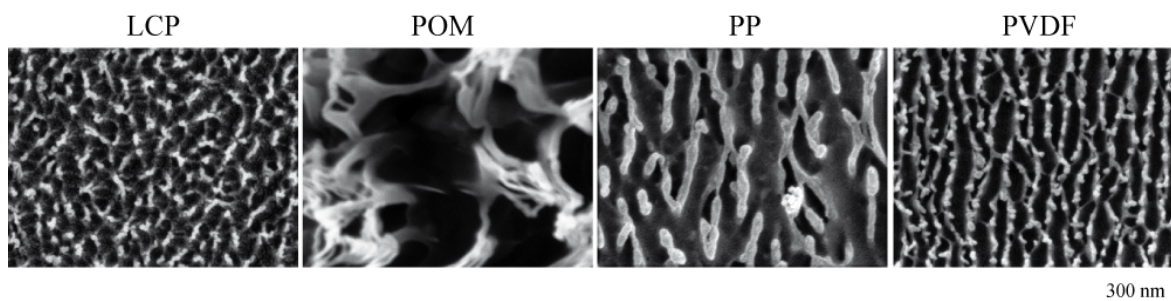


Figure 4. The SEM images of the injection-molded polymers after 50 W oxygen plasma treatment prove the presence of homogeneously distributed nanostructures on the polymer surface. The nanostructures on liquid crystal polymer (LCP) and polyoxymethylene (POM) appear to be isotropic, whereas the ones on polypropylene (PP) and polyvinylidene (PVDF) show an elongated shape with a clear preferential orientation. Size and density of the nanostructures depend on the material selected.

3.4 Injection molding combined with plasma treatment leads to highly anisotropic nanostructures

In injection molded polymer materials, the polymer chains are usually highly oriented as the result of the shear forces occurring during the manufacturing process. Figure 5 shows such anisotropy of injection-molded polyethylene (PE) and polypropylene (PP), as present at the support for the array of the eight micro-cantilevers. For comparison, a polarizer film made of polyvinyl alcohol (PVA) that consists of highly ordered polymer chains is given, cp. ref. [15]. It shows ramified nanostructures but no preferential orientation of the islands. This behavior becomes also clear from images obtained with lower magnification, as shown in the second row of Figure 5.

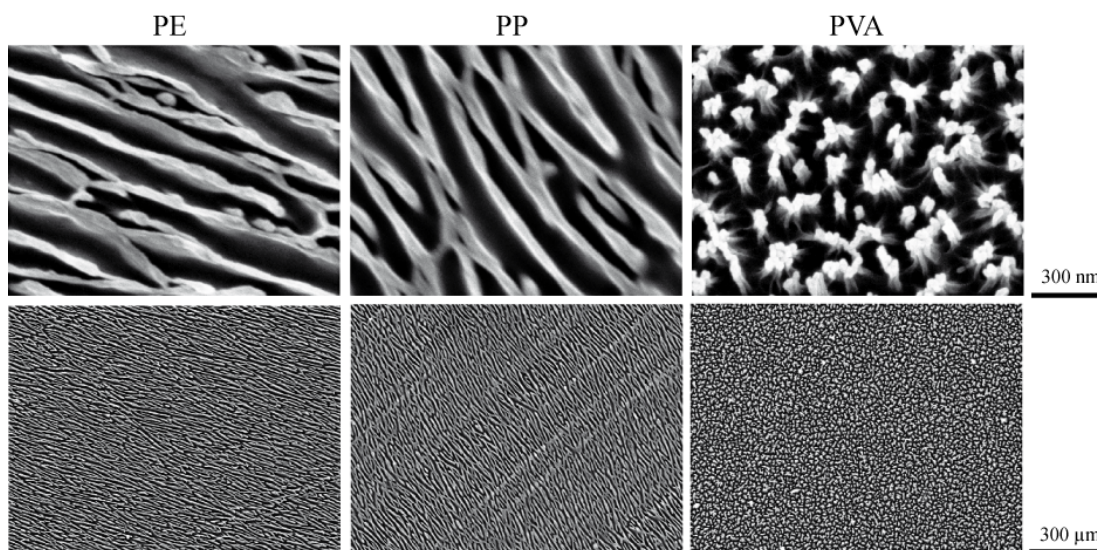


Figure 5. The SEM images of anisotropic polymers treated with 50 W oxygen plasma for five minutes prove that injection molded polyethylene (PE) and polypropylene (PP) exhibit strongly anisotropic nanostructures but the polyvinyl alcohol (PVA) polarizer film that is regularly used for optical purposes does not.

3.5 Comparing oxygen and ammonia plasma treatments of PEEK films

Applying a series of oxygen plasma powers on PEEK films one finds nanostructures of characteristic sizes [12]. For plasma powers up to at least 200 W the size of the pillar-like structures increases with the applied power (see upper part of Figure 6). For ammonia plasma treatments this plasma power dependent phenomenon is also present as shown in the

lower part of Figure 6. Here, the patterning effect is weaker under overall identical conditions (plasma power, duration of treatment and gas flow). This relationship was investigated in detail: A linear dependence between plasma power and roughness and an inverse linear relationship between plasma power and pillar density was demonstrated [12].

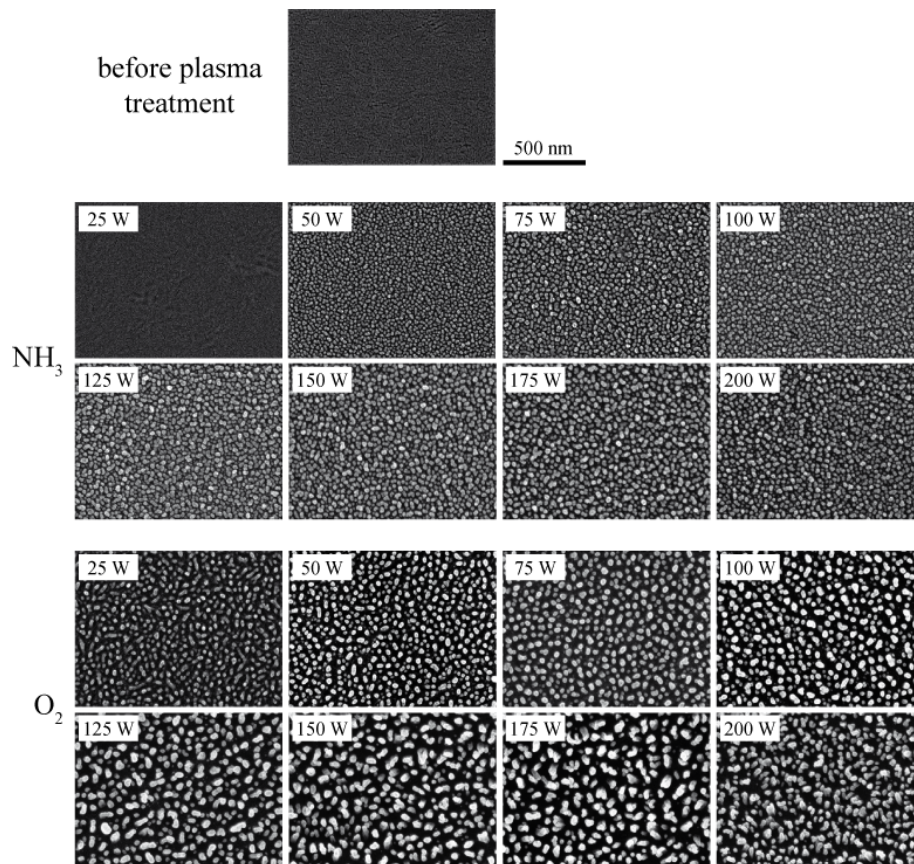


Figure 6. SEM images of oxygen and ammonia plasma treated polyetheretherketone (PEEK) films after applying plasma powers from 25 to 200 W during five minutes. The pillar-like, nanometer-size features increase with plasma power. Ammonia plasma is less abrasive than oxygen plasma.

3.6 Stability of generated nanostructures

In order to investigate the stability of the generated nanostructures on the PEEK films for planned cell studies, washing and sterilization procedures were performed. Figure 7 displays the related SEM images. Neither excessive rinsing with water nor the standard sterilization procedure consisting of a 70% ethanol wash followed by rinsing with phosphate buffered saline and water destroyed the nanostructures. The washing procedures, however, change the size and shape of the pillar-like PEEK nanostructures. The larger nanostructures show a ramified shape, which seems to be the result of aggregated pillars.

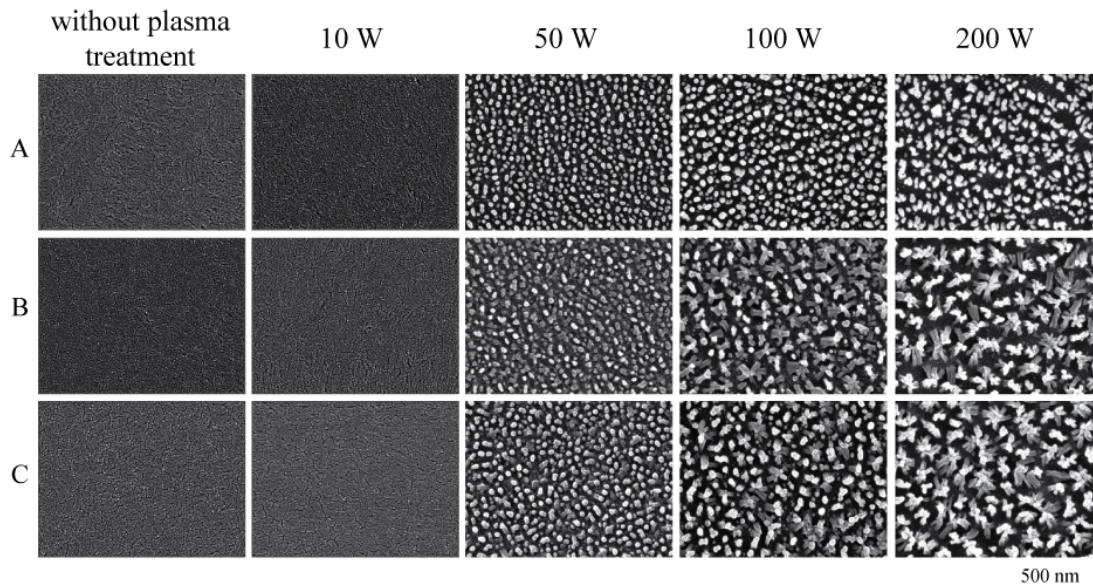


Figure 7. The SEM images of oxygen plasma treated PEEK substrates show (A) the morphology of dry films directly after the plasma treatment, (B) the morphology of the substrates after rinsing with water twice and dried in air, and (C) the morphology of the plasma-treated PEEK substrate after rinsing with 70% ethanol, with PBS twice and four times with water before dried in air.

3.7 Zeta-potential measurements

Plasma-excited oxygen and ammonia are reactive gaseous species that not only etch the PEEK surface and give rise to characteristic nanostructures but also induce a chemical alteration of the PEEK surface. In the field of biomaterials science and engineering such changes are often characterized by zeta-potential measurements that describe the surface charge as a function of the pH. Note surface charges crucially determine the protein adsorption thermodynamics and kinetics. For films, as given in the present case, the zeta-potential is commonly determined by the pH-dependent streaming measurements as shown in the diagram of Figure 8. The pH-value found for a zeta-potential of zero, i.e. at a net charge of zero, corresponds to the iso-electric point of the surface. The original flat PEEK substrate revealed an iso-electric point of 3.9. The oxygen plasma treated films showed a substantial shift towards lower iso-electric points. Ammonia plasma treatments caused a shift of the iso-electric point to slightly more basic pH-values. The ammonia plasma-treated PEEK surface seemed to be less stable than the oxygen plasma-treated surface since the zeta-potential shifted during the equilibration at the beginning of the measurement from higher values towards the values of the untreated PEEK film. The oxygen plasma-treated PEEK films exhibited a constant zeta-potential from the start of the experiment.

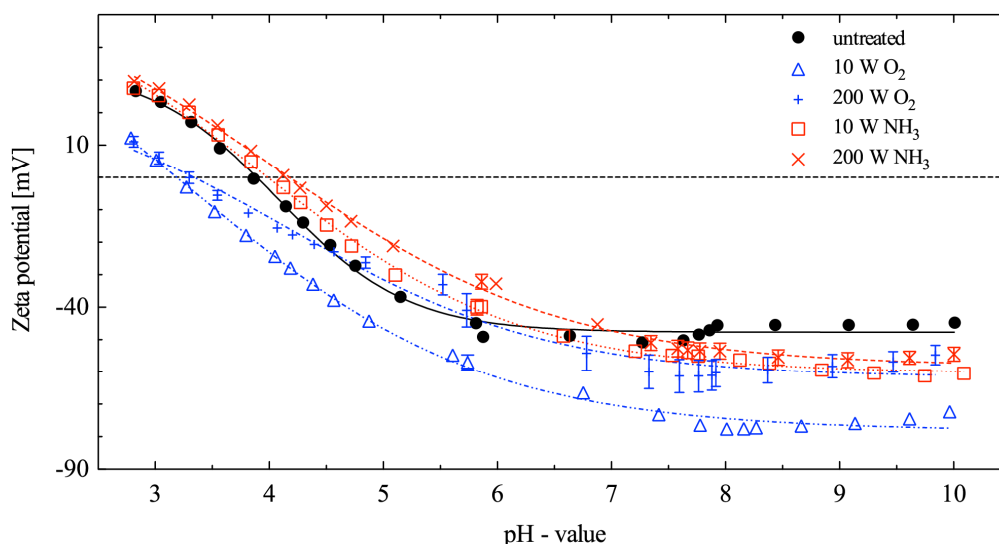


Figure 8. The zeta-potential of oxygen plasma treated PEEK films is shifted to smaller values with respect to the original PEEK film, whereas the ammonia plasma treatment resulted in higher values than the original PEEK substrate.

3.8 Chemical analysis of the plasma treated PEEK films using XPS

To gain more detailed information about the chemical modification of the PEEK film surfaces induced by the plasma treatment, XPS measurements were performed. The summary of the results for the oxygen plasma treated PEEK substrates is displayed in Figure 9. The survey scans in the first column show an increase of oxygen with increasing applied plasma power. Significant amounts of fluorine and aluminum are also present on the plasma treated surfaces, generally increasing with applied plasma power.

The highly intense peak at 284.5 eV of the C1s spectrum corresponds to the aromatic carbon atoms [20]. The peaks of higher binding energy are attributed to the following functional groups: ether bonds (C-O-C, 286.1 eV), keto bonds (C=O, 286.9 eV), carbonyl, ester and carbonate bonds (COO_x, CO₃, 288.3 eV) and shake-up satellite bonds from the π -electrons of the aromatic rings [20]. The C1s spectra revealed the formation of C-OOH and carbonate groups upon oxygen plasma treatment, which was previously well documented [16, 21]. A plasma power dependent decrease of the carbonyl groups and the aromatic C-C bonds was caused by the bombardment and associated fragmentation of the surface PEEK molecules. The O1s spectrum of the original PEEK film showed two main peaks for the ether bonds (532.7 eV) and keto bonds (531.3 eV) [20] and a minor peak at higher binding energy due to absorbed water [22]. The differences in peak-shape and the increased intensity in the O1s spectra are assigned to the various oxygen-containing species formed in the plasma process. A minor amount of nitrogen was found on the oxygen plasma treated PEEK surfaces at binding energies of 400 and 402 eV, which can be attributed to aliphatic amine groups (-C-NH₂) and charged amine groups, respectively, [23].

Ammonia plasma treatment introduced additional amounts of nitrogen and oxygen on the substrate surface as can be seen in Figure 10. The fitted N1s peaks (at 399.8 eV and 402.1 eV) are assigned to the formation of amine groups, which only a minor amount was charged. Surprisingly the nitrogen content was highest at intermediate plasma power. This is most probably due to increased sputtering of the surface at high plasma power. Sputtering leads removal of formed surfaces species and to the formation of surface radicals which undergo further reactions, e.g. with oxygen and water of the environment when the samples are removed from the plasma chamber. These reactions explain the increased intensity of the O1s signals upon NH₃-plasma treatment and are in line with the additional peaks found in the C1s spectra. Similar to the O₂-plasma-treatment we also found increasing fluorine and aluminum concentrations with increasing plasma power.

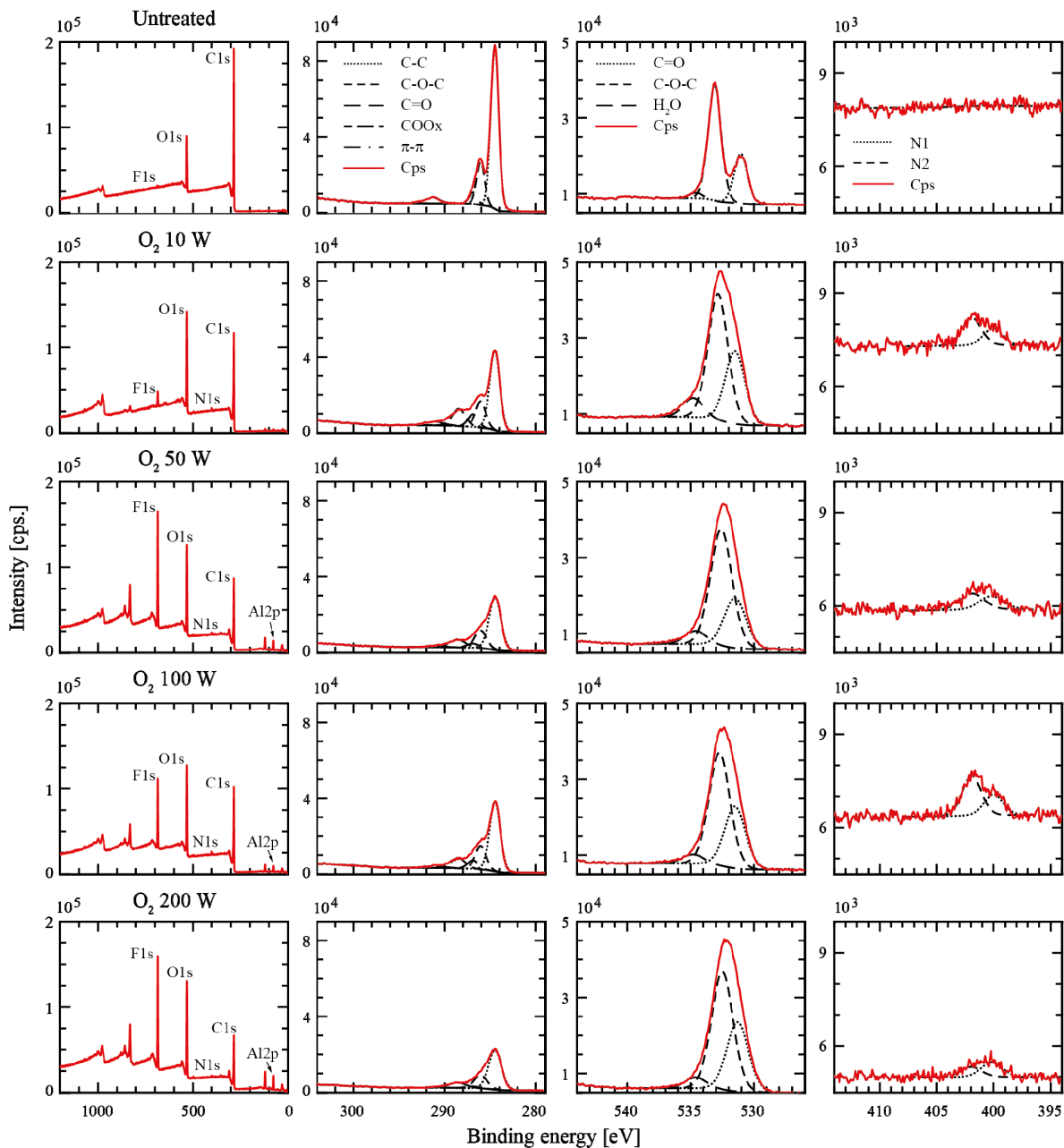


Figure 9. XPS spectra of oxygen plasma treated PEEK films. Survey spectra (first column) and detailed spectra of C1s, O1s and N1s.

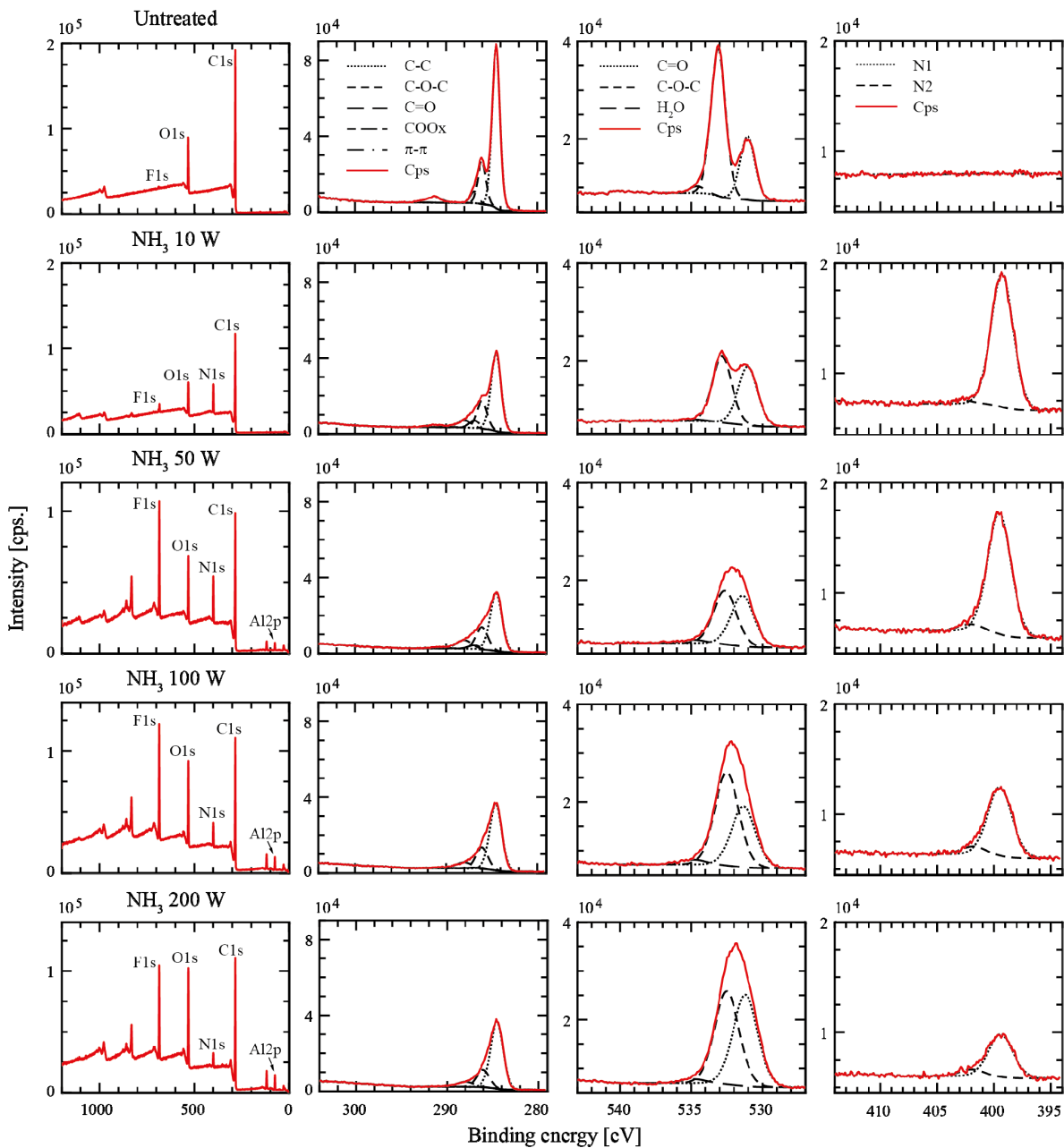


Figure 10. XPS spectra of ammonia plasma treated PEEK films. Survey spectra (first column) and detailed spectra of C1s, O1s and N1s.

3.9 Cell response to plasma-treated PEEK substrates

The initial cell adhesion on the plasma-treated PEEK substrates with two primary cells types, HDMEC (human dermal microvascular endothelial cells) and ASC (adipose tissue derived stem cells), is depicted in Figure 11 by optical micrographs of the stained cells (vital staining). Both cell types did not adhere homogenously on the original, not plasma-treated PEEK substrate but were well spread and grew to confluence after 48 h on the polystyrene control (tissue culture polystyrene – TCPS) and the ammonia plasma-treated PEEK substrates.

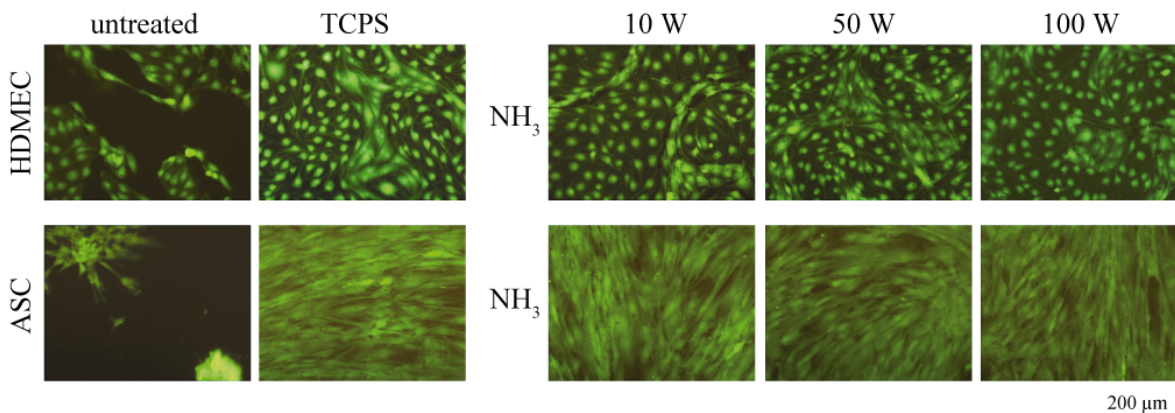


Figure 11. The optical micrographs show adipose tissue derived human mesenchymal stem cells (ASC) and human dermal microvascular endothelial cells (HDMEC) on ammonia plasma-treated PEEK substrates 48 h after seeding. The cells were stained by means of the green fluorescent intracellular calcein-AM vital stain. Both cell types do not homogeneously adhere to the untreated PEEK substrate but on the ammonia plasma treated substrates without exception.

Cells are known to react to their underlying substrate on the micrometer and nanometer scale [10, 24, 25]. Therefore, micro-structured PEEK substrates with grooves 1 μm deep and 20 μm wide were fabricated and additionally plasma treated to activate the substrate and to realize the nanometer-size features on top. ASC stretched and aligned parallel to such grooves and displayed an elongated phenotype as clearly verified in Figure 12. The control measurement on TCPS without grooves showed a random orientation of the adherent ASC. The ASC adhered to the original PEEK substrate did not reveal such homogeneous distribution as on the plasma-treated PEEK films. Both oxygen and ammonia plasma treated PEEK substrates allowed homogenous ASC adhesion. Adding a 5 nm-thin titanium film onto the PEEK surfaces always resulted in a homogeneously distributed cell layer.

The images taken in the red emission channel are supposed to uncover the dead cells stained by propidium iodide (PI). No dead ASC were found on the substrates. The images, however, allow detecting the micro grooves of the PEEK films because of the strong broadband auto-fluorescence of PEEK [12].

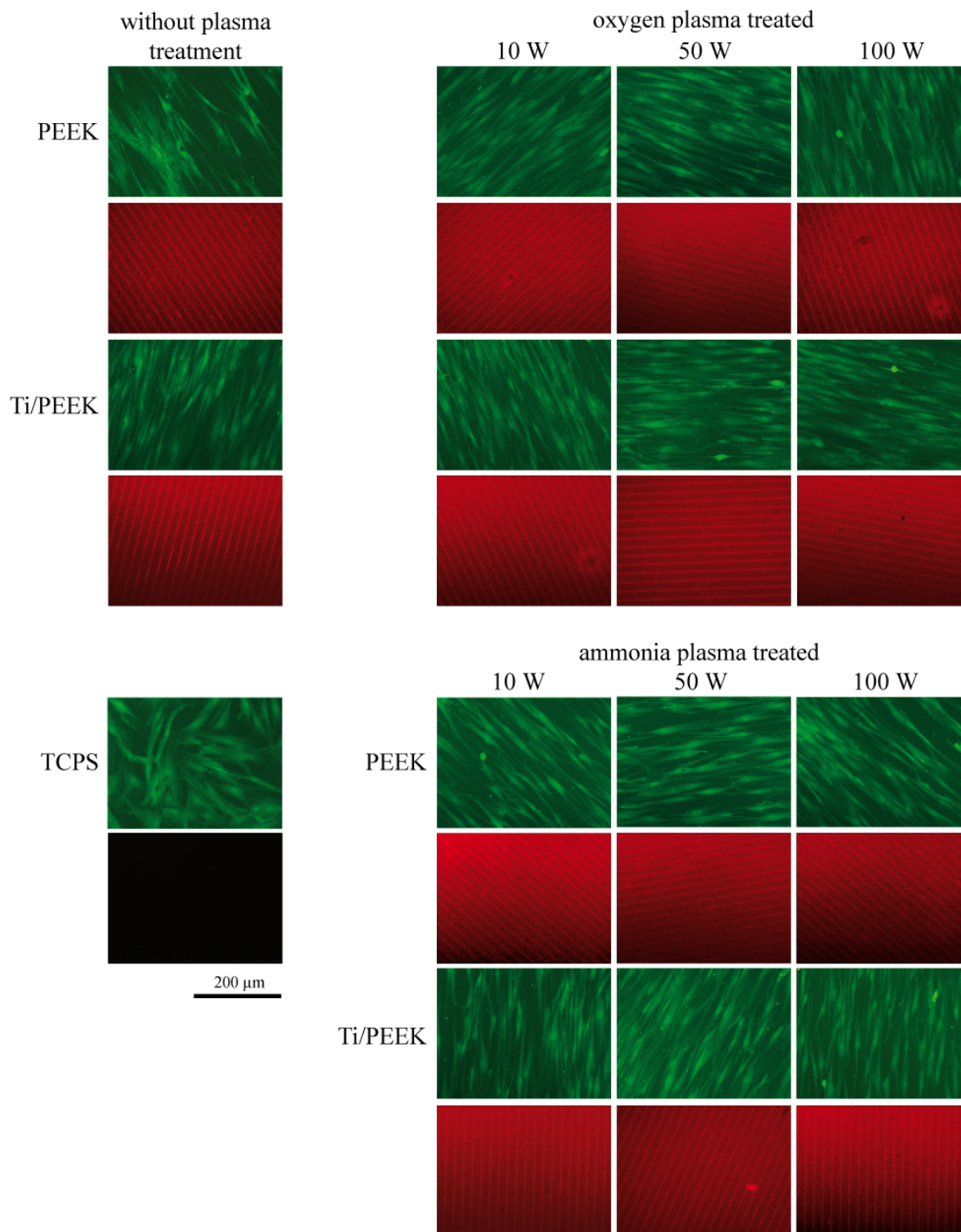


Figure 12. ASC aligned along micro-grooves on oxygen and ammonia plasma treated PEEK substrates 48 h after seeding. Vital cells were stained with calcein-AM. The micro-grooves including their orientation are visible in the red-colored images.

4. DISCUSSION

Improved design of injection molds and optimized processing allow the fabrication of polymer parts with dimensions in the micrometer range, which can be successfully applied as biosensors to detect DNA sequences or nM copper ion concentrations [6]. Such tiny products, however, are not yet medical implants, although microstructures such as grooves can be simultaneously generated integrating the thermally and mechanically stable negative pattern into the mold. The polymer surfaces, for example of PEEK implants, have to be activated to obtain the desired interaction with the biosystem. For bone implants one also needs a nanometer-scale roughness to mimic the apatite crystallites and further nanostructures present in human bone [26].

This study showed that ASC homogeneously adhere on oxygen and ammonia plasma treated PEEK substrates, which is a prerequisite for adequate cell differentiation and proliferation, since cytoskeletal tension plays a crucial role in stem cell differentiation [18, 27] and is closely related to the adequate density of focal adhesions, which is associated with the micro- and especially with the nanostructure of the implant's surface. McBeath et al. [27] proved that the cell shape regulates commitment of human mesenchymal stem cells (hMSCs) towards the osteogenic and adipogenic lineage. hMSCs allowed to adhere, flatten, and spread underwent osteogenesis, while unspread, round cells became adipocytes. Kilian et al. [18] verified that when exposed to competing soluble differentiation signals, cells cultured in rectangles with increasing aspect ratio and in shapes with pentagonal symmetry but with different sub-cellular curvature, and with each occupying the same area, display different adipogenesis and osteogenesis profiles. The results reveal that geometric features that increase cytoskeletal tension promote osteogenesis and maybe an approximation to the *in vivo* characteristics of the microenvironment of the differentiated cells.

To tailor the micro- and nanostructures on the polymer surface, however, is not enough. Surface chemistry is another important parameter, which determines the adsorption of proteins and thus cell behavior. Consequently, it is vital to characterize the net surface charge and the chemical composition of the polymer surface. Both experiments were carefully performed and agree with the expectations. The only exceptions are the presence of fluorine and aluminum. The presence of fluorine is associated with the segregation of moieties from fluorine containing precursors of PEEK. Aluminum probably arises from the vacuum chamber as the result of the high-energetic plasma.

Preparing micro-cantilevers with well-defined nanostructures after chemical activation to measure contractile cell forces as demonstrated by means of Si cantilevers [9] could therefore become an important tool to evaluate the performance of bone implants and to improve their biocompatible properties.

5. CONCLUSIONS

In order to realize load-bearing polymer implants, the mold defining the shape of the implant should be covered with microstructures. These surface structures can be directly replicated into the implant surface in a single step. Hence injection molding allows for easy replication of human tissue topography. In a second processing step, surfaces can be further modified by plasma treatments. This does not only chemically activate the surface, but also creates nanostructures, which can be tailored choosing the process gas composition, the plasma power and the duration of the treatment. One has to consider, however, aging phenomena of the metastable nanostructures and changes owing to contact with water and other species. Stem cell differentiation analysis will support the optimization of the implant surfaces to reach biocompatible properties approximately to that of human tissue itself.

ACKNOWLEDGEMENTS

The authors thank K. Jefimovs (Dübendorf) for the laser micro-machining of the mold, O. Häfeli (Windisch) for the injection molding, A. Caspari (Dresden) for the zeta-potential measurements, S. Adam for the cell-culture work, A. Salamon (Rostock) for methodical support in cell experiment analysis, M. Waser (Muttentz), K. Vogelsang, M. Altana, C. Spreu, S. Stutz, V. Guzenko (Villigen) for their technical assistance. The APTIV™ PEEK films were kindly provided by VICTREX. Financial support was provided by grants from the Swiss Nanoscience Institute (SNI-project 6.2), the Rectors Conference of the Swiss Universities (CRUS), the European Union and the Federal State of Mecklenburg-Vorpommern, Germany (ESF/IV-WM-B34-0006/08).

REFERENCES

- [1] J. Park, "Real time measurement of the contactile forces of self organized cardiomyocytes on hybrid biopolymer microcantilevers," *Anal. Chem.* 77, 6571 (2005).
- [2] X. R. Zhang, and X. Xu, "Development of a biosensor based on laser fabricated polymer microcantilevers," *Appl. Phys. Lett.* 85(12), 2423 (2004).
- [3] J. Thaysen, A. D. Yalçinkaya, P. Vettiger *et al.*, "Polymer-based stress sensor with integrated readout," *J. Phys. D: Appl. Phys.* 35, 2698-2703 (2002).
- [4] M. Calleja, M. Nordström, M. Álvarez *et al.*, "Highly sensitive polymer-based cantilever-sensors for DNA detection," *Ultramicroscopy* 105, 215-222 (2005).
- [5] P. Urwyler, O. Häfeli, H. Schiff *et al.*, "Disposable polymeric micro-cantilever arrays for sensing," *Procedia Eng.* 5, 347-350 (2010).
- [6] P. Urwyler, J. Köser, H. Schiff *et al.*, "Nano-mechanical transduction of polymer micro-cantilevers to detect bio-molecular interactions," *Biointerphases* 7(1), 8 (2012).
- [7] P. Urwyler, H. Schiff, J. Gobrecht *et al.*, "Surface patterned polymer micro-cantilever arrays for sensing," *Sensors and Actuators A: Physical* 172(1), 2-8 (2011).
- [8] F. Battiston, J. Ramseyer, H. Lang *et al.*, "A chemical sensor based on a microfabricated cantilever array with simultaneous resonance-frequency and bending readout," *Sensors and Actuators B* 77, 122-131 (2001).
- [9] J. Köser, S. Gaiser, and B. Müller, "Contractile cell forces exerted on rigid substrates," *Eur. Cells Mater.* 2, 479-487 (2011).
- [10] M. Riedel, B. Müller, and E. Wintermantel, "Protein adsorption and monocyte activation on germanium nanopyrramids," *Biomaterials* 22(16), 2307-16 (2001).
- [11] B. Müller, "Natural Formation of nanostructures: from fundamentals in metal heteroepitaxy to applications in optics and biomaterials science," *Surf. Rev. Lett.* 8(1-2), 169-228 (2001).
- [12] J. Althaus, C. Padeste, J. Köser *et al.*, "Nanostructuring polyetheretherketone for medical implants," *Eur. J. Nanomed.* 4, DOI: 10.1515/ejnm-2011-0001 (2012).
- [13] C. Chan, T. Ko, and H. Hiraoka, "Polymer surface modification by plasmas and photons," *Surf. Sci. Rep.* 24, 1-54 (1996).
- [14] S. M. Kurtz, and J. N. Devine, "PEEK biomaterials in trauma, orthopedic, and spinal implants," *Biomaterials* 28, 4845-4869 (2007).
- [15] J. Althaus, H. Deyhle, O. Bunk *et al.*, "Anisotropy in polyetheretherketone films," *J. Nanophoton.* accepted, (2012).
- [16] S. W. Ha, R. Hauert, K. H. Ernst *et al.*, "Surface analysis of chemically-etched and plasma-treated polyetheretherketone (PEEK) for biomedical applications," *Surf. Coatings Technol.* 96, 293-299 (1997).
- [17] K. Grundke, H. Jacobatsch, F. Simon *et al.*, "Physico-chemical properties of surface modified polymers," *J. Adhesion Sci. Technol.* 9, 327-350 (1995).
- [18] K. A. Kilian, B. Bugarija, B. T. Lahn *et al.*, "Geometric cues for directing the differentiation of mesenchymal stem cells," *Proc. Nat. Acad. Sci.* 107(11), 4872-4877 (2010).
- [19] K. Peters, Unger, Barth *et al.*, "Induction of apoptosis in human microvascular endothelial cells by divalent cobalt ions. Evidence for integrin-mediated signaling via the cytoskeleton," *J. Mater. Sci.: Mater. in Med.* 12, 955-958 (2001).
- [20] G. Beamson, and D. Briggs, [High resolution XPS of organic polymers—the scienta ESCA 300 data base.] John Wiley & Sons Ltd, Chichester (1992).
- [21] D. Clark, B. Cromarty, and A. Dilks, "A theoretical investigation of molecular core binding and relaxation energies in a series of oxygen-containing organic molecules of interest in the study of surface oxidation of polymers," *J. Polymer Sci.: Polymer Chem.* 16, 3173-84 (1978).
- [22] M. Olla, G. Navarra, B. Elsener *et al.*, "Nondestructive in-depth composition profile of oxy-hydroxide nanolayers on iron surfaces from ARXPS measurement," *Surf. Interface Anal.* 38(5), 964-974 (2006).

- [23] C. Jones and E. Sammann, "The effect of low power plasmas on carbon fibre surfaces," *Carbon* 28(4), 509-514 (1990).
- [24] D. Dohan Ehrenfest, P. Coelho, B. Kang *et al.*, "Classification of osseointegrated implant surfaces: materials, chemistry and topography," *Trends Biotechnol.* 28(4), 198-206 (2010).
- [25] F. Variola, J. B. Brunski, G. Orsini *et al.*, "Nanoscale surface modifications of medically relevant metals: state-of-the art and perspectives," *Nanoscale* 3(2), 335-353 (2011).
- [26] B. Müller, H. Deyhle, D. Bradley *et al.*, "Scanning x-ray scattering: Evaluating the nanostructure of human tissues," *Eur. J. Nanomed.* 3, 30-33 (2010).
- [27] R. McBeath, D. M. Pirone, C. M. Nelson *et al.*, "Cell shape, cytoskeletal tension, and RhoA regulate stem cell lineage commitment," *Developmental Cell* 6(4), 483-495 (2004).

Differentiation of human mesenchymal stem cells on plasma-treated polyetheretherketone

Jasmin Waser-Althaus · Achim Salamon ·
 Marcus Waser · Celestino Padeste · Michael Kreutzer ·
 Uwe Pieleles · Bert Müller · Kirsten Peters

Received: 29 May 2013 / Accepted: 10 October 2013 / Published online: 8 November 2013
 © Springer Science+Business Media New York 2013

Abstract Polyetheretherketone (PEEK) generally exhibits physical and chemical characteristics that prevent osseointegration. To activate the PEEK surface, we applied oxygen and ammonia plasma treatments. These treatments resulted in surface modifications, leading to changes in nanostructure, contact angle, electrochemical properties and protein adhesion in a plasma power and process gas dependent way. To evaluate the effect of the plasma-induced PEEK modifications on stem cell adhesion and differentiation, adipose tissue-derived mesenchymal stem cells (adMSC) were seeded on PEEK specimens. We demonstrated an increased adhesion, proliferation, and osteogenic differentiation of adMSC in contact to plasma-treated PEEK. In dependency on the process gas (oxygen or ammonia) and plasma power (between 10 and 200 W for 5 min), varying degrees of osteogenic differentiation

were induced. When adMSC were grown on 10 and 50 W oxygen and ammonia plasma-treated PEEK substrates they exhibited a doubled mineralization degree relative to the original PEEK. Thus plasma treatment of PEEK specimens induced changes in surface chemistry and topography and supported osteogenic differentiation of adMSC in vitro. Therefore plasma treated PEEK holds perspective for contributing to osseointegration of dental and orthopedic load-bearing PEEK implants in vivo.

1 Introduction

Polyetheretherketone (PEEK) is a high-temperature thermoplastic used as biomaterial for trauma, orthopedic and in this connection especially spine implants [1]. Owing to the chemical structure, it possesses relatively high mechanical stability as well as chemical and radiation resistance. Neither in vitro nor in vivo cell studies on PEEK showed signs of cytotoxicity, immunogenicity or mutagenicity [2–4]. In contrast to metals, PEEK is radiolucent and magnetic resonance imaging compatible, which allows diagnostic examination in implant's vicinity [4]. Young's modulus E of pure PEEK is between 3 and 4 GPa [5]. To increase elasticity of PEEK implants to that of cortical bone (~ 18 GPa), carbon fiber reinforcement was successfully used [3].

PEEK is hydrophobic and exhibits a low surface energy, which limits cell adhesion capacity [6]. Therefore, PEEK has been so far successfully used for applications where implant osseointegration is not essential [1]. Due to its relative inertness, several attempts were made to activate PEEK implant surfaces. Coatings with Ti and hydroxyapatite [2] as well as plasma treatment were shown to be compatible with PEEK [2, 7]. Processing without coating,

J. Waser-Althaus · A. Salamon · K. Peters (✉)
 Department of Cell Biology, Rostock University Medical Center,
 Schillingallee 69, 18057 Rostock, Germany
 e-mail: kirsten.peters@med.uni-rostock.de

J. Waser-Althaus · B. Müller
 Biomaterials Science Center, University of Basel, 4031 Basel,
 Switzerland

J. Waser-Althaus · M. Waser · U. Pieleles
 Institute for Chemistry and Bioanalytics, University of Applied
 Sciences and Arts Northwestern Switzerland, 4132 Muttenz,
 Switzerland

J. Waser-Althaus · C. Padeste
 Laboratory for Micro- and Nanotechnology, Paul Scherrer
 Institut, 5232 Villigen PSI, Switzerland

M. Kreutzer
 Center for Medical Research (ZEMFO), Rostock University
 Medical Center, 18057 Rostock, Germany

i.e. wet chemical activation [7–9] and plasma treatments [7, 10, 11] were shown to be alternatives. Treatment with oxygen and ammonium plasma creates functional groups at the surface of polymers, which can increase the surface energy (hydrophilicity) and modify the surface topography without affecting the bulk properties [12]. Therefore, oxygen and ammonia plasma show promise for surface activation of PEEK [13] potentially replacing elaborate coating techniques. It was shown that plasma treatment generates nanostructures on polymer surfaces such as polydimethylsiloxane [14], polymethyl methacrylate and PEEK [15]. Controlling plasma power and exposure time, nanostructures of defined size can be fabricated by oxygen and ammonia plasma treatments [13].

A decade ago, Zuk et al. [16] characterized a stem cell population within the adipose tissue that is of mesenchymal origin and able to undergo e.g. adipogenic (AS), osteogenic (OS), and chondrogenic differentiation. These cells are termed adipose tissue-derived stem cells (adMSC). Due to their primarily mesenchymal differentiation potential, their frequent occurrence and the ease of harvesting, adMSC are a potential alternative to mesenchymal stem cells (MSC) from bone marrow for utilization in regenerative therapies such as bone and adipose tissue regeneration [17–19].

In recent years, a number of studies demonstrated that the underlying substrate is a critical determinant of stem cell behaviour. The key material properties affecting stem cell or primary cell behaviour have been categorized into elasticity [20], surface morphology on micro- and nanometer scale [21–24] and surface chemistry [25]. Thus, successful adhesion and differentiation of MSC towards osteoblasts would significantly contribute to the development of iso-elastic, coating-free PEEK implants for orthopaedic applications.

In this study, we examined the differentiation of adMSC towards the OS and AS lineage *in vitro* in dependence of plasma treatment of PEEK substrates. To determine surface activation conditions for optimized cell differentiation, PEEK specimens were oxygen and ammonia plasma-treated using a series of plasma powers.

2 Materials and methods

2.1 Materials

The chemicals, enzymes, antibiotics and biological factors were supplied, if not indicated otherwise, by Sigma-Aldrich (Steinheim, Germany). Cell culture plastics were from Nunc and Greiner (Frickenhausen, Germany).

2.2 PEEK sheet pretreatment

Hot embossing with a HEX03 press (JENOPTIK Mikro-technik GmbH, Oberkochen, Germany) at a temperature of 160 °C and a pressure of 100 kN served to flatten commercially available amorphous APTIV™ PEEK sheets (Series 2000, Victrex Europa GmbH, Hofheim, Germany) with a thickness of 25 µm between two polished 4-inch silicon wafers. During this process the PEEK changes from amorphous to a partially crystalline state [26].

2.3 Plasma treatment (plasma etching)

Oxygen/argon or ammonia plasma treatments (Piccolo system, Plasma Electronic, Neuenburg, Germany) activated the embossed PEEK sheets. PEEK specimens were placed at the bottom of the plasma chamber (RF-system, 13.56 MHz). Subsequently, the chamber was evacuated, flushed for a period of 5 min with oxygen/argon (200/100 sccm, 99.5/99.2 %, Messer, Lenzburg, Switzerland) or ammonia (200 sccm, 99.98 %, Messer, Lenzburg, Switzerland) and then equilibrated for further 5 min with oxygen/argon (20/10 sscm) or ammonia (30 sccm) gas. The plasma treatments of 5 min using a power of 10–200 W resulted in pressures between 0.5 and 1.8 Pa and bias voltages between 55 and 400 V. Argon was used to support the oxygen plasma.

Since plasma-activated polymer surfaces are subjected to molecular changes termed ageing [27], we performed the presented experiments with the activated PEEK specimens 7 days after plasma treatment.

2.4 Water contact angle measurements

The wettability of (plasma-treated) PEEK was determined with double distilled water (ddH₂O) by the sessile drop contact angle method using a contact angle goniometer (Drop Shape Analysis System PSA 10Mk2, Krüss, Hamburg, Germany). Contact angles were measured 5 s after placing the 4 µL drop at room temperature in triplicate.

2.5 Scanning electron microscopy

The plasma-treated PEEK specimens were coated with Au/Pd (9 nm) during 30 s using a current of 20 mA in a vacuum of 6 Pa (sputter coater Polaron, Thermo VG Scientific, East Grinstead, United Kingdom). Substrate surfaces were investigated with the field emission scanning electron microscope Supra 40 VP (Carl Zeiss, Jena, Germany) at an applied acceleration voltage of 10 kV using an InLens detector.

2.6 Protein adsorption

The protein amount is quantified via the colorimetric conversion of a bichinonic acid Cu^+ complex in solution. In this manner the protein was quantified directly when adsorbed on the substrate. The PEEK specimens were stamped out in a 12 mm diameter format, the treated side was wetted with phosphate-buffered saline (PBS) and then incubated on a 200 μL drop of 10 % foetal calf serum (FCS, PAN-Biotech GmbH, Aidenbach, Germany) or 10 mg/mL bovine serum albumin (BSA, Cohn fraction V) in PBS for 2 h at 37 °C using the inverted drop method: the 200 μL drop was placed on a parafilm in a wet chamber and the PEEK specimen was placed on the drop with the treated side. The incubated PEEK was subsequently washed with PBS using the inverted drop method to remove excess protein. The specimens were then incubated with 600 μL micro BCA reagent (Thermo Scientific, Rockford, USA) at 60 °C for 1 h and the protein concentration was determined via the optical density at 562 nm.

2.7 Zeta-potential measurements

All streaming potential measurements to determine the zeta potential values were carried out with the Electrokinetic Analyzer (Anton Paar KG, Graz, Austria) and the measuring cell for flat plates as described previously [28].

2.8 XPS measurements

XPS studies were carried out by means of an Axis Nova photoelectron spectrometer (Kratos Analytical, Manchester, England). The spectrometer was equipped with a monochromatic Al $\text{K}\alpha$ ($h\nu = 1,486.6$ eV) X-ray source operated at a power of 225 W. The kinetic energy of the photoelectrons was determined with a hemispheric analyser set to a pass energy of 160 eV for the wide-scan spectra and 40 eV for the high-resolution spectra (full-width-at-half-maximum of $\text{Ag}3d_{5/2}$ was 1.8 and 0.6 eV, respectively). During the measurements, electrostatic charging of the specimen was overcompensated by means of a low-energy electron source. The peak fitting was performed with the CasaXPS software (Version 2.3.15, Casa Software Ltd.). The energy scale of the spectra was calibrated against the C_{1s} line of aliphatic carbon at $E_b = 285.0$ eV. An iterated Shirley background was subtracted from the spectra. Quantitative elemental compositions were determined from peak areas.

2.9 Cell culture

Human adMSC from liposuction-derived adipose tissue were isolated by collagenase digestion (collagenase NB4

from *Clostridium histolyticum*, 0.12 PZ units (Wünsch)/mg, 6 mg/mL adipose tissue, Serva, Heidelberg, Germany). The enzymatic digestion was performed for 0.5 h at 37 °C (slight shaking). Afterwards the homogeneous solution was filtered through a 100 μm filter (nylon cell strainer, BD Falcon, Heidelberg, Germany) and the resulting cell suspension was washed three times with PBS containing 10 % FCS (PAN, Aidenbach, Germany) and repeated centrifugation at $400\times g$ for 5 min. The final cell pellet was resuspended in DMEM (Gibco Invitrogen, Karlsruhe, Germany) containing 10 % FCS and antibiotics (final concentration: 100 U/mL penicillin, 100 $\mu\text{g}/\text{mL}$ streptomycin, Invitrogen, Germany), seeded in cell culture flasks and cultivated at 37 °C and 5 % CO_2 in a humidified atmosphere. 24 h after cell isolation the CD34-positive subpopulation was isolated by the Dynal[®] CD34 progenitor cell isolation system (Invitrogen, Karlsruhe, Germany) as described previously [19]. These experiments were conducted with the approval of the ethics committee (Medical Faculty, University of Rostock) and the full consent of the patients.

In the fourth passage seeding of cells into experimentation was done at 20,000 cells per cm^2 . Absence of contaminating monocytes/macrophages and endothelial cells was confirmed by flow cytometry (FACSCalibur; BD Biosciences AG, Heidelberg, Germany) proving the absence of $\text{CD}14^+/\text{CD}68^+$ (eBioscience, Frankfurt a. M., Germany) and $\text{CD}31^+$ (Millipore, Schwabach, Germany) cells, respectively. After seeding, adMSC were cultured until confluence was reached and then stimulated to differentiate using OS differentiation stimulating medium (OS: basal medium plus 0.25 g/L ascorbic acid, 1 μM dexamethasone and 10 mM beta-glycerophosphate) or AS differentiation stimulating medium (basal medium plus 1 μM dexamethasone, 500 μM IBMX, 500 μM indomethacin, 10 μM insulin). For the unstimulated (US) adMSC control cultures the basal medium did not contain any specific differentiation factors. Start of stimulation is termed day zero of experimentation. The plasma treated PEEK specimens were punched out to fit into a 96 well format, sterilized with 70 % ethanol (LiChrosolv, MERCK, Darmstadt, Germany) washed two times with Dulbecco's PBS (without Ca^{2+} and Mg^{2+} , sterile; PAA Laboratories GmbH, Cölbe, Germany), and incubated with medium for 2 h before adMSC seeding. All experiments represented as box plots were performed at least 4 different liposuction-derived adipose tissue donors.

2.10 Cell number quantification

Quantification of adMSC number at the distinct experimental conditions was done indirectly using the basic dye crystal violet [29]. Due to a linear correlation, cell numbers

can indirectly be determined quantifying the optical density of the re-solubilised dye [30]. Briefly, cells were washed with PBS, fixed with 2-propanol (SERVA Electrophoresis GmbH, Heidelberg, Germany), permeabilised (0.05 % Tween 20 in PBS), stained with crystal violet (0.1 % in PBS) for 60 min and washed with ddH₂O. Subsequently, bound crystal violet was dissolved in acetic acid (33 %; Merck KGaA, Darmstadt, Germany), transferred to an optical plate and quantified via its optical density at 600 nm (anthos 2010 optical density microplate reader; anthos Mikrosysteme GmbH, Krefeld, Germany).

2.11 Quantification of alkaline phosphatase (ALPL) activity

ALPL catalyses the hydrolysis of an arylphosphate residue of its synthetic substrate para-nitrophenyl phosphate (pNPP) into the coloured product paranitrophenol [31]. Thus, by quantification of the optical density of the coloured product generated in a given time, the ALPL activity can be determined.

For this analysis cells were washed with Tris-buffered saline, lysed using a detergent- and protease inhibitor-containing buffer (1 % Tween 20 and 100 µM phenylmethanesulfonylfluoride/PMSF (AppliChem GmbH, Darmstadt, Germany) in ddH₂O, incubated with ALPL substrate solution (10 mM pNPP, AppliChem GmbH, Darmstadt, Germany), 100 mM 2-amino-2-methyl-1,3-propanediol and 5 mM MgCl₂ (AppliChem GmbH, Darmstadt, Germany) in ddH₂O for 60 min at 37 °C, 5 % CO₂ in a humidified atmosphere. pNPP conversion was stopped using 2 M NaOH, and the optical density of the supernatant was quantified at 405 nm.

2.12 Quantification of extracellular matrix calcium content

Extracellular matrix calcium content was optically quantified using cresolphthalein. In order to quantify only the concentration of calcium ions in solution, magnesium ions have to be masked. This was accomplished by adding the chelating agent 8-hydroxy chinoline [30]. The procedure used was adapted from Proudfoot et al. [32] and involves acidic liberation of calcium ions from the extracellular matrix and subsequent complexation under alkaline conditions. For that purpose, cells were washed with PBS, fixed with 4 % paraformaldehyde (PFA) pre-warmed to 37 °C, washed with ddH₂O and then incubated in cresolphthalein buffer (0.1 mg/mL ortho-cresolphthalein complexon, 1 mg/mL 8-hydroxy chinolin and 6 % (v/v) of 37 % HCl in ddH₂O) for 5 min. Then, 2-amino-2-methyl-1-propanol (AMP) buffer (15 % AMP) in ddH₂O, pH = 10.7 was added, and after 20 min, the

supernatant was transferred to an optical plate to quantify the optical density at 580 nm.

2.13 Quantification of cellular lipid content

Cellular lipid content was determined using an unmodified lipophilic boron dipyrromethene (Bodipy) dye which dissolves well in cellular neutral lipids, most of which being triglycerides, that build the core of lipid droplets and that are surrounded by a monolayer of phospholipids [33]. Bodipy fluoresces upon excitation at 480 nm or maximal at 493 nm and emits a green fluorescence at 503 nm. Thus, the intensity of the fluorescence emitted by the Bodipy stain is proportional to the total amount of lipid stored within a cell. Briefly, cells were washed with PBS, fixed in 4 % PFA pre-warmed to 37 °C, washed with PBS, incubated in Bodipy solution (1 µg/mL, BODIPY 493/503 (Life Technologies GmbH, Darmstadt, Germany) in 150 mM NaCl) for 10 min in the dark, washed with PBS and subsequently with ddH₂O. The stained cells were investigated under the microscope in standard filter-based fluorescence microscopy (Axio Scope.A1 with AxioCam MRc, both Carl Zeiss MicroImaging GmbH, Göttingen, Germany). To quantify the cellular lipid content, images were converted into linear grey scale mode, the background level was calculated judging the histograms of a group of images of US adMSC, and a PHP-script (www.php.org), complemented by functions of the ImageMagick (www.imagemagick.org) software suite, was used to assess all pixels, cumulated their number as area and their intensity as voxel.

2.14 Live cell staining

Visualization of living cells was done by fluorescence staining with calcein AM. Cells were incubated in basal medium containing calcein AM (Biomol GmbH, Hamburg, Germany) at 1 µM for 15 min at 37 °C, 5 % CO₂ in a humidified atmosphere. Then, this staining solution was exchanged by basal medium, and cells were examined under the microscope in standard filter-based fluorescence microscopy at 496 nm (excitation) and 516 nm (emission).

2.15 Data normalization

To facilitate statistical analysis of the metrical data obtained, data were normalized. To this end, the data, as e.g. ALPL activity, for each adipose tissue donor was collected, and the minimum (x_{\min}) and maximum (x_{\max}) value for all treatment conditions and time points were determined. The position of a distinct value x obtained for this parameter and individual with respect to the extremes x_{\min} and x_{\max} was then represented as $x_{\text{norm}} = (x - x_{\min}) /$

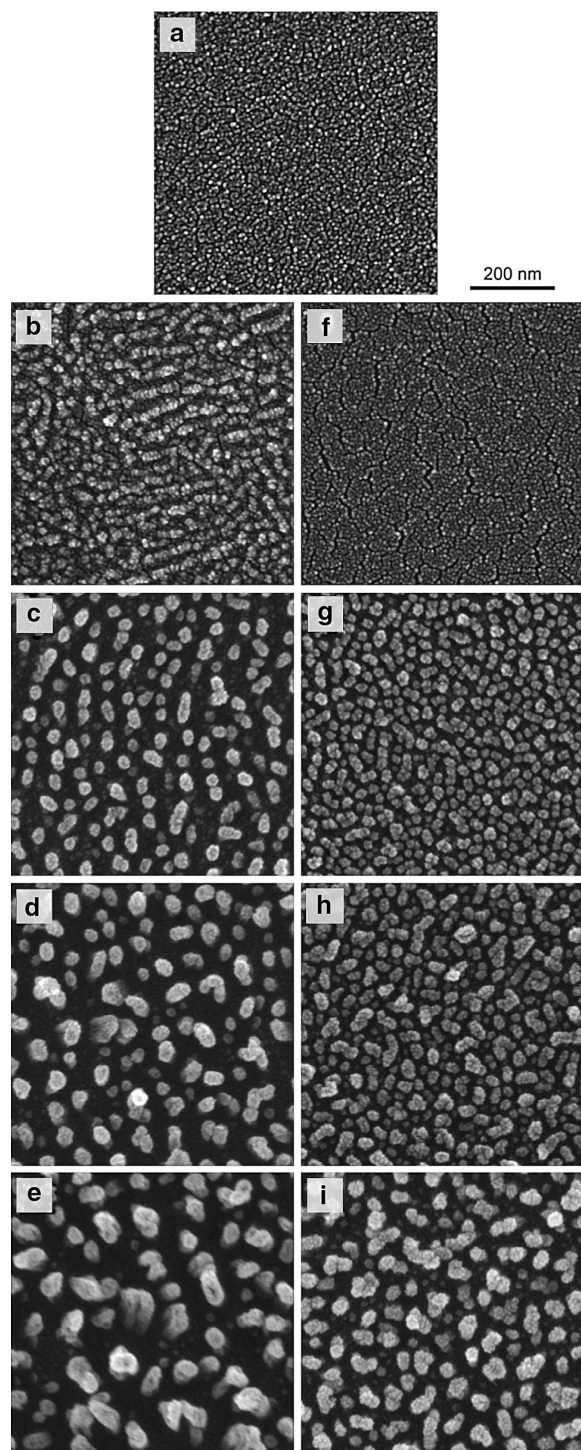


Fig. 1 SEM images of original PEEK (a) and 10, 50, 100, 200 W oxygen plasma-treated (b–e) and 10, 50, 100, 200 W ammonia plasma-treated (f–i) PEEK specimens

$(x_{\max} - x_{\min})$. This operation scales the values obtained for each individual and parameter to a range from zero to one.

2.16 Data presentation

Data are habitually presented as box plots. Here, the solid box represents 50 % of the measured values that assemble around the median indicated by a horizontal line. The box ranges from the 25th to the 75th percentile, i.e. that 25 % of the measured values lay below the lower border of the box and 25 % of them lay above the upper border of the box. Error bars starting below and above the box indicate the 5th and 95th percentile.

2.17 Statistics

All mean values were compared by a non-parametric one-way ANOVA test using Prism 5 (GraphPad Software, Inc., La Jolla, USA). Statistical significance of differences was accepted for $P < 0.05$.

3 Results

3.1 Plasma treatment of PEEK substrates

For activation of the hydrophobic PEEK surface, we applied oxygen and ammonia plasma with powers between 10 and 200 W for a period of 5 min. Both plasma treatments generated a homogenous nanopatterning of the surface with increased roughness. As demonstrated in Fig. 1, oxygen plasma had a stronger effect (Fig. 1b–e) than ammonia plasma (Fig. 1f–i) for identical plasma duration and power. While 10 W oxygen plasma treatment led to pillar-like structures in the range of 10 nm, 200 W treatment resulted in structures with a size of about 50 nm. 200 W ammonia plasma created structures with sizes of about 25 nm.

To further characterize the plasma-treated PEEK surfaces, static water contact angle and protein adsorption measurements were performed. The results of static water contact angle measurements are shown in Fig. 2a. The original PEEK specimen revealed a contact angle of more than 80° . Increasing oxygen plasma power resulted in reduction of contact angles, i.e. being 40° for 10 W and 5° for 200 W. Ammonia plasma treatments also resulted in a decrease of contact angle which, however, increased in dependency of the plasma power, i.e. being 45° for 10 W and 90° for 200 W. In all cases, the amount of adsorbed protein gained with increasing plasma power as illustrated

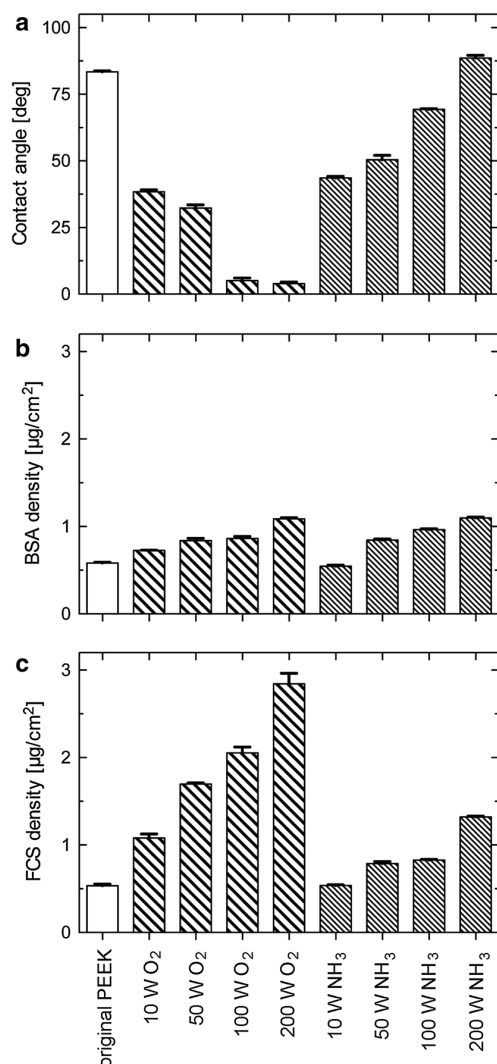


Fig. 2 **a** Static water contact angle of original and of oxygen and ammonia plasma-treated PEEK specimens at day 7 after processing. **b** BSA and **c** FCS adsorption (2 h, 37 °C) of original, oxygen and ammonia plasma-treated PEEK specimens at day 7 after processing, quantified by the micro BCA assay

in Fig. 2b and c. BSA density on oxygen and ammonia plasma-treated specimens as well as FCS on ammonia plasma-treated PEEK was doubled with respect to the original specimens for powers of 200 W, whereas the FCS density on oxygen plasma-treated specimens raised by a factor of six.

Furthermore, the electrochemical surface properties, i.e. the charge of the plasma-treated PEEK specimens, were investigated by zeta-potential measurements via the streaming potential at varying pH-values (Fig. 3). The original PEEK showed a zeta potential of zero at a pH of 3.9, which is the point of zero net charge and therefore

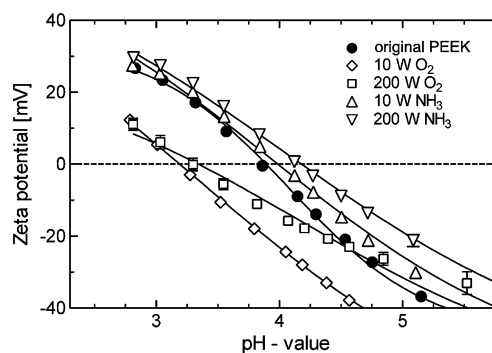


Fig. 3 Zeta-potential measurements of original, oxygen (10 and 200 W) and ammonia plasma-treated (10 and 200 W) PEEK specimens via the streaming potential at given pH-values. The isoelectric points (zeta potential zero) correspond to 3.9, 3.2, 3.3, 4.0, and 4.2, respectively

Table 1 XPS analysis of non-treated and plasma-treated PEEK specimens. Relative concentrations of the detected elements and O/C and N/C ratios as a function of plasma processing parameters

PEEK type	C %	O %	N %	F %	Al %	O/C	N/C
Original PEEK	85.4	13.4	0.1	0.3	0	0.16	0.00
O ₂ (0 W plasma)	67.9	25.2	1.2	3.4	1.2	0.37	0.02
O ₂ (50 W plasma)	56.7	22.0	1.5	14.6	4.7	0.39	0.03
O ₂ (100 W plasma)	45.9	21.8	0.9	22.7	8.0	0.48	0.02
O ₂ (200 W plasma)	37.5	25.8	0.8	23.4	11.7	0.69	0.02
NH ₃ (10 W plasma)	72.0	11.9	13.1	2.3	0.4	0.17	0.18
NH ₃ (50 W plasma)	57.9	10.9	11.8	15.4	4.0	0.19	0.20
NH ₃ (100 W plasma)	54.6	15.4	6.7	16.2	7.0	0.28	0.12
NH ₃ (200 W plasma)	53.8	19.2	4.5	13.4	8.5	0.35	0.08

corresponds to its isoelectric point (pI). Oxygen plasma treatment resulted in lower pIs, i.e. of 3.2 for a power of 10 W and 3.3 for 200 W, because of the generation of negatively charged groups at the PEEK surface. Ammonia plasma treatment shifted the pI to higher values, i.e. to 4.0 for a power of 10 W and to 4.2 for 200 W.

To gain information about the chemical composition of the plasma-treated PEEK surfaces, XPS spectra were acquired. As summarized in Table 1, there are significant differences between the plasma-treated and the original PEEK surfaces as already shown in more detail elsewhere [34]. The treatment with oxygen plasma led to surface oxidation, as indicated by the O/C ratio which increased steadily with increasing treatment power. Comparably, NH₃-plasma treatment leads to introduction of surface-amino groups. However this effect and therefore the N/C ratio decreased with increasing plasma power. Unexpectedly, the XPS measurements revealed also an enrichment of

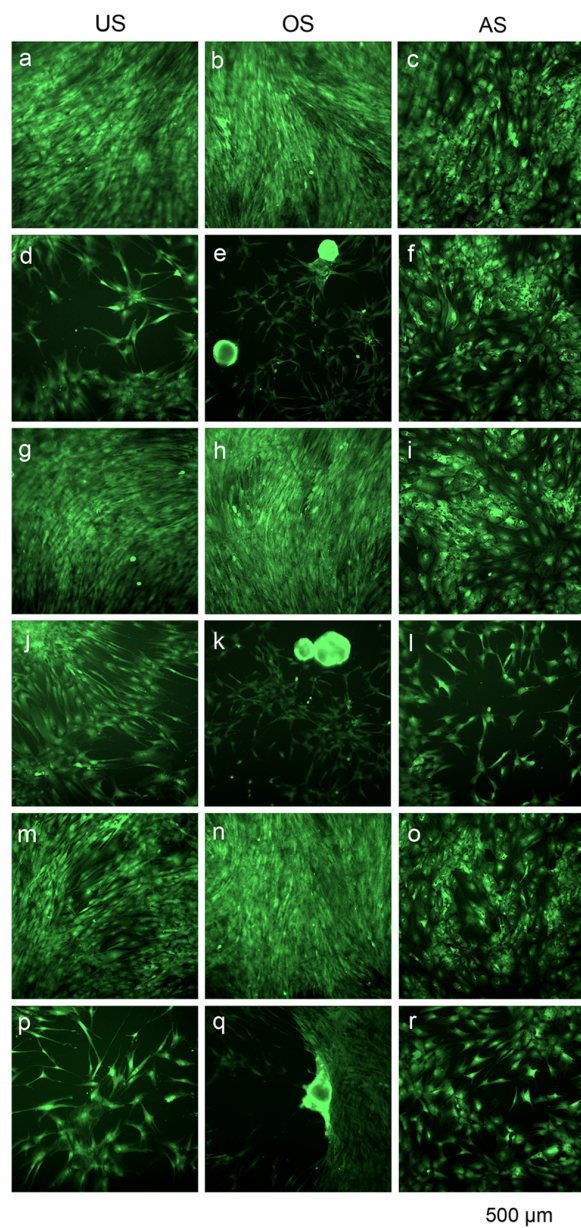


Fig. 4 Calcein AM stain of adMSC at day 14 of culture on TCPS (a–c), original PEEK (d–f), 10 W oxygen plasma-treated (g–i), 200 W oxygen plasma-treated (j–l), 10 W ammonia plasma-treated (m–o) and 200 W ammonia plasma-treated (p–r) PEEK specimens

fluorine and aluminium (present in the oxidized state) on the specimen surfaces at 50–200 W plasma power (Table 1).

3.2 adMSC adhesion and phenotype on plasma-treated PEEK substrates

The effect of the plasma-treated PEEK substrates on adMSC phenotype, vitality, proliferation and differentiation

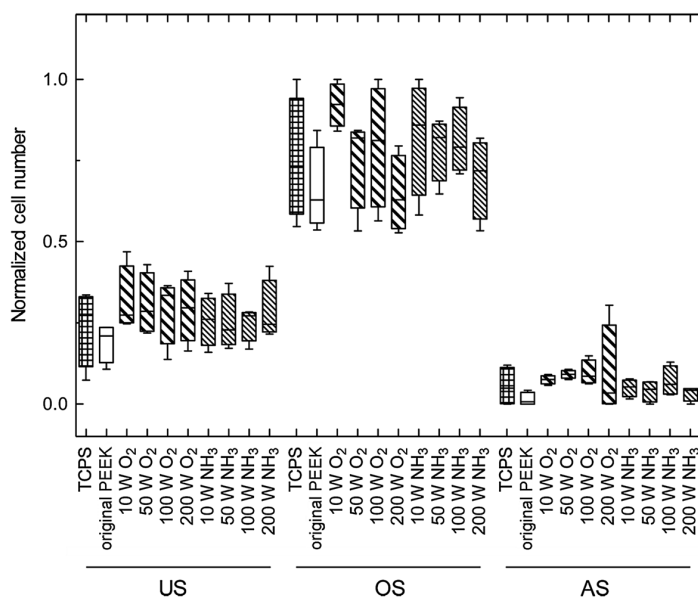
was analysed for US, OS and AS cell culture conditions. The vital staining revealed that the adMSC adhered on standard tissue culture polystyrene (TCPS) and proliferated until confluence under US, OS and AS differentiation conditions at day 14 (Fig. 4a–c). On the original PEEK substrates, adhesion of the adMSC under US and OS conditions was weak and the cells frequently formed spheroids (Fig. 4d, e). adMSC adhesion under AS conditions contrastingly was unaffected in comparison to TCPS (Fig. 4f). Low power oxygen plasma treatment (10 W) resulted in reproducible adMSC adhesion on PEEK (Fig. 4g–i) similar to adhesion on TCPS, whereas high-power oxygen plasma treatment (200 W) allowed only sparse adMSC adhesion for all treatment conditions (Fig. 4j–l). Similar to the oxygen plasma-treated PEEK substrates, adMSC adhered well to the 10 W ammonia plasma-treated PEEK substrates (Fig. 4m–o), but weakly to the 200 W ammonia plasma-treated specimens (Fig. 4p–r). 50 and 100 W oxygen plasma and ammonia plasma-treated specimens gave rise to similar behaviour as noticed for 10 W plasma-treated PEEK specimens (data not shown). Notably, the spheroid formation was only observed up to day 14 of cultivation. After 21 and 28 days, the substrates were completely cell-covered.

adMSC proliferation was quantified for day 14, day 21 and day 28 (results from day 14 see Fig. 5). For all time points measured, the oxygen and ammonia plasma treatments of PEEK specimens up to a power of 100 W led to higher cell numbers than on TCPS and on original PEEK substrates. Under OS conditions, adMSC proliferation was increased, whereas it was halted under AS conditions. We found a dependence of cell number on plasma power for oxygen plasma-treated PEEK substrates under OS conditions, increasing plasma powers resulting in decreasing cell numbers, as qualitatively observed on the live stain images (cp. Fig. 4).

3.3 Differentiation of adMSC on plasma-treated PEEK substrates

OS differentiation was investigated analysing the ALPL activity at day 14 and the mineralization degree at day 28 under OS and US conditions (Fig. 6). ALPL activity was generally increased for OS conditions compared to the US control (Fig. 6a). We observed a plasma power dependent regulation of ALPL activity, being increased on 10 and 50 W plasma-treated PEEK substrates compared to TCPS, the original PEEK substrate and the US controls, but decreased for higher plasma powers. This phenomenon was observed for both reaction gases, while oxygen plasma showed a stronger impact. At day 21 and day 28, such a clear dependency was not found (data not shown).

Fig. 5 adMSC quantification at day 14 of culture on TCPS, original PEEK and oxygen and ammonia plasma-treated PEEK specimens with crystal violet. Data were normalized to values between 0 and 1, $n = 4$



Mineralization was quantified at day 28 (Fig. 6b). Again, we discovered a plasma power dependent regulation of OS differentiation as seen for ALPL activity, since mineralization was increased for the lower plasma power treated PEEK specimens (10 and 50 W) in comparison to the TCPS and the original PEEK substrate controls, but it was decreased for higher plasma power treated PEEK specimens (100 and 200 W).

Furthermore, we investigated the AS differentiation potential of adMSC on plasma-treated PEEK substrates. Cellular lipid accumulation was analysed at day 14 and day 21 under AS and US conditions. Generally, lipid accumulation occurred only under AS conditions. Quantification of cellular lipid content revealed a slight and homogenous increase on ammonia plasma-treated PEEK between 10 and 100 W (approx. 120 % compared to original PEEK), whereas the lipid content was reduced on 200 W ammonia plasma-treated PEEK (approx. 80 %). The lipid accumulation on oxygen plasma-treated PEEK substrates was generally lower compared to original and ammonia plasma-treated PEEK (10–100 W approx. 90 % and 200 W approx. 60 % compared to original PEEK).

4 Discussion

4.1 Surface characteristics

To refine PEEK as suitable polymer for load-bearing implants, its hydrophobic surface needs to be activated to allow cell attachment. Plasma treatments can specifically affect the chemistry and the nanostructure of the substrate's

surface [6, 7, 13, 15]. The nanometer-scale topography can be tailored controlling the plasma power, exposure time and process gas composition [13]. Since an increased root-mean-square roughness leads to enhanced protein adsorption, the plasma-induced changes of PEEK surface topography could affect protein adsorption [35]. We could show that plasma treatment strongly impacts water contact angle and protein adsorption. In accordance to literature suggesting that neither extremely hydrophobic nor hydrophilic surfaces bind proteins in conformations accessible for cells [36], adMSC adhesion and proliferation was highest on oxygen and ammonia plasma treated PEEK substrates showing contact angles between 30° and 50°. With increasing plasma power an increase in surface roughness and higher amounts of BSA and FCS were detected. The detected BSA density of 0.6 $\mu\text{g}/\text{cm}^2$ on the original PEEK substrates agrees well with the values calculated for monolayer coverage, which corresponds to 0.7 $\mu\text{g}/\text{cm}^2$ assuming an area of 4 nm \times 4 nm per BSA molecule. According to line profiles from AFM measurements, the increase of surface area for the roughest PEEK substrates treated with 200 W plasma is about 15 % for ammonia and about 90 % for oxygen processing compared to the original PEEK. These values for the surface increase was extracted from previous detailed AFM studies on the plasma treated PEEK [13]. While for BSA and FCS one observes a doubling of protein adsorption on 200 W ammonia-treated substrates, 200 W oxygen-plasma led to twofold and sixfold densities for BSA and FCS, respectively, compared to the original PEEK. The consideration of surface enlargement can, therefore, only partly explain the increased protein adsorption. Hence, one may conclude that the

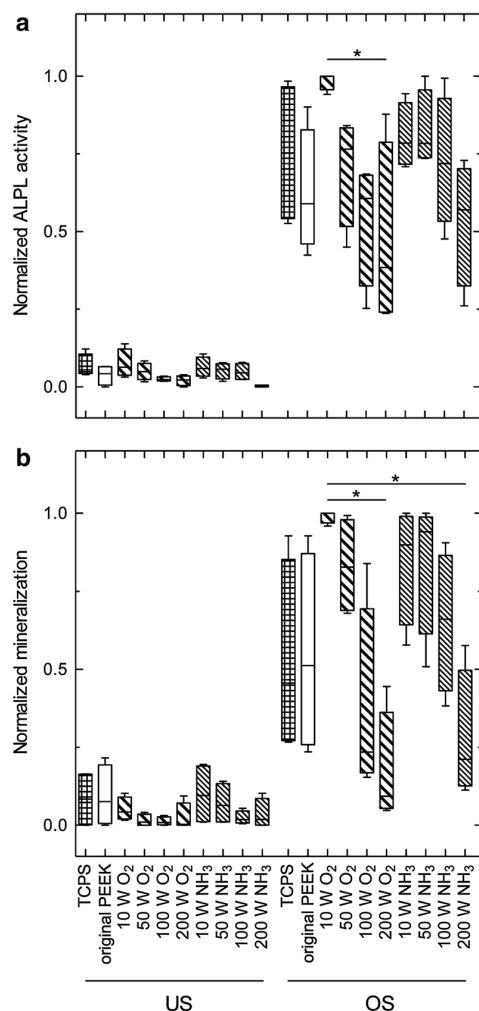


Fig. 6 Osteogenic differentiation of adMSC on TCPS, original, oxygen and ammonia plasma-treated PEEK substrates. **a** ALPL activity at day 14 of culture under US and OS conditions. **b** In vitro mineralization at day 28 under US and OS conditions. Data were normalized to values between 0 and 1, $n = 4$

nanostructures act as nucleation centres for the proteins, an effect that was described for immunoglobulins and BSA on nanopyramidal surfaces [37, 38]. In contrast to BSA, FCS contains a mixture of proteins, potentially enabling selective protein adsorption. In this context, the local surface charge plays a crucial role. For instance, it was shown that hydroxyapatite functionalized with differently charged amino acids, namely arginine or aspartic acid, selectively bound more BSA or lysozyme in a competitive protein adsorption assay [39]. Oxygen plasma treatments shifted the pI of the PEEK specimens significantly towards the acidic range through creation of negatively charged carboxylic acid or ester groups, whereas ammonia plasma treatments gave rise to a more alkaline pI because of the

creation of positively charged amine groups [34]. In accordance to our observations, Safinia et al. [40] noted that air plasma shifted the pI towards the acidic range, whereas ammonia plasma in combination with water treatment resulted in a pI slightly shifted towards the basic pH range.

Interestingly, our XPS measurements revealed a decreasing N/C ratio with increasing ammonia plasma power. High ammonia plasma powers cause etching and loss of NH₂ radicals from the surface, resulting in lower amounts of incorporated nitrogen on the PEEK surface [27]. This may also explain why contact angles increased with increasing plasma power. The higher plasma powers resulted in increasing amounts of fluorine and aluminium on the PEEK surface for both process gases. As one of the starting materials in the production of PEEK is fluorinated, the accumulation of fluorine with increasing plasma power is explained by thermally activated surface segregation of fluorinated residues in the PEEK specimens [41]. The plasma chamber, which is made from aluminium, is most likely the source of the aluminium oxide on the plasma treated specimens. Since Mendonça et al. [42] and Cooper et al. [43] have shown that aluminium oxide or fluoride-containing coatings of titanium implants may enhance OS differentiation we do not expect impairing effects from the accumulation of aluminium and fluorine on our substrates.

4.2 Cellular reactions

Adhesion of adMSC was higher on low power oxygen and ammonia plasma-treated PEEK specimens (10 and 50 W) where the root-mean-squared (RMS) roughness is smaller (average height for oxygen plasma is 9 and 18 nm, for ammonia plasma 3 and 7 nm, respectively) than for the more powerful plasma treatments (i.e. 100 and 200 W) (average height for oxygen plasma is 24 and 37 nm, for ammonia plasma 11 and 13 nm, respectively), according to AFM line scans. Dalby and colleagues have demonstrated that nanostructures in the height-range of 13 nm positively influence fibroblast adhesion and proliferation, whereas 95 nm high nanostructures have a negative effect [23, 44]. PEEK substrates that supported adMSC adhesion also induced pronounced OS differentiation (i.e. 10 and 50 W oxygen and ammonia plasma-treated PEEK), whereas PEEK substrates that impaired adMSC adhesion also impaired OS differentiation (i.e. 200 W oxygen and ammonia plasma-treated PEEK). This correlation was first described by Spiegelman and Ginty [45]. These authors examined a dependency of the differentiation characteristics of the AS cell line 3TE-F442A on the adhesion substrate and demonstrated that well-spread cells exhibited less AS differentiation than cells with weaker adhesion. McBeath et al. [22] showed that bone marrow MSC that

were allowed to adhere, flatten, and spread underwent osteogenesis, while unspread, round cells became adipocytes. These cell shape induced differentiation changes of MSC were accounted to the signalling of the small GTPase RhoA, which is involved in the regulation of cytoskeletal tension [22]. Furthermore, our experimental findings correlate well with the observations of Poulsson and Richards, who found that human primary osteoblast-like cells show higher levels of in vitro mineralization on oxygen plasma treated PEEK in comparison to unmodified PEEK surfaces [6].

Noticeably, while US and osteogenically stimulated adMSC did not adhere comprehensively on original PEEK, adipogenically stimulated adMSC exhibited a homogenous growth even on original PEEK. These differences in adhesion of adMSC could evolve from the mode of action of a ligand-activated transcription factor termed peroxisome proliferator-activated receptor γ (PPAR γ) that is activated in AS stimulation [46]. Activation of PPAR γ increases cellular motility via changes in cytoskeletal organization [47], i.e. the increased adhesion observed for adipogenically stimulated adMSC could have resulted from reduced cytoskeletal tension due to activation of PPAR γ .

Although the ammonia and oxygen plasma-treated PEEK specimens significantly differ with respect to surface chemistry and roughness, adMSC adhesion, proliferation and differentiation were largely similar. This raises the question whether surface nanostructure or surface chemistry dominates the observed adMSC differentiation. The nanostructure may be of secondary importance, as the nanostructures on oxygen and ammonia plasma-treated substrates significantly differ in height and density and as there is no direct correlation with the protein adsorption. The chemical modification of the PEEK surfaces through the oxygen and ammonia plasma treatments, as revealed by the XPS and contact angle measurements, is complex. The electrochemical properties showed reaction gas dependent but not plasma power dependent effects. Therefore, we have to conclude that both surface chemistry and nanostructuring lead to the positive effect on adMSC differentiation. 10 and 50 W oxygen and ammonia plasma-treated PEEK surfaces proved to be suitable substrates to promote OS differentiation in vitro.

5 Conclusion

Activation of PEEK surfaces using 10 and 50 W oxygen and ammonia plasma treatments (exposure time 5 min) generated nanostructured substrates allowing extensive adMSC adhesion, proliferation, and OS differentiation compared to the original PEEK. These in vitro data indicate that plasma-treated PEEK-implants are osteopromotive

in vitro and thus may permit osseointegration of these isoelastic, magnetic resonance imaging compatible, and X-ray transparent load-bearing implants in vivo.

Acknowledgments This work was funded by the Swiss Nanoscience Institute (project 6.2), the Rector's Conference of the Swiss Universities (CRUS) and the Federal State of Mecklenburg-Vorpommern, Germany. The authors thank Stefanie Adam (Department of Cell Biology, Rostock University Medical Center, Germany) for her excellent technical assistance and Dr. med. habil. Jürgen Weber (Ästhetikklinik Rostock, Germany) for providing liposuction tissue. Further acknowledgements go to Prof. Dr. Dieter Scharnweber (Technical University Dresden, Germany) and Anja Caspari (Leibnitz Institute for Polymer Research, Dresden, Germany) for support with the zeta-potential measurements and to Dr. Roman Heuberger (RMS Foundation, Bettlach, Switzerland) for the XPS measurements and related data analysis. We thank Victrex for kindly providing us with APTIV™ PEEK sheets.

References

1. Kurtz SM, Devine JN. PEEK biomaterials in trauma, orthopedic, and spinal implants. *Biomaterials*. 2007;28(32):4845–69. doi:10.1016/j.biomaterials.2007.07.013.
2. Cook SD, Rust-Dawicki AM. Preliminary evaluation of titanium-coated PEEK dental implants. *J Oral Implantol*. 1995;21(3):176–81.
3. Skinner HB. Composite technology for total hip-arthroplasty. *Clin Orthop Relat Res*. 1988;235:224–36.
4. Toth JM, Wang M, Estes BT, Scifert JL, Seim HB 3rd, Turner AS. Polyetheretherketone as a biomaterial for spinal applications. *Biomaterials*. 2006;27(3):324–34. doi:10.1016/j.biomaterials.2005.07.011.
5. Ratner BD, Hoffman AS, Schoen FJ, Lemons JE. *Biomaterials science: an introduction to materials in medicine*. San Diego: Academic Press; 1996.
6. Poulsson AHC, Richards GR. Surface modification techniques of polyetheretherketone, including plasma surface treatment. In: Kurtz SM, editor. *PEEK biomaterials handbook*. 1st ed. Walham: William Andrew/Elsevier Inc.; 2012. p. 145–61.
7. Ha SW, Gisep A, Mayer J, Wintermantel E, Gruner H, Wieland M. Topographical characterization and microstructural interface analysis of vacuum-plasma-sprayed titanium and hydroxyapatite coatings on carbon fibre-reinforced poly(etheretherketone). *J Mater Sci*. 1997;8(12):891–6. doi:10.1023/A:1018562023599.
8. Noiset O, Schneider YJ, Marchand-Brynaert J. Fibronectin adsorption or and covalent grafting on chemically modified PEEK film surfaces. *J Biomater Sci Polym Ed*. 1999;10(6):657–77.
9. Noiset O, Schneider YJ, Marchand-Brynaert J. Adhesion and growth of CaCo₂ cells on surface-modified PEEK substrata. *J Biomater Sci Polym Ed*. 2000;11(7):767–86.
10. Briem D, Strametz S, Schroder K, Meenen NM, Lehmann W, Linhart W, et al. Response of primary fibroblasts and osteoblasts to plasma treated polyetheretherketone (PEEK) surfaces. *J Mater Sci*. 2005;16(7):671–7. doi:10.1007/s10856-005-2539-z.
11. Schroder K, Meyer-Plath A, Keller D, Ohl A. On the applicability of plasma assisted chemical micropatterning to different polymeric biomaterials. *Plasmas Polym*. 2002;7(2):103–25. doi:10.1023/A:1016239302194.
12. Chan CM, Ko TM, Hiraoka H. Polymer surface modification by plasmas and photons. *Surf Sci Rep*. 1996;24(1–2):3–54.
13. Althaus J, Padeste C, Köser J, Pielers U, Peters K, Müller B. Nanostructuring polyetheretherketone for medical implants. *Eur J Nanomed*. 2012;4(1):7–15. doi:10.1515/ejnm-2011-0001.

14. Vlachopoulou ME, Tserepi A, Beltsios K, Boulousis G, Gogolides E. Nanostructuring of PDMS surfaces: dependence on casting solvents. *Microelectron Eng.* 2007;84(5–8):1476–9. doi:10.1016/j.mee.2007.01.169.
15. Tsougeni K, Vourdas N, Tserepi A, Gogolides E, Cardinaud C. Mechanisms of oxygen plasma nanotexturing of organic polymer surfaces: from stable super hydrophilic to super hydrophobic surfaces. *Langmuir.* 2009;25(19):11748–59. doi:10.1021/La901072z.
16. Zuk PA, Zhu M, Mizuno H, Huang J, Futrell JW, Katz AJ, et al. Multilineage cells from human adipose tissue: implications for cell-based therapies. *Tissue Eng.* 2001;7(2):211–28. doi:10.1089/107632701300062859.
17. Rider DA, Dombrowski C, Sawyer AA, Ng GH, Leong D, Huttmacher DW, et al. Autocrine fibroblast growth factor 2 increases the multipotentiality of human adipose-derived mesenchymal stem cells. *Stem Cells.* 2008;26(6):1598–608. doi:10.1634/stemcells.2007-0480.
18. Levi B, Nelson ER, Li SL, James AW, Hyun JS, Montoro DT, et al. Dura mater stimulates human adipose-derived stromal cells to undergo bone formation in mouse calvarial defects. *Stem Cells.* 2011;29(8):1241–55. doi:10.1002/Stem.670.
19. Peters K, Salamon A, Van Vlierberghe S, Rychly J, Kreutzer M, Neumann HG, et al. A new approach for adipose tissue regeneration based on human mesenchymal stem cells in contact to hydrogels—an in vitro study. *Adv Eng Mater.* 2009;11(10):B155–61. doi:10.1002/adem.200800379.
20. Engler AJ, Sen S, Sweeney HL, Discher DE. Matrix elasticity directs stem cell lineage specification. *Cell.* 2006;126(4):677–89. doi:10.1016/j.cell.2006.06.044.
21. Dalby MJ, Gadegaard N, Tare R, Andar A, Riehle MO, Herzyk P, et al. The control of human mesenchymal cell differentiation using nanoscale symmetry and disorder. *Nat Mater.* 2007;6(12):997–1003. doi:10.1038/nmat2013.
22. McBeath R, Pirone DM, Nelson CM, Bhadriraju K, Chen CS. Cell shape, cytoskeletal tension, and RhoA regulate stem cell lineage commitment. *Dev Cell.* 2004;6(4):483–95. doi:10.1016/S1534-5807(04)00075-9.
23. McNamara LE, McMurray RJ, Biggs MJ, Kantawong F, Oreffo RO, Dalby MJ. Nanotopographical control of stem cell differentiation. *J Tissue Eng.* 2010;2010:120623. doi:10.4061/2010/120623.
24. Kolind K, Leong KW, Besenbacher F, Foss M. Guidance of stem cell fate on 2D patterned surfaces. *Biomaterials.* 2012;33(28):6626–33. doi:10.1016/j.biomaterials.2012.05.070.
25. Anselme K, Ponche A, Bigerelle M. Relative influence of surface topography and surface chemistry on cell response to bone implant materials. Part 2: biological aspects. *Proc Inst Mech Eng H.* 2010;224(H12):1487–507. doi:10.1243/09544119jeim901.
26. Althaus J, Deyhle H, Bunk O, Kristiansen PM, Müller B. Anisotropy in polyetheretherketone films. *J Nanophotonics.* 2012;6(63510):1–11. doi:10.1117/1.JNP.6.063510.
27. d'Agostino R, Favia P, Kawai Y, Ikegami H, Sato N, Arefi-Khonsari F. *Advanced plasma technology.* Weinheim: Wiley-VCH; 2008.
28. Grundke K, Jacobasch HJ, Simon F, Schneider S. Physicochemical properties of surface-modified polymers. *J Adhes Sci Technol.* 1995;9(3):327–50. doi:10.1163/156856195x00536.
29. Noeske K. Die Bindung von Kristallviolett an Desoxyribonukleinsäure—Cytrophotometrische Untersuchungen an normalen und Tumorzellkernen. *Histochemie.* 1966;7(3):273–87.
30. Sarkar BC, Chauhan UP. A new method for determining micro quantities of calcium in biological materials. *Anal Biochem.* 1967;20(1):155–66.
31. Montalibet J, Skorey KI, Kennedy BP. Protein tyrosine phosphatase: enzymatic assays. *Methods.* 2005;35(1):2–8. doi:10.1016/j.ymeth.2004.07.002.
32. Proudfoot D, Skepper JN, Hegyi L, Bennett MR, Shanahan CM, Weissberg PL. Apoptosis regulates human vascular calcification in vitro—evidence for initiation of vascular calcification by apoptotic bodies. *Circ Res.* 2000;87(11):1055–62.
33. Spandl J, White DJ, Peychl J, Thiele C. Live cell multicolor imaging of lipid droplets with a new dye, LD540. *Traffic.* 2009;10(11):1579–84. doi:10.1111/j.1600-0854.2009.00980.x.
34. Althaus J, Urwyler P, Padeste C, Heuberger R, Deyhle H, Schiff H, et al. Micro- and nanostructured polymer substrates for biomedical applications. *Proc SPIE.* 2012;8339:83390Q. doi:10.1117/12.915235.
35. Rechendorff K, Hovgaard MB, Foss M, Zhdanov VP, Besenbacher F. Enhancement of protein adsorption induced by surface roughness. *Langmuir.* 2006;22(26):10885–8. doi:10.1021/la0621923.
36. Altankov G, Groth T. Reorganization of substratum-bound fibronectin on hydrophilic and hydrophobic materials is related to biocompatibility. *J Mater Sci.* 1994;5(9–10):732–7.
37. Müller B. Natural formation of nanostructures: from fundamentals in metal heteroepitaxy to applications in optics and biomaterials science. *Surf Rev Lett.* 2001;8(1–2):169–228. doi:10.1142/S0218625X01000859.
38. Muller B, Riedel M, Michel R, De Paul SM, Hofer R, Heger D, et al. Impact of nanometer-scale roughness on contact-angle hysteresis and globulin adsorption. *J Vac Sci Technol B.* 2001;19(5):1715–20.
39. Lee WH, Loo CY, Van KL, Zavgorodny AV, Rohanizadeh R. Modulating protein adsorption onto hydroxyapatite particles using different amino acid treatments. *J R Soc Interface.* 2012;9(70):918–27. doi:10.1098/rsif.2011.0586.
40. Safinia L, Datan N, Hohse M, Mantalaris A, Bismarck A. Towards a methodology for the effective surface modification of porous polymer scaffolds. *Biomaterials.* 2005;26(36):7537–47. doi:10.1016/j.biomaterials.2005.05.078.
41. Iyengar DR, Perutz SM, Dai CA, Ober CK, Kramer EJ. Surface segregation studies of fluorine-containing diblock copolymers. *Macromolecules.* 1996;29(4):1229–34.
42. Mendonca G, Mendonca DBS, Simoes LGP, Araujo AL, Leite ER, Duarte WR, et al. Nanostructured alumina-coated implant surface: effect on osteoblast-related gene expression and bone-to-implant contact in vivo. *Int J Oral Maxillofac Implant.* 2009;24(2):205–15.
43. Cooper LF, Zhou YS, Takebe J, Guo JL, Abron A, Holmen A, et al. Fluoride modification effects on osteoblast behavior and bone formation at TiO₂ grit-blasted c.p. titanium endosseous implants. *Biomaterials.* 2006;27(6):926–36. doi:10.1016/j.biomaterials.2005.07.009.
44. Dalby MJ, Riehle MO, Johnstone HJ, Affrossman S, Curtis AS. Polymer-demixed nanotopography: control of fibroblast spreading and proliferation. *Tissue Eng.* 2002;8(6):1099–108. doi:10.1089/107632702320934191.
45. Spiegelman BM, Ginty CA. Fibronectin modulation of cell-shape and lipogenic gene-expression in 3T3-adipocytes. *Cell.* 1983;35(3):657–66.
46. Lazar MA. PPAR gamma, 10 years later. *Biochimie.* 2005;87(1):9–13. doi:10.1016/j.biochi.2004.10.021.
47. Chen L, Necela BM, Su WD, Yanagisawa M, Anastasiadis PZ, Fields AP, et al. Peroxisome proliferator-activated receptor gamma promotes epithelial to mesenchymal transformation by rho GTPase-dependent activation of ERK1/2. *J Biol Chem.* 2006;281(34):24575–87. doi:10.1074/jbc.M604147200.

CONCLUSIONS AND OUTLOOK

Thin semi-crystalline PEEK films exhibit an anisotropy in machine direction originating from the glass casting process that can be investigated by two complementary methods: optical transmission measurements and wide-angle as well as small-angle X-ray scattering.

The found anisotropy corresponds to the orientation of the lamellar stacks in semi-crystalline PEEK films and is aligned along the c-axis of the PEEK monomer unit. The long-range order of 14.6 nm found in the X-ray scattering experiments corresponds to the lamellar stacks, consisting of alternating amorphous and crystalline regions.

Simple optical transmission measurements in dependence of annealing temperature allow the determination of intermolecular binding energies responsible for the crystallization of PEEK via the Arrhenius behavior. The observed binding energies for PEEK crystallization of 0.12 ± 0.03 eV correspond exactly to the $\pi - \pi$ binding energy of benzene.

As PEEK exhibits a strong auto-fluorescence, cells stained for specific cell compartments such as the actin cytoskeleton or focal adhesions can only be visualized by confocal microscopy due to the strong fluorescent background of PEEK.

Fluorescence scans revealed a broadband fluorescence for an excitation range of 350 to 550 nm. By synthesizing pure PEEK, we were able to proof that the fluorescence is inherent to the material and is not caused by any additive.

Oxygen and ammonia plasma induced homogenous nano-structuring on PEEK substrates. The nano-structuring is caused by an etching effect.

The size of the pillar-like nano-structures is plasma power dependent, increasing with applied plasma power. Oxygen plasma revealed a stronger patterning effect than ammonia plasma at identical power and exposure time.

AFM allowed quantification of the produced nano-structures. Roughness increased and island density decreased linearly with plasma power for oxygen and ammonia plasma treated PEEK substrates. This finding enables tailored nano-structuring of large-area PEEK substrates in the investigated size-range. 10 W and 200 W oxygen plasma treated PEEK revealed an RMS roughness of 1.5 and 15 nm, respectively, whereas 10 W and 200 W ammonia plasma treated PEEK revealed an RMS roughness of 1.0 and 7.5 nm, respectively. The island density on ammonia plasma treated PEEK was three-fold compared to oxygen plasma treated PEEK:

200 W oxygen plasma resulted in approximately 170 islands per μm^2 , whereas the island density on 200 W ammonia plasma treated PEEK was 500 islands per μm^2 .

Oxygen plasma treatment is a dry and fast method to (nano)structure and activate large-area PEEK and other polymer surfaces. Oxygen plasma of injection-molded polymers such as PP or PE revealed anisotropic nano-structures, probably associated with the molecular orientation of the molecules. Therefore, oxygen plasma treatment might be a valuable method to visualize polymer chain orientations in injection-molded materials. Furthermore, the oriented nano-structures might serve as templates for a wide variety of applications such as protein crystallography or cell-material interaction studies.

Oxygen and ammonia plasma treatment are powerful methods to activate polymer surfaces, since they induce nano-structures and chemical modifications of the PEEK substrates simultaneously. The chemical changes of the surface are reflected in zeta-potential measurements and XPS measurements. Contact angle and protein adsorption depend on both, chemical and topographical changes induced by plasma treatment.

Oxygen or ammonia plasma treatment is necessary to activate the bio-inert PEEK surface in order to reach reproducible and homogenous spreading of ASC.

ASC viability on the PEEK substrates under OS stimulation conditions decreased with increasing plasma power for both reaction gases. 10 and 50 W plasma treatment results in increased cell numbers, 100 and 200 W plasma treatment resulted in decreased cell numbers compared to the original and the TCPS control.

ASC differentiation under OS conditions towards the osteogenic lineage revealed also a plasma power dependent effect: both, ALPL activity and *in vitro* mineralization increases on 10 and 50 W plasma treated PEEK substrates for both reaction gases, oxygen and ammonia. Differentiation towards the adipogenic lineage under AS conditions was slightly higher on 10, 50 and 100 W ammonia plasma treated PEEK substrates compared to the oxygen plasma treated substrates, the original PEEK substrate and the TCPS control.

10 and 50 W oxygen and ammonia plasma treatment appeared to enable ASC adhesion and positively influence osteogenic differentiation *in vitro*. Thus, these *in vitro* data indicate an osteopromotive effect of plasma-treated PEEK on tissue-resident mesenchymal stem cells. However, this assumption must be confirmed by *in vivo* experimentation.

Jasmin Waser-Althaus

Hemmikerstrasse 26
4466 Ormalingen
Switzerland
+ 41 79 225 26 52
waser.jasmin@gmail.ch

PERSONAL DATA

Date of birth 02.07.1981
Nationality Swiss
Place of origin Lauperswil, BE
Languages German, English, French (basics)
Marital Status married

EDUCATION

2008-2012 PhD thesis
Medical Faculty, University of Basel
Doctoral supervisor: Prof. Dr. Bert Müller, Director Biomaterials
Science Center
PhD Thesis: *“Plasma-activated polymer films for mesenchymal stem
cell differentiation”*
“Cotutelle de Thèse” with the University of Rostock (Kirsten Peters,
Department of Cell Biology, Junior Research Group), granted by the
Rectors` Conference of the Swiss Universities (CRUS)

2006-2007 Master of Science in Molecular Biology
Major in Immunology
Prof. Dr. Antonius Rolink, Center for Biomedicine (CBM), University
of Basel
Master Thesis: *“Notch signaling in mouse and human T cell
development”*

Recombinant BAFF rescues mature B cell development in baff deficient mice”

- 2004-2006 Bachelor of Science in Molecular Biology
Biocenter, University of Basel
- 2000-2004 Chemist FH
University of Applied Sciences, Basel (FHBB)
Diploma Thesis: “Quantification of (C-Man-)Trp in human urine with LC-MS/MS”
Prof. Dr. Jan Hofsteenge, Friedrich Miescher Institute (FMI), Basel
- 1997-2000 Laboratory assistant
Ciba, Basel
Extra-occupational professional maturity

WORK EXPERIENCE

- Since 2012 Project Manager R&D
Thommen Medical AG
- 2008 Research associate (6 months)
ICB / Nanotechnology, FHNW
3D α -TCP scaffolds for implantology
Modification of collagen membranes for increased cell attachment
- 2005 Project work (3 months during studies)
Geistlich Pharma AG
Literature research
Initial cell culture experiments on bone replacement scaffold with stroma cells
- 2004-2005 Research assistant (50% during studies)
Prof. Dr. Jan Hofsteenge, Friedrich Miescher Institute (FMI), Basel

AWARDS

- 2011 Travel Award from Swiss Society of Biomaterials
- 2010 Selected for CCMX conference sponsorship at Gordon Conference Biointerface Science
- 2004 Prize for best interdisciplinary diploma thesis (Novartis)

OTHER ACTIVITIES

- 2010 Selected as participant for the 10th women into industry (WIN) program, a joined mentoring program between the University of Basel and Novartis
- Participation as core team member

PUBLICATIONS

- J. Waser-Althaus, A. Salamon, M. Waser, C. Padeste, M. Kreutzer, U. Pieleles, B. Müller, K. Peters. Differentiation of human mesenchymal stem cells on plasma-treated polyetheretherketone. *Journal of Materials Science: Materials in Medicine* 25 (2014) 515-525.
- J. Althaus, P. Urwyler, C. Padeste, R. Heuberger, H. Deyhle, H. Schiff, J. Gobrecht, U. Pieleles, D. Scharnweber, K. Peters, B. Müller Micro- and nanostructured polymer substrates for biomedical applications. *Proc. SPIE* 8339 (2012) 83390Q.
- J. Althaus, H. Deyhle, O. Bunk, P.M. Kristiansen, B. Müller. Anisotropy in polyetheretherketone films. *Journal of Nanophotonics* 6 (2012) 063510.
- J. Althaus, C. Padeste, J. Köser, U. Pieleles, K. Peters, B. Müller. Nanostructuring polyetheretherketone for medical implants. *European Journal of Nanomedicine* 4 (1) (2012) 7-15.

PEER-REVIEWED CONFERENCE ABSTRACTS

J. Althaus, H. Deyhle, O. Bunk and B. Müller Structural anisotropies of PEEK foils revealed by optical dichroism and X-ray scattering methods. *European Cells and Materials* 22 (2011) 29.

J. Althaus, Stefanie Adam, H. Schiff, J. Gobrecht, U. Pieves, B. Müller and K. Peters. Plasma treated and nano/micro-structured PEEK substrates for adipose tissue-derived stem cell studies. *European Cells and Materials* 20 (2010) 3.

J. Althaus, Uwe Pieves, K. Peters, and B. Müller. PEEK Substrates for Measurement of Contractile Cell Forces of Primary Cells. *European Cells and Materials* 20 (2010) 1.

CONFERENCE CONTRIBUTIONS

J. Althaus, J. Köser, U. Pieves, and B. Müller. Effects of plasma-treatment and nanostructuring of PEEK substrates on osteogenic differentiation of adipose tissue-derived stem cells. *European Society for Biomaterials 2011, Dublin, Ireland*. Talk.

J. Althaus, J. Köser, U. Pieves, and B. Müller. Auto-fluorescence of polyetheretherketone (PEEK) foils. *European Society for Biomaterials 2011, Dublin, Ireland*. Poster contribution.

J. Althaus, J. Köser, Stefanie Adam, H. Schiff, J. Gobrecht, U. Pieves, B. Müller and K. Peters. Plasma treated and nano/micro-structured PEEK substrates for adipose tissue-derived stem cell studies. *Gordon Conference on Biointerface Science 2010*. Poster contribution.

J. Althaus, Stefanie Adam, H. Schiff, J. Gobrecht, U. Pieves, B. Müller and K. Peters Plasma treated and nano/micro-structured PEEK substrates. *3rd European Conference for Clinical Nanomedicine 2010, Basel, Switzerland*. Poster contribution.

J. Althaus, J. Gobrecht, H. Schiff, Mirco Altana, U. Pieves, J. Köser, and B. Müller. Quantification of contractile cell forces on PEEK substrates. *Third Switzerland-Japan Workshop on Biomechanics 2009, Engelberg, Switzerland*. Poster contribution.

REFERENCES

1. Kurtz SM, Devine JN. PEEK biomaterials in trauma, orthopedic, and spinal implants. *Biomaterials* 2007;28:4845-69.
2. Dawson PC, Blundell DJ. X-ray data for poly(aryl ether ketones). *Polymer* 1980;21:577-8.
3. Hunter A, Archer CW, Walker PS, Blunn GW. Attachment and proliferation of osteoblasts and fibroblasts on biomaterials for orthopaedic use. *Biomaterials* 1995;16(4):287-95.
4. Briem D, Strametz S, Schröder K, Meenen NM, Lehmann W, Linhart W, et al. Response of primary fibroblasts and osteoblasts to plasma treated polyetheretherketone (PEEK) surfaces. *J Mater Sci Mater Med* 2005;16(7):671-7.
5. Protecting batteries in heart pacemakers. *Kunststoffe* 2011;2:98.
6. Sobieraj M, Murphy J, Brinkman J, Kurtz S. Notched fatigue behavior of PEEK. *Biomaterials* 2010;31(35):9156-62.
7. Ratner B, Hoffman A, Schoen F, Lemons J. *Biomaterials science: an introduction to materials in medicine*. Waltham: Academic Press; 1996.
8. Skinner H. Composite technology for total hip arthroplasty. *Clin Orthop Relat Res* 1988;235:224-36.
9. Cook S, Rust-Dawicki A. Preliminary evaluation of titanium-coated PEEK dental implants. *J Oral Implantol* 1995;21(3):176-81.
10. Ha S, Mayer J, Koch B, Wintermantel E. Plasma-sprayed hydroxylapatite coating on carbon fibre reinforced thermoplastic composite materials. *J Mater Sci* 1994;5:481-4.
11. Ha S, Gisep A, Mayer J, Wintermantel E, Gruner H, Wieland M. Topographical characterization and microstructural interface analysis of vacuum-plasma-sprayed titanium and hydroxyapatite coatings on carbon fibre-reinforced poly(etheretherketone). *J Mater Sci Mater Med* 1997;8:891-6.
12. Noiset O, Schneider Y, Marchand-Brynaert J. Fibronectin adsorption or/and covalent grafting on chemically modified PEEK film surfaces. *J Biomater Sci Polym Ed* 1999;10(6):657-77.
13. Noiset O, Schneider Y, Marchand-Brynaert J. Adhesion and growth of CaCo2 cells on surface-modified PEEK substrata. *J Biomater Sci Polym Ed* 2002;11(7):767-86.
14. Ha SW, Hauert R, Ernst KH, Wintermantel E. Surface analysis of chemically-etched and plasma-treated polyetheretherketone (PEEK) for biomedical applications. *Surface and Coatings Technology* 1997;96(2-3):293-9.
15. Schroder K, Meyer-Plath A, Keller D, Ohl A. On the applicability of plasma assisted chemical micropatterning to different polymeric biomaterials. *Plasmas Polym* 2002;7(2):103-25.
16. Akhavan S, Matthiesen M, Schulte L, Penoyar T, Kraay M, Rimnac C, et al. Clinical and histologic results related to a low-modulus composite total hip replacement stem. *J Bone Jt Surg Am* 2006;88(6):1308-14.
17. Petrovic L, Pohle D, Munstedt H, Rechtenwald T, Schlegel K, Rupprecht S. Effect of betaTCP filled polyetheretherketone on osteoblast cell proliferation in vitro. *J Biomed Sci* 2006;13(1):41-6.
18. Yu S, Kithva PH, Kumar R, Cheang P, Khor KA. In vitro apatite formation and its growth kinetics on hydroxyapatite/polyetheretherketone biocomposites. *Biomaterials* 2005;26(15):2343-52.
19. Bakar MA, Cheng M, Tang S, Yu S, Liao K, Tan C, et al. Tensile properties, tension-tension fatigue and biological response of polyetheretherketone-hydroxyapatite composites for load-bearing orthopedic implants. 2003;24(13):2245-50.

20. Fan J, Tsui C, Tang C, Chow C. Influence of interphase layer on the overall elasto-plastic behaviors of HA/PEEK biocomposite. *Biomaterials* 2004;25(23):5363-73.
21. Tang S, Cheang P, AbuBakar M, Khor K, Liao K. Tension-tension fatigue behavior of hydroxyapatite reinforced polyetheretherketone composites. *Int J Fatigue* 2004;26(49-57).
22. Chan C, Ko TM, Hiraoka H. Polymer surface modification by plasmas and photons. *Surface Science Reports* 1996;24(1-2):1-54.
23. Vlachopoulou M, Tserepi A, Beltsios K, Boulousis G, Gogolides E. Nanostructuring of PDMS surfaces: Dependence on casting solvents. *Microelectronic Engineering* 2007;84:1476-79.
24. Tsougeni K, Vourdas N, Tserepi A, Gogolides E, Cardinaud C. Mechanisms of oxygen plasma nanotexturing of organic polymer surfaces: from stable super hydrophilic to super hydrophobic surfaces. *Langmuir* 2009;6(25):11748-59.
25. Ponche A, Bigerelle M, Anselme K. Relative influence of surface topography and surface chemistry on cell response to bone implant materials. Part 1: Physico-chemical effects. *Proc Inst Mech Eng H* 2010;224:1471-86.
26. Anselme K, Ponche A, Bigerelle M. Relative influence of surface topography and surface chemistry on cell response to bone implant materials. Part 2: biological aspects. *Proc Inst Mech Eng H* 2010;224(12):1487-507.
27. Engler AJ, Sen S, Sweeney HL, Discher DE. Matrix elasticity directs stem cell lineage specification. *Cell* 2006;126(4):677-89.
28. Riedel M, Müller B, Wintermantel E. Protein adsorption and monocyte activation on germanium nanopylamids. *Biomaterials* 2001;22(16):2307-16.
29. Variola F, Brunski JB, Orsini G, Tambasco de Oliveira P, Wazen R, Nanci A. Nanoscale surface modifications of medically relevant metals: state-of-the art and perspectives. *Nanoscale* 2011;3(2):335-53.
30. Dohan Ehrenfest D, Coelho P, Kang B, Sul Y, Albrektsson T. Classification of osseointegrated implant surfaces: materials, chemistry and topography. *Trends Biotechnol* 2010;28(4):198-206.
31. McBeath R, Pirone DM, Nelson CM, Bhadriraju K, Chen CS. Cell Shape, Cytoskeletal Tension, and RhoA Regulate Stem Cell Lineage Commitment. *Developmental Cell* 2004;6(4):483-95.
32. Tuan R. Role of adult stem/progenitor cells in osseointegration and implant loosening. *Int J Oral Maxillofac Implants* 2011;26:Suppl. 50-62.
33. Wilson C, Clegg R, Leavesley D, Percy M. Mediation of biomaterial-cell interactions by adsorbed proteins: a review. *Tissue Eng* 2005;11(1-2):1-18.
34. Dalby MJ, Gadegaard N, Tare R, Andar A, Riehle MO, Herzyk P, et al. The control of human mesenchymal cell differentiation using nanoscale symmetry and disorder. *Nat Mater* 2007;6(12):997-1003.
35. Müller B. Natural Formation of nanostructures: from fundamentals in metal heteroepitaxy to applications in optics and biomaterials science. *Surface Review and Letters* 2001;8(1-2):169-228.
36. Huang N, Patlolla B, Abilez O, Sharma H, Rajadas J, Beygui R, et al. A matrix micropatterning platform for cell localization and stem cell fate determination. *Acta Biomaterialia* 2010;6:4614-21.
37. Zuk P, Zhu M, Mizuno H, Huang J, Futrell W, Katz A, et al. Multi-lineage cells from human adipose tissue: Implications for cell-based therapies. *Tissue Eng* 2001;7:211-26.
38. Choi J, Kim S, Jung J, Lim Y, Kang K, Park S, et al. Wnt5a-mediating neurogenesis of human adipose tissue-derived stem cells in a 3D microfluidic cell culture system. *Biomaterials* 2011;32(29):7013-22.

39. Banas A. Purification of adipose tissue mesenchymal stem cells and differentiation toward hepatic-like cells. *Methods Mol Biol* 2012;826:61-72.
40. Peters K, Salamon A, Vlierberghe SV, Rychly J, Kreutzer M, Neumann H, et al. A new approach for adipose tissue regeneration based on human mesenchymal stem cells in contact to hydrogels – an in vitro study. *Adv Eng Mat* 2009;11(10):B 151-61.
41. Levi B, Nelson E, Li S, James A, Hyun J, Montoro D, et al. Dura mater stimulates human adipose tissue-derived stromal cells to undergo bone formation in mouse calvarial defects. *Stem Cells* 2011;29:1241-55.
42. Bunk O, Bech M, Jensen T, Feidenhans'l R, Binderup T, Menzel A, et al. Multimodal x-ray scatter imaging. *New Journal of Physics* 2009;11:123016.
43. Heinrich B, Bergamaschi A, Brönnimann C, Dinapoli R, Eikenberry EF, Jhonson I, et al. PILATUS: A single photon counting pixel detector for X-ray applications. *Nuclear Instruments and Methods in Physics Research A* 2009;607:247-9.
44. Risse W, Sogha DY. Synthesis of Soluble High Molecular Weight Poly(ary1 ether ketones) Containing Bulky Substituents. *Macromolecules* 1990;23(18):4029-33.
45. Peters K, Salamon A, Van Vlierberghe S, Rychly J, Kreutzer M, Neumann H-G, et al. A new approach for adipose tissue regeneration based on human mesenchymal stem cells in contact to hydrogels - an in vitro study. *Advanced Engineering Materials* 2007;11(10):B155-61.
46. Urwyler P, Schiff H, Gorecht J, Häfeli O, Altana M, Battiston F, et al. Surface patterned polymer micro-cantileverarrays for sensing. *Sensors and Actuators A: Physical* 2011;172(1):2-8.
47. Urwyler P, Häfeli O, Schiff H, Gobrecht J, Battiston F, Müller B. Disposable polymeric micro-cantilever arrays for sensing. *Procedia Eng* 2010;5:347-50.
48. Althaus J, Deyhle H, Bunk O, Kristiansen P, Müller B. Anisotropy in polyetheretherketone films. *J Nanophoton*;submitted.
49. d'Agostino R, Favia P, Kawai Y, Ikegami H, Sato N, Arefi-Khonsari F. *Advanced plasma technology*. Weinheim: Wiley-VCH; 2008.
50. Grundke K, Jacobatsch H, Simon F, Schneider S. Physico-chemical properties of surface modified polymers. *J Adhesion Sci Technol* 1995;9:327-50.
51. Noeske K. The binding of crystal violet on deoxyribonucleic acid. *Cytophotometric studies on normal and tumor cell nuclei*. *Histochemie* 1966;7(3):273–87.
52. Sarkar B, Chauhan U. A new method for determining micro quantities of calcium in biological materials. *Anal Biochem* 1967;20(1):155-66.
53. Montalibet J, Skorey K, Kennedy B. Protein tyrosine phosphatase: enzymatic assays. *Methods* 2005;35(1):2-8.
54. Proudfoot D, Skepper J, Hegyi L, Bennett M, Shanahan C, Weissberg P. Apoptosis regulates human vascular calcification in vitro: evidence for initiation of vascular calcification by apoptotic bodies. *Circ Res* 2000;87(11):1055-62.
55. Spandl J, White D, Peychl J, Thiele C. Live cell multicolor imaging of lipid droplets with a new dye, LD540. *Traffic* 2009;10(11):1579-84.
56. Hay JN, Kemmish DJ, Langford JI, Rae AIM. The structure of crystalline PEEK. *Polymer Commun* 1984;25:175-8.
57. Reiter G, Sommer JU. *Semicrystalline Polymers at Variable Temperature*. *Polymer Crystallization*: Springer; 2003. p. 116-8.
58. Lauritzen J, Hoffman J. Theory of formation of polymer crystals with folded chains in dilute solution. *J Res Nat Bur Stand A Phys Ch* 1960;64:73-102.
59. Ryan A, Stanford J, Bras W, Nye T. A synchrotron X-ray study of melting and recrystallization in isotactic polypropylene. *Polymer* 1997;38(4):759-68.